

LEVEL II

12

AD

SR

AD A100965

TECHNICAL REPORT ARBRL-TR-02319

QUANTITATIVE ASSESSMENT OF
PRESSURE WAVES IN GUNS

A. W. Horst
F. R. Lynn
J. N. Walbert

DTIC
ELECTE
JUL 0 6 1981
S D E

May 1981



US ARMY ARMAMENT RESEARCH AND DEVELOPMENT COMMAND
BALLISTIC RESEARCH LABORATORY
ABERDEEN PROVING GROUND, MARYLAND

Approved for public release; distribution unlimited.

DTIC FILE COPY

81 7 02 090

Destroy this report when it is no longer needed.
Do not return it to the originator.

Secondary distribution of this report by originating
or sponsoring activity is prohibited.

Additional copies of this report may be obtained
from the National Technical Information Service,
U.S. Department of Commerce, Springfield, Virginia
22161.

The findings in this report are not to be construed as
an official Department of the Army position, unless
so designated by other authorized documents.

*The use of trade names or manufacturers' names in this report
does not constitute endorsement of any commercial product.*

UNCLASSIFIED

SECURITY CLASSIFICATION OF THIS PAGE (When Data Entered)

REPORT DOCUMENTATION PAGE		READ INSTRUCTIONS BEFORE COMPLETING FORM
1. REPORT NUMBER TECHNICAL REPORT ARBRL-TR-02319	2. GOVT ACCESSION NO. AD-100965	3. RECIPIENT'S CATALOG NUMBER
4. TITLE (and Subtitle) QUANTITATIVE ASSESSMENT OF PRESSURE WAVES IN GUNS.	5. TYPE OF REPORT & PERIOD COVERED Technical Report.	
7. AUTHOR(s) A.W./Horst F.R./Lynn J.N./Walbert	8. CONTRACT OR GRANT NUMBER(s)	
9. PERFORMING ORGANIZATION NAME AND ADDRESS U.S. Army Ballistic Research Laboratory ATTN: DRDAR-BLI Aberdeen Proving Ground, MD 21005	10. PROGRAM ELEMENT, PROJECT, TASK AREA & WORK UNIT NUMBERS IL162618AH80	12. REPORT DATE MAY 1981
11. CONTROLLING OFFICE NAME AND ADDRESS U.S. Army Armament Research Laboratory U.S. Army Ballistic Research Laboratory ATTN: DRDAR-BL Aberdeen Proving Ground, MD 21005	13. NUMBER OF PAGES 86	
14. MONITORING AGENCY NAME & ADDRESS (if different from Controlling Office)	15. SECURITY CLASS. (of this report) UNCLASSIFIED	
16. DISTRIBUTION STATEMENT (of this Report) Approved for public release; distribution unlimited		
17. DISTRIBUTION STATEMENT (of the abstract entered in Block 20, if different from Report)		
18. SUPPLEMENTARY NOTES		
19. KEY WORDS (Continue on reverse side if necessary and identify by block number) Pressure Waves Interior Ballistics Guns Breechblows		
20. ABSTRACT (Continue on reverse side if necessary and identify by block number) Combustion instability in conventional guns is often manifested by the presence of longitudinal pressure waves traveling between the breech face and base of the projectile. Such waves are of concern because of their causal connection with high chamber pressures and pressurization rates which may in turn lead to breechblows, projectile or fuze malfunctions, and ballistic variability. While design approaches which minimize pressure waves are routinely employed today, the problem remains of specifying acceptable pressure-wave levels. (continued on next page)		

DD FORM 1 JAN 73 1473

EDITION OF 1 NOV 65 IS OBSOLETE

UNCLASSIFIED

SECURITY CLASSIFICATION OF THIS PAGE (When Data Entered)

UNCLASSIFIED

SECURITY CLASSIFICATION OF THIS PAGE(When Data Entered)

One of the most-used indicators of the severity of pressure waves in guns is the initial reverse pressure difference ($-\Delta P_i$) measured between the breech and forward (mouth) ends of the chamber at the time of stagnation of the ignition front at the projectile base. The U.S. Army employs a correlation between this quantity and the maximum chamber pressure in order to project statistically the expected probability of exceeding a given pressure limit. A fundamental concern exists, however, as to whether $-\Delta P_i$ is a physically appropriate indicator of pressure-wave problems.

→ This study addresses the establishment of the basis for an improved procedure for assessment of pressure waves. Several techniques are described for "detecting" the true pressure-wave signal from its carrier by removing what is essentially the classical Lagrangian pressure gradient from the experimental pressure-difference-versus-time profile, formed by subtracting the pressure-versus-time signal recorded at the forward end of the chamber from that recorded at the breech. The most successful approach is shown to be a digital Fourier-analysis technique involving multiple bandpass filtering of the recorded pressure-difference-versus-time profile. The resulting pressure-wave signal is characterized by an initial amplitude which is believed to be a physically well-motivated measure of the level of pressure waves and which offers procedural advantages in terms of both measurement and statistical processing of data. Integration of this technique into existing safety-assessment procedures is outlined.

UNCLASSIFIED

SECURITY CLASSIFICATION OF THIS PAGE(When Data Entered)

TABLE OF CONTENTS

	Page
LIST OF ILLUSTRATIONS.	5
I. INTRODUCTION	7
II. TECHNICAL DISCUSSION	9
A. Current Procedure.	9
B. Inadequacies Of The Current Procedure.	16
C. Consideration Of Other Indicators.	18
D. A New Approach: Removal Of The Classical Gradient .	24
III. CONCLUSIONS AND RECOMMENDATIONS.	45
REFERENCES	49
APPENDIX	51
DISTRIBUTION LIST.	81

Accession For	
NTIS GRA&I	<input checked="" type="checkbox"/>
DTIC TAB	<input type="checkbox"/>
Unannounced	<input type="checkbox"/>
Justification	
By _____	
Distribution/	
Availability Codes	
Dist	Avail and/or Special
A	

LIST OF ILLUSTRATIONS

Figure	Page
1. Bag Charge/Gun Chamber Interface.	8
2. Experimental Pressurization Profiles for a Properly-Ignited, High-Performance Bag Charge.	10
3. Experimental Pressurization Profiles Exhibiting High-Amplitude, Longitudinal Pressure Waves.	11
4. Induced Breechblow, 175-mm Gun.	12
5. Sensitivity of Maximum Chamber Pressure to Pressure Waves; 175-mm, M107 Gun; M86A2 (Zone 3) Propelling Charge. . .	14
6. Cumulative Distribution of $-\Delta P_i$; 175-mm, M107 Gun; M86A2 (Zone 3) Propelling Charge.	15
7. Projected Probability of $-\Delta P_i$; 175-mm, M107 Gun; M86A2 (Zone 3) Propelling Charge.	15
8. Profiles of Pressure Difference (Breech Minus Forward) Versus Time	17
9. Best-Fit Cumulative Distribution for Population of $-\Delta P_i$ Data Including Assigned Zeros	19
10. Effect of 10% Linear Calibration Errors on Recorded Pressure-Difference-Versus-Time Data of Figure 8(c) . .	20
11. Schematic Definitions of Alternative Indicators of Pressure-Wave Magnitude	21
12. Plots of Maximum Chamber Pressure Versus Alternative Indicators of Figure 11 for a 155-mm, Special-Charge Data Base	22
13. Conceptualized Scheme for Extracting Longitudinal Pressure-Wave Signal.	25
14. Sensitivity of Detected Pressure-Wave Signal to Alternative Cubic-Spline Techniques for Removal of Lagrangian Profile.	27
15. Conceptualized Application of Fourier-Analysis/Digital Filtering Technique	30
16. Alternative Schemes for Application of Digital Filters.	31

LIST OF ILLUSTRATIONS

Figure	Page
17. Character of Digital Bandpass Filter.	32
18. Multiple Application of Bandpass Filter	32
19. Application of Fourier-Analysis/Digital-Bandpass- Filtering Technique to Experimental 155-mm Howitzer Firing Data - A	33
20. Application of Fourier-Analysis/Digital-Bandpass- Filtering Technique to Experimental 155-mm Howitzer Firing Data - B	34
21. Application of Fourier-Analysis/Digital-Bandpass- Filtering Technique to Experimental 155-mm Howitzer Firing Data - C	35
22. Application of Fourier-Analysis/Digital-Bandpass- Filtering Technique to Experimental 155-mm Howitzer Firing Data - D	36
23. Application of Fourier-Analysis/Digital-Bandpass- Filtering Technique to Experimental 155-mm Howitzer Firing Data - E	37
24. Application of Fourier-Analysis/Digital-Bandpass- Filtering Technique to Experimental 155-mm Howitzer Firing Data - F	38
25. Application of Fourier-Analysis/Digital-Bandpass- Filtering Technique to Experimental 155-mm Howitzer Firing Data - G	39
26. Sensitivity of Detected Pressure-Wave Profile to Two Alternative Digital-Filtering Schemes	41
27. Sensitivity of Detected Pressure-Wave Profile to 10% Linear Calibration Errors.	43
28. Sensitivity of Detected Pressure-Wave Profile to Severe Signal Drift	44
29. Best-Fit Cumulative Distribution for Populations Based on Three Alternative Indicators of Pressure-Wave Magnitude.	46

I. INTRODUCTION

The presence of longitudinal pressure waves in guns can influence overall system safety in a variety of manners. As pointed out by Budka and Knapton in their survey on pressure waves in guns¹, "...researchers have revealed one common characteristic associated with the occurrence of unexpected high pressure excursions - namely, the existence of strong pressure waves in the gun system." Such unintended overpressures can damage gun and ammunition components, leading to breechblows, prematures, increased dud rates, and other forms of performance degradation. However, even without increases in maximum chamber pressure, nonuniform ignition and pressurization in the gun chamber can cause very high local pressurization rates and solid-phase (propellant and packaging components) transient loads on the projectile base that can lead to projectile or fuze damage^{2,3}. An even further concern with pressure waves exists in terms of their effect on ballistic reproducibility, as variation in the magnitude of pressure waves is often accompanied by a variation in other performance parameters⁴.

Yet many weapons with excellent safety, reliability, and performance records exhibit pressure waves, some at substantial levels. Techniques for distinguishing between acceptable and unacceptable levels of pressure waves are based on philosophies that range all the way from "she ain't blown yet, so why worry now" to "all pressure waves are unacceptable"! While both views may be considered impractical, the more conservative approach finds its origin in the costly experiences of numerous catastrophic gun malfunctions, for which strong pressure waves served as precursors to the overpressure or premature functioning of the payload. Further motivation arises from our lack of understanding of the detailed phenomenology of such failures, as articulated nearly three decades ago

¹A.J. Budka and J.D. Knapton, "Pressure Wave Generation in Gun Systems: A Survey," BRL MR 2567, USA Ballistic Research Laboratories, Aberdeen Proving Ground, MD, December 1975. (AD #B008893L)

²D.W. Culbertson, M.C. Shamblen, and J.S. O'Brasky, "Investigation of 5"/38 Gun In-Bore Ammunition Malfunctions," NWL-TR-2624, Naval Weapons Laboratory, Dahlgren, VA, December 1971.

³L. Kell, "The 5-Inch Illuminating Projectile Dud Investigation," NSWL/DL-TR-3792, Naval Surface Weapons Center, Dahlgren Laboratory, Dahlgren, VA, January 1979.

⁴E.V. Clarke, Jr. and I.W. May, "Subtle Effects of Low-Amplitude Pressure Wave Dynamics on the Ballistic Performance of Guns," 11th JANNAF Combustion Meeting, CPIA Publication 261, Vol. 1, pp. 141-155, December 1974.

by the British interior ballisticians Lockett⁵:

"It might be pertinent to point out...that there is always some uncertainty in the interpretation of what might be dismissed as minor irregularities in the pressure-time curve. We have by bitter experience learned to regard such irregularities with a degree of suspicion...because of the apparent ease with which such minor flaws can turn over to major irregularities by some mechanism not yet understood."

The problem of pressure waves has been of most concern to the U.S. Army with respect to the design of high-performance artillery bag charges. A typical layout for such a charge is presented schematically in Figure 1. Principal components of the charge include a basepad igniter (usually containing black powder or CBI*), a centercore igniter (containing additional igniter material), and a main charge (typically multi-perforated, triple-base, granular propellant). A cloth bag is employed to contain the charge, and other components such as a flash inhibitor or wear-reducing additive may be present. We postulate functioning of the charge to be described by the following sequence of events: the basepad igniter is initiated by the impingement of hot combustion products from a percussion primer. The basepad then ignites the centercore charge, and together they ignite nearby propellant grains. Combined igniter and propellant gases penetrate the propellant bed, convectively heating the grains and resulting in flamespread. During this process, the pressure gradient and interphase drag forces accelerate the propellant grains, largely in the forward direction, thrusting them and any intervening elements against the projectile base. Upon stagnation, a reflected compression wave in the gas phase is formed, its magnitude being subject to increase by the combined effects of reduction in free volume (due to bed compaction) and combustion in this low-porosity region.

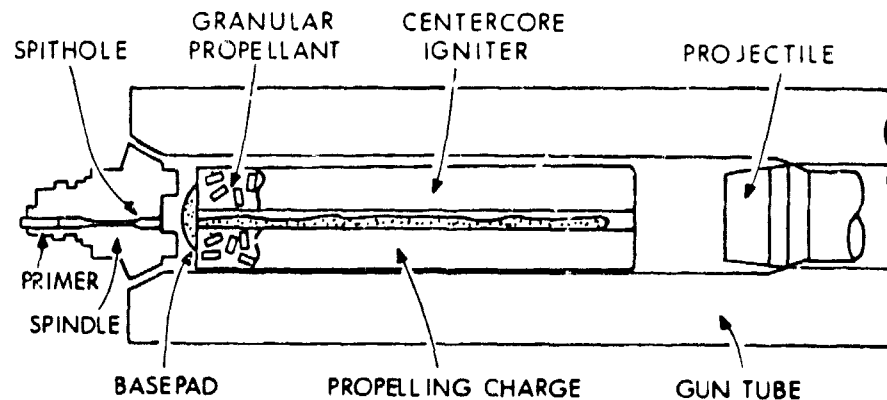


Figure 1. Bag Charge/Gun Chamber Interface

⁵N. Lockett, "British Work on Solid Propellant Ignition," *Bulletin of the First Symposium on Solid Propellant Ignition*, Solid Propellant Information Agency, Silver Spring, MD, October 1956.

*Clean-Burning Igniter, a nitrocellulose-base ignition material

If the charge functions as intended, smooth pressure-versus-time curves as shown in Figure 2 are obtained. A pressure-difference-versus-time history, formed by subtracting the pressure measured by a gage in the chamber wall near the initial position of the projectile base from the breech pressure as a function of time, reveals only the normal forward-facing gradient associated with motion of the projectile down the tube. On occasion, however, pressure-time histories as shown in Figure 3 are obtained. Strong longitudinal pressure waves are clearly manifested in the pressure-difference plot. Such phenomena have been traditionally associated with localized ignition of the propellant bed and thus may imply non-functioning or at least late functioning of the centercore charge. Whether this wave dissipates or grows is dependent on a complex interplay of events controlled by gas production rates, ullage, bed permeability and projectile motion. Thus, other factors in addition to proper functioning of the ignition train may be of importance. Finally, increases in maximum chamber pressure may or may not accompany such increases in pressure-wave dynamics, with extreme amplitudes resulting in breechblows (see Figure 4.)

In a recent study⁶, we addressed the validity of the assumption that a unique relationship existed between the initial reverse pressure difference ($-\Delta P_i$), as indicated on Figure 3, and the maximum chamber pressure (P_{max}) for a given charge/weapon combination. The quantity $-\Delta P_i$ can be interpreted as a measure of the severity of the flow stagnation event at the conclusion of flamespread, and as such serves as a measure of "badness" of the ignition event. This assumption of uniqueness between $-\Delta P_i$ and P_{max} is fundamental to the breechblow safety assessment procedure currently employed by the U.S. Army. It was concluded that while initial charge temperature significantly impacts this relationship, an essentially unique sensitivity relationship between $-\Delta P_i$ and P_{max} can be assumed for any given temperature to facilitate a quantitative assessment of the probability of breechblow for a given charge/weapon combination.

In this study, however, we probe the adequacy of $-\Delta P_i$ formulism as an indicator of the magnitude of pressure waves and evaluate the use of several alternative parameters in terms of physical motivation, ease of measurement, and impact on established safety-assessment procedures.

II. TECHNICAL DISCUSSION

A. Current Procedure

As one facet of the overall safety-assessment procedure for new propelling charges for artillery, the Ballistic Research Laboratory is

⁶C.R. Ruth and A.W. Horst, "Experimental Validation for the Uniqueness of the Differential Pressure-Maximum Pressure Sensitivity Curves Used for Charge Safety Assessment", Ballistic Research Laboratory, USA ARRADCOM, Aberdeen Proving Ground, MD, (report in preparation).

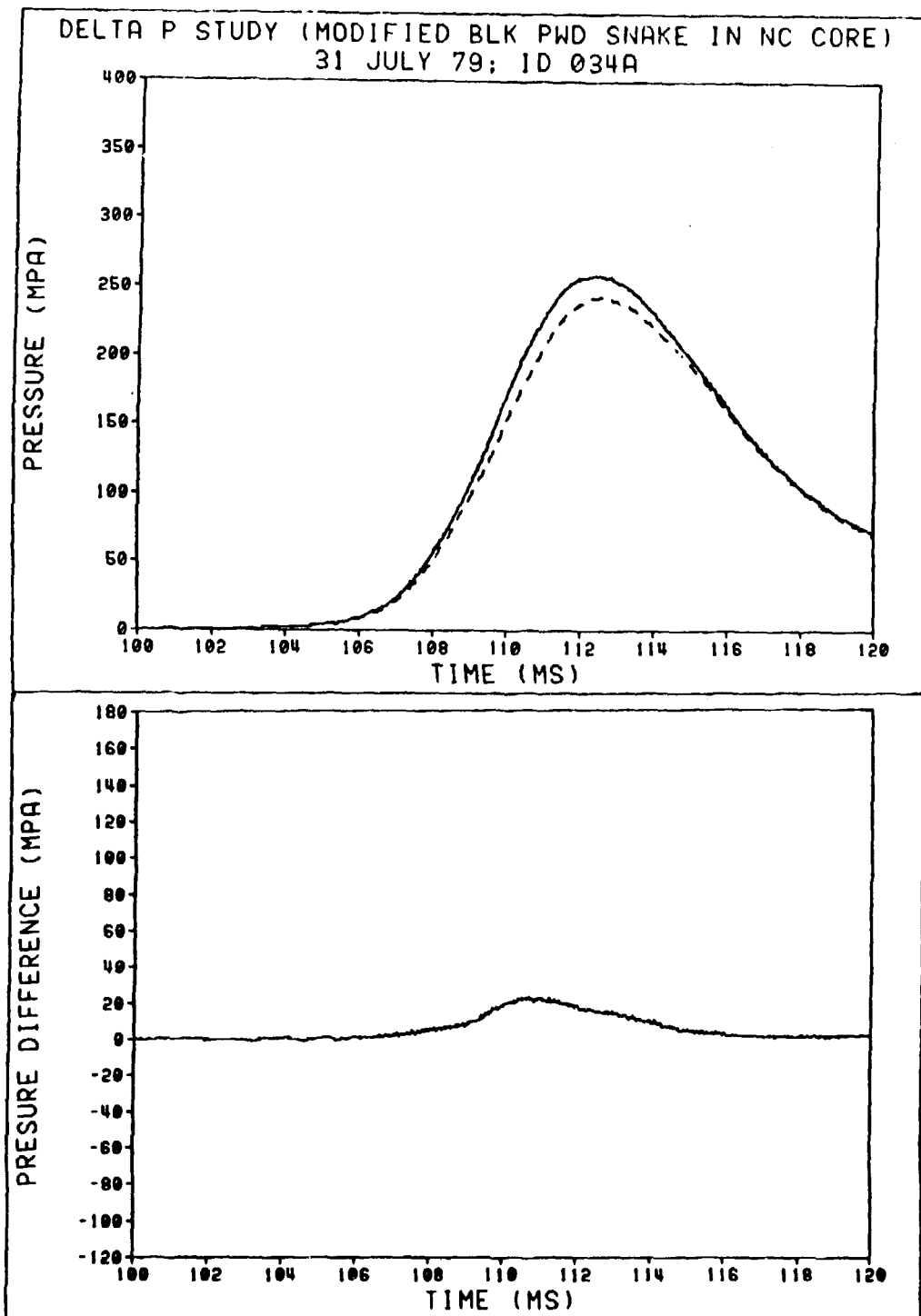


Figure 2. Experimental Pressurization Profiles for a Properly-Ignited, High-Performance Bag Charge

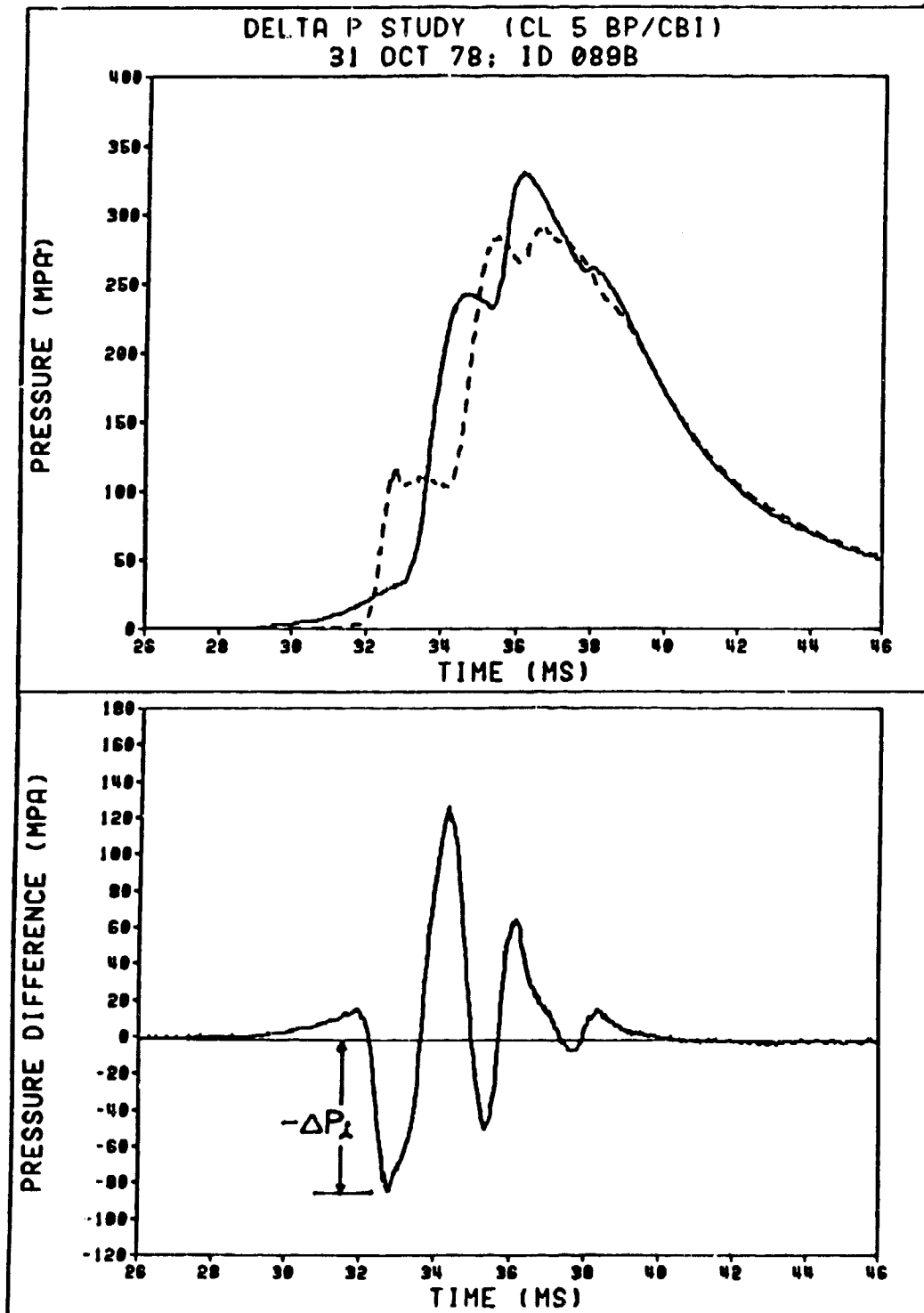
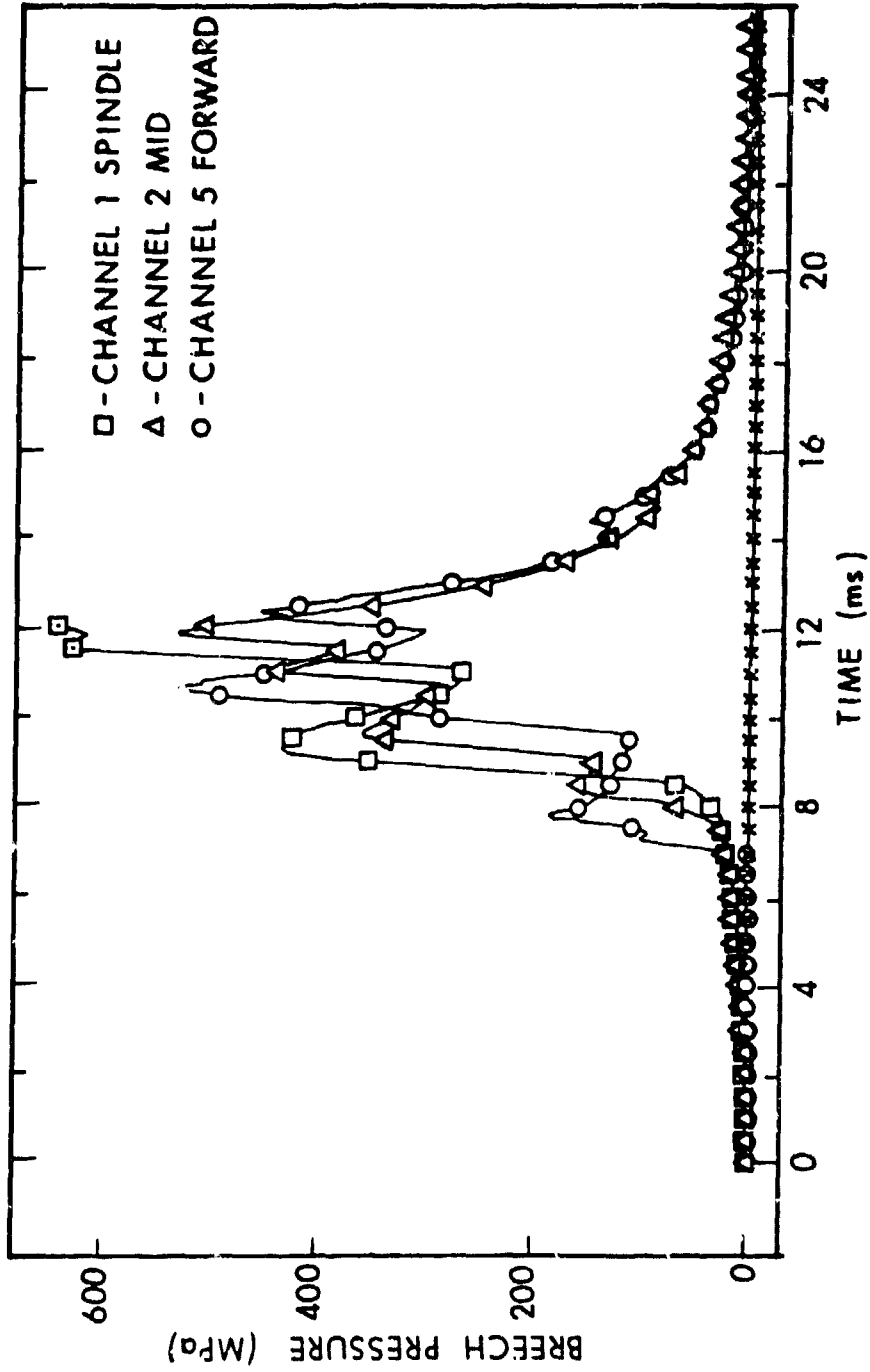


Figure 3. Experimental Pressurization Profiles Exhibiting High-Amplitude, Longitudinal Pressure Waves



APG FR P-82501

Figure 4. Induced Breachblow, 175-mm Gun

often asked to comment on safety of the charge, particularly with respect to any deleterious effects of pressure waves. While problems arising from transient loads on the projectile base (both gas- and solid-phase) associated with the presence of pressure waves are not amenable to so direct a treatment, the influence of pressure waves on maximum chamber pressure can be assessed in the following manner:

(1) Sensitivity firings are conducted to determine the relationship between $-\Delta P_i$ and maximum chamber pressure for that charge/weapon combination. Intentionally-defeated centercore igniters may be included in this series to assure that data from a localized-ignition/high-pressure-wave firing can be obtained with a reasonable number of tests. More recent assessments of base ignited charges have included sensitivity testing with special charges in which faster-burning igniter materials have been substituted for the standard material.

(2) A failure criterion is identified, usually in terms of some maximum chamber pressure, dictated most often by breech or payload failure.

(3) This failure level is reinterpreted in terms of a $-\Delta P_i$ level, determined from the sensitivity curve developed in Step (1).

(4) A sample of firing data is then obtained which is believed to be representative of "real-world" propelling charges, typical of those to be fielded for use. One or more statistical distributions are fit to these data.

(5) The probability of failure as defined in Step (3) can then be statistically determined with respect to the distribution of $-\Delta P_i$ values from Step (4).

An alternate form of this procedure is possible if the firing data described in Step (4) are available prior to sensitivity testing. Based on these data, the $-\Delta P_i$ value to be associated with the highest, acceptable probability for failure can be statistically projected, and sensitivity testing to determine the corresponding chamber pressure need not be continued beyond that point. In this fashion, while we do not necessarily determine the $-\Delta P_i$ value corresponding to the maximum-pressure failure criterion, we do ensure that this pressure limit is not exceeded at that $-\Delta P_i$ level projected to occur at a frequency equal to the highest allowable probability for failure. This alternate plan, in some cases, may significantly reduce the risk of catastrophic overpressure during sensitivity testing.

Application of the basic procedure can be demonstrated with respect to a data base available for the 175-mm, M107 Gun. The relationship between $-\Delta P_i$ and maximum chamber pressure for M86A2 (Zone 3) Charges fired in the M107 Gun, based on sensitivity firings, is presented in Figure 5. A $-\Delta P_i$ failure criterion can also be identified on this curve,

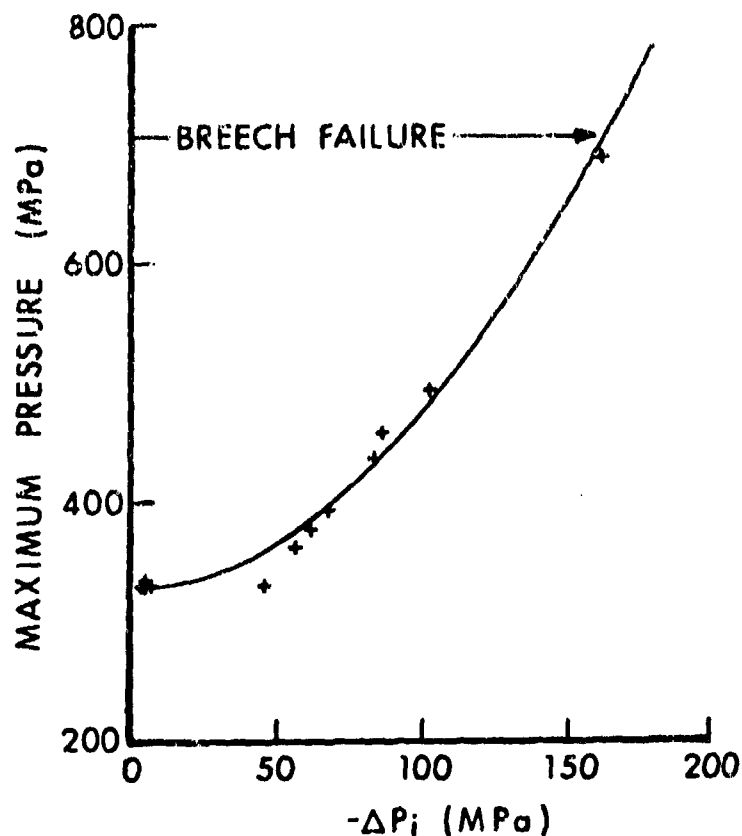


Figure 5. Sensitivity of Maximum Chamber Pressure to Pressure Waves; 175-mm, M107 Gun; M86A2 (Zone 3) Propelling Charge

corresponding to a known breech pressure failure level. Figure 6 then presents the cumulative distribution of $-\Delta P_i$ values for a data base considered to represent a typical population of "real-world" charges. The probability of achieving the $-\Delta P_i$ failure criterion, as determined using Kolmogorov-Smirnov statistics and two different population distribution functions, is presented in Figure 7. The prediction of one failure in about half a million firings compares quite favorably with empirical data of half a dozen breechblows in some two and one-half million firings to date. This agreement, although satisfying, must be considered somewhat fortuitous.

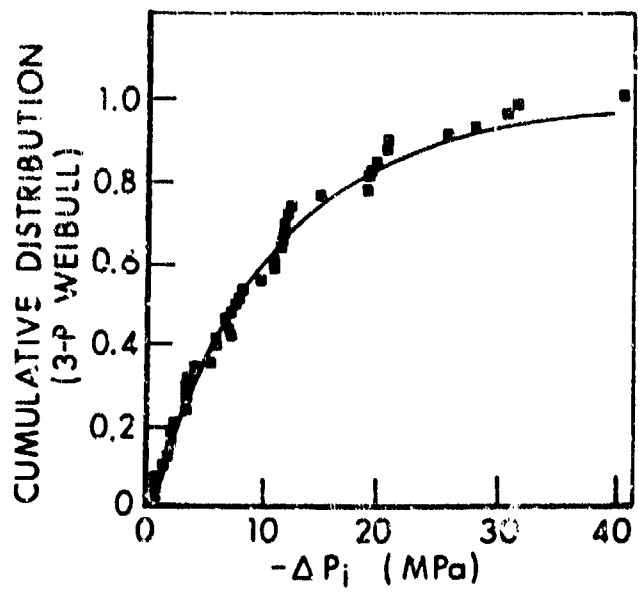


Figure 6. Cumulative Distribution of $-\Delta P_i$; 175-mm, M107 Gun; M86A2 (Zone 3) Propelling Charge

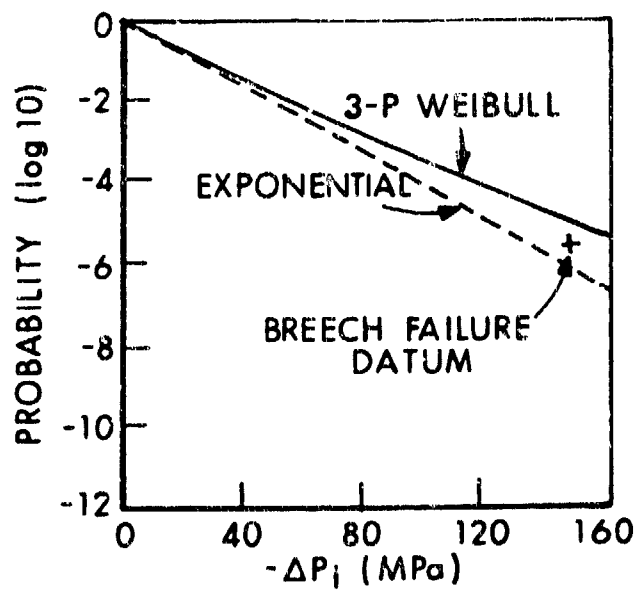


Figure 7. Projected Probability of $-\Delta P_i$; 175-mm, M107 Gun; M86A2 (Zone 3) Propelling Charge

B. Inadequacies Of The Current Procedure

As mentioned earlier, the subject of the uniqueness of the $-\Delta P_i$ versus P_{max} relationship which constitutes the sensitivity curve has been discussed elsewhere⁶. In this report, we confine our discussion to problems arising from use of $-\Delta P_i$ as the specific indicator of the severity of longitudinal pressure waves present in the gun chamber. Certainly, many studies, both theoretical and experimental, of the interior ballistic environment over the past decade have employed quite effectively this parameter in particular and the entire pressure-difference-versus-time profile in general to characterize the pressure waves in guns. A partial listing of such work has been provided recently by May and Horst⁷. Moreover, our current understanding of such pressure waves as a consequence of an axially-localized ignition stimulus applied to an often nonuniform distribution of propellant in the gun chamber tends to provide a clear physical basis for some type of quantifier which reflects the axial nonuniformity of chamber pressure immediately following the ignition event. Again, the initial reverse pressure difference, $-\Delta P_i$, appears to be a proper choice. Use of this parameter has provided the propelling charge modeler, designer, and diagnostician alike with a valuable measure of ballistic acceptability facilitating significant advances in our understanding of interior ballistics phenomenology. Nevertheless, it is to problems associated with use of this parameter that we address ourselves in the remainder of this report.

Let us proceed by considering the four interior ballistic environments as depicted by a series of pressure-difference-versus-time profiles, all based on experimental data and reproduced on the same scale in Figure 8. Few observers would not agree that this figure depicts a sequence of environments characterized by ever-increasing pressure waves. Consider first Curves (a) and (b). While the former exhibits virtually no hint of pressure waves, the latter reveals clearly defined modulation associated with the presence of longitudinal pressure waves traveling between projectile base and the breech end of the chamber. However, by established procedures, a $-\Delta P_i$ value of zero would be arbitrarily assigned to both curves. This result is both physically and procedurally undesirable.

The undesirability of this situation with respect to providing a quantitative physical description of pressure waves is obvious; its effects on the procedural analysis of the safety implications of pressure waves, however, requires some explanation. Recalling our description of the current safety-assessment procedure with respect to pressure waves, we note the necessity of providing a statistical description of a sample

⁷ I.W. May and A.W. Horst, "Charge Design Considerations and Their Effect on Pressure Waves in Guns," *Interior Ballistics of Guns*, H. Krier and M. Summerfield, Editors, *Progress in Astronautics and Aeronautics*, Vol. 66, AIAA, New York, NY, 1979, pp. 197-227.

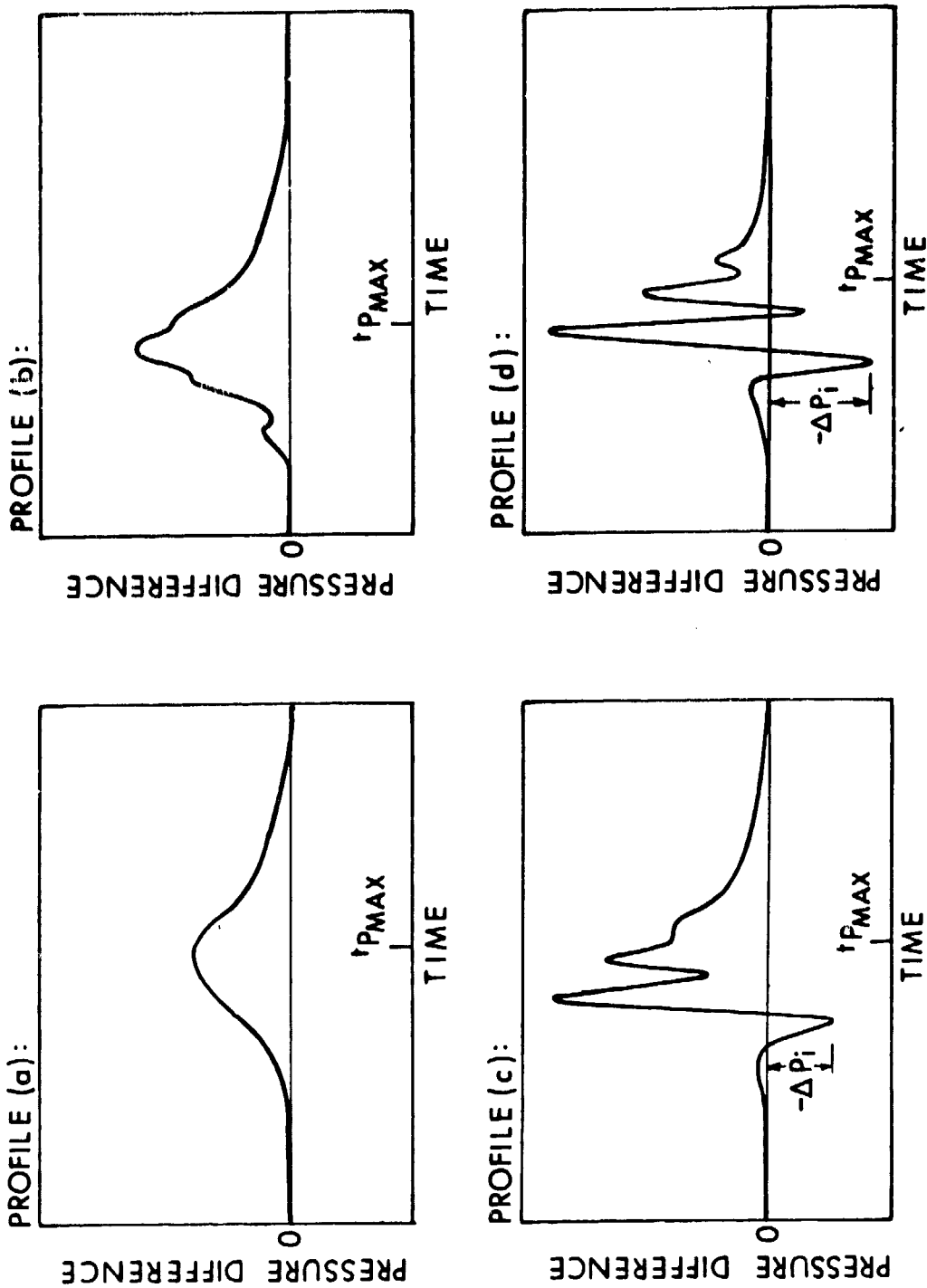


Figure 8. Profiles of Pressure Difference (Breech Minus Forward) Versus Time

population of $-\Delta P_i$ values determined experimentally. An artificial preponderance of zeros can strongly bias the fit at the low end of the spectrum of $-\Delta P_i$ values and seriously degrade our confidence in the fit at the high end, rendering extrapolations to some even higher failure level of questionable worth. This problem is depicted in Figure 9, which displays the result of an attempt to fit several statistical distributions to a body of $-\Delta P_i$ data for 155-mm, M203 Propelling Charges which included numerous zeros. The assurance level at which this best-fit distribution would have met the null hypothesis using a Kolmogorov-Smirnov test was only 0.11. The deletion of zeros from these data significantly improved the fit, but the data base was then no longer a complete representation of the experimental results of interest.

At the other end of the spectrum, let us now consider Curves (c) and (d) of Figure 8. Not only are the levels of $-\Delta P_i$ greater in these views, but the overall levels of pressurization in the gun chamber, not shown in the figure, at the time of $-\Delta P_i$ have significantly increased. If we assume the presence of a linear calibration error somewhere in one of the instrumentation data channels (forward and rear pressure versus time), not only will the absolute error in $-\Delta P_i$ similarly suffer a linear increase, this discrepancy will reflect the percentage error of the measured chamber pressures themselves, not just of the difference in forward and rear pressures. Figure 10 demonstrates that gage calibration errors of 10% can impact the value for $-\Delta P_i$ in the experimentally based curve depicted in Figure 8(c) by as much as 50%. Depending on the magnitude of the chamber pressure at the time of $-\Delta P_i$, even greater errors are possible, influencing not only the goodness-of-fit problem discussed in reference to Curves 8(a) and (b), but also impacting the generation of the $-\Delta P_i$ versus P_{\max} curve itself, the most fundamental aspect of the existing procedure for assessment of the influence of pressure waves on safety.

C. Consideration of Other Indicators

Since recording pressure-difference-versus-time data is an established procedure and a great quantity of such data is already in existence, we felt it reasonable to consider first the use of alternative indicators for the magnitude of pressure waves that might be extracted from this profile. Such quantities as peak-to-peak (or inflection-to-inflection for low-magnitude waves) wave amplitude and the ratio of successive peak-to-peak amplitudes to indicate growth or damping factors are obvious choices.

Application of this approach has been evaluated in reference to a large body of experimentally measured pressure-difference-versus-time profiles discussed in detail in a previous work⁶. The following quantities, defined in Figure 11, were considered: $-\Delta P_1$ (equivalent to $-\Delta P_i$ except that positive values rather than zeros are assigned when this minimum falls above the baseline); $(+\Delta P_1+-\Delta P_1)$; $(-\Delta P_1++\Delta P_2)$; $(+\Delta P_2+-\Delta P_2)$; $(-\Delta P_2++\Delta P_3)$; $(-\Delta P_1++\Delta P_2)/(+\Delta P_2+-\Delta P_2)$; and $(+\Delta P_2+-\Delta P_2)/(-\Delta P_2++\Delta P_3)$. Since

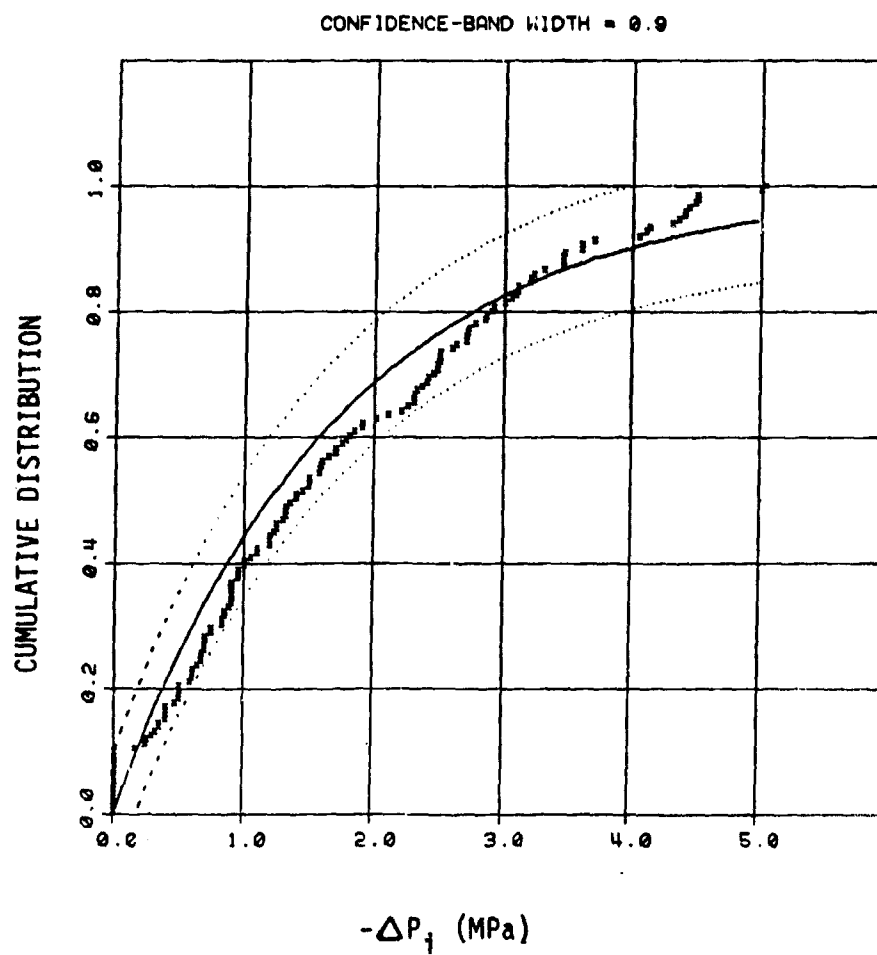


Figure 9. Best-Fit Cumulative Distribution for Population of $-\Delta P_1$
Data Including Assigned Zeros

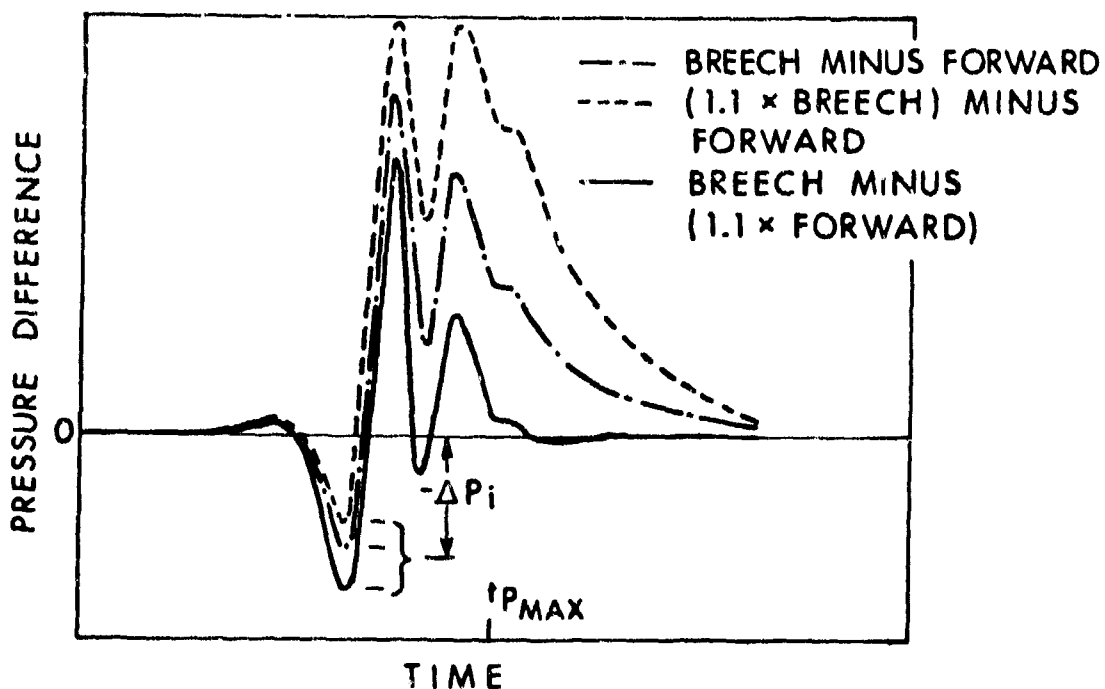


Figure 10. Effect of 10% Linear Calibration Errors on Recorded Pressure-Difference-Versus-Time Data of Figure 8(c)

these data had been generated using propelling charges intentionally altered in a variety of different ways to promote the formation of pressure waves, a good statistical fit with the various probability distribution functions was not to be expected. However, the relationship of each of these parameters to maximum chamber pressure for the subject body of data can be examined in Figure 12.

The relationship which is best approximated by a quadratic fit using the method of least squares is that of $(-\Delta P_1 \leftrightarrow \Delta P_2)$ versus P_{max} . The amplitude factor $(-\Delta P_1 \leftrightarrow \Delta P_2)$ may be physically related to the driving amplitude of the longitudinal pressure wave over its first transit of the chamber after conclusion of the ignition/flamespread event. While $-\Delta P_1$ (or $-\Delta P_i$ as termed earlier) is really the first indicator of this driving pressure gradient, its shortcomings have already been noted; use of $-\Delta P_2$ alone is even more susceptible to large measurement errors which

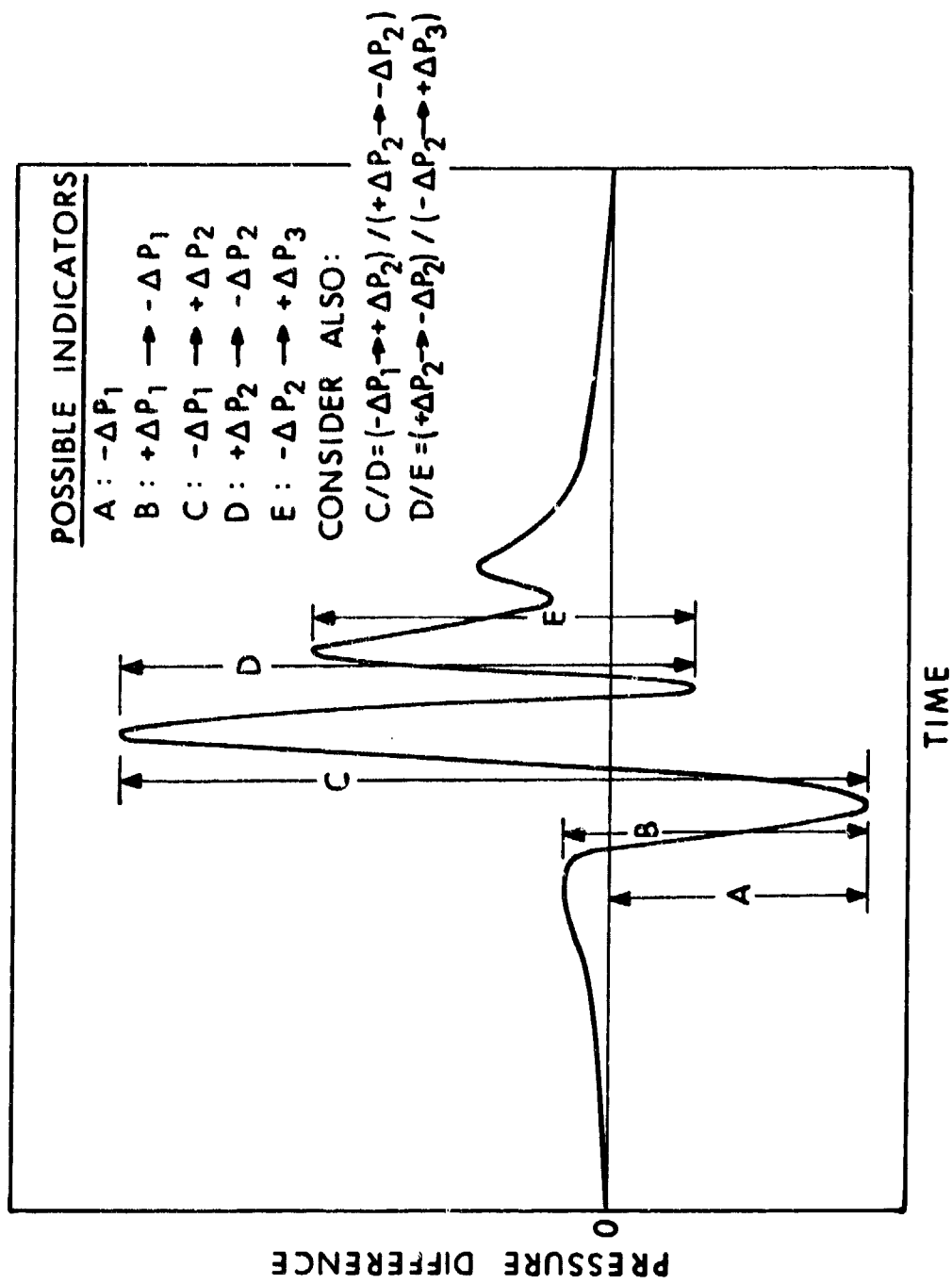


Figure 11. Schematic Definitions of Alternative Indicators of Pressure-Wave Magnitude

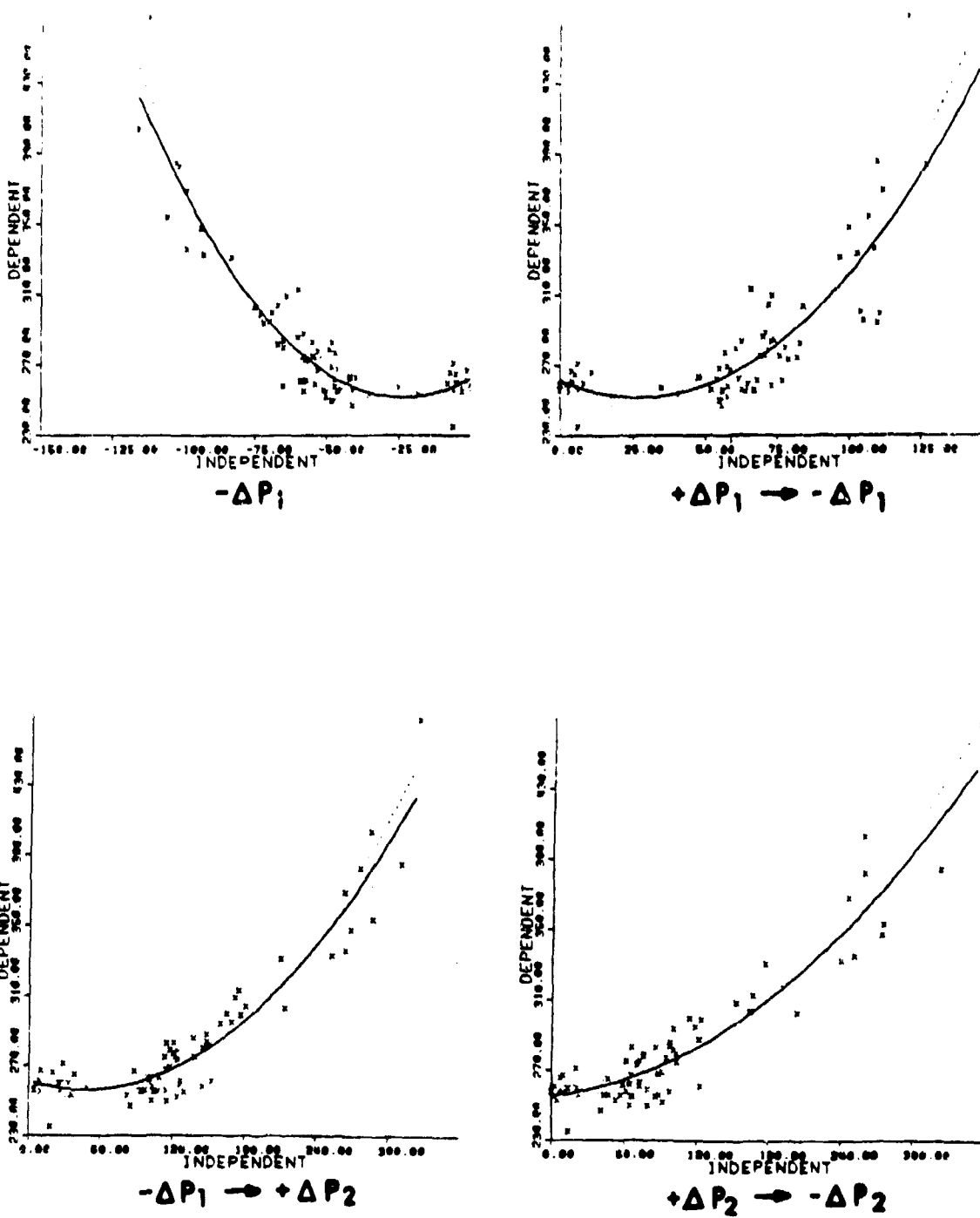
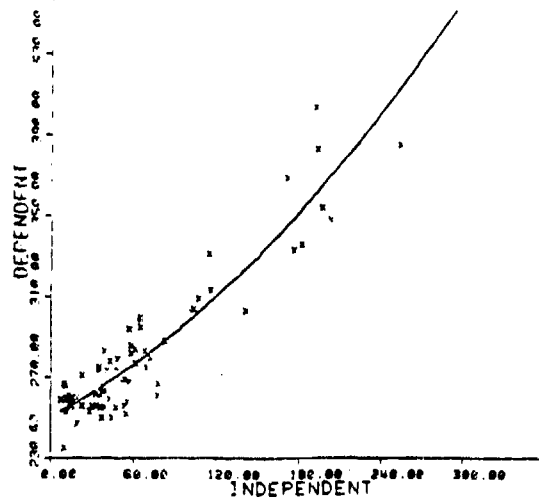
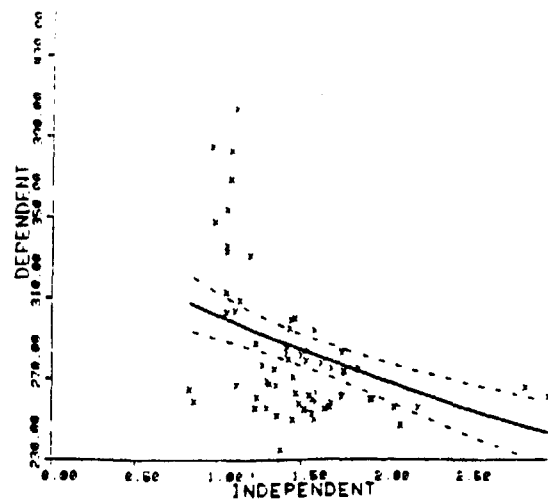


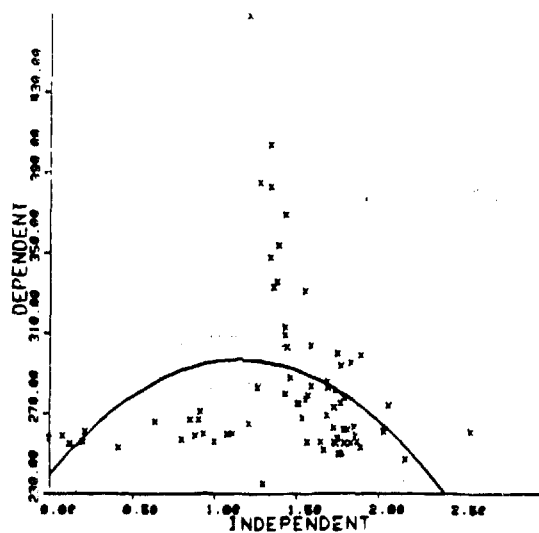
Figure 12. Plots of Maximum Chamber Pressure Versus Alternative Indicators of Figure 11 for a 155-mm, Special-Charge Data Base



$$-\Delta P_2 \rightarrow +\Delta P_3$$



$$(-\Delta P_1 \rightarrow +\Delta P_2) / (+\Delta P_2 \rightarrow -\Delta P_2)$$



$$(+\Delta P_2 \rightarrow -\Delta P_2) / (-\Delta P_2 \rightarrow +\Delta P_3)$$

Figure 12 (continued). Plots of Maximum Chamber Pressure Versus Alternative Indicators of Figure 11 for a 155-mm, Special-Charge Data Base

may be related linearly to the chamber pressure, typically much greater by the time of the occurrence of $-\Delta P_2$. On the other hand, the value for $+\Delta P_1$ appears to reflect the combined effect of local combustion at the base of the charge (basepad and perhaps first propellant combustion) and the availability of local free volume. While very large values of $+\Delta P_1$ were usually followed by large pressure-wave amplitudes, large pressure-wave amplitudes were not always preceded by a large value of $+\Delta P_1$. Apparently, its failure to reflect the interaction of gas production rates with overall bed permeability render it inadequate as an indicator of subsequent wave growth. The indicators based on the ratio of subsequent amplitudes apparently fail because of the occasional presence of undamped, low-amplitude pressure waves which have no effect on chamber pressure, while a similar persistence of high-amplitude waves almost always leads to increases in maximum chamber pressure.

Returning to the most successful of the above indicators, $(-\Delta P_1 \rightarrow \Delta P_2)$, we find that while it should remove the problem associated with non-physical zeros experienced with $-\Delta P_1$, the location and magnitude of the $+\Delta P_2$ inflection required to assign a value to $(-\Delta P_1 \rightarrow \Delta P_2)$ is not always unambiguous, particularly for low-amplitude pressure waves. Thus, the new measure suffers a similar failure to that which it is proposed to replace. Further, the level of the $+\Delta P_2$ inflection is subject to the same calibration error, increasing with overall chamber pressure, as discussed previously. While some improvement is apparently offered by this indicator, clearly a better approach is needed.

D. A New Approach: Removal Of The Classical Gradient

General. One approach to this problem involves removal, by some means yet undefined, of what may be thought of as the classical pressure gradient of Lagrange⁸ from the pressure-difference-versus-time profile, leaving only that part of the signal which results from the presence of longitudinal pressure waves. Such a procedure may be thought of as being somewhat analogous to the detection of an intelligent audio frequency signal from a radio frequency carrier, though in our case the intelligence we are interested in is higher in frequency than its Lagrangian carrier.

For our purposes, such a technique offers several obvious advantages. Consider the schematic offered in Figure 13. Upon removal of that part of the pressure-difference signal associated simply with motion of the projectile down the tube, the remaining signal should reflect only perturbations to the classical pressure gradient, now displayed as variations about the zero baseline. Hence, the new $-\Delta P_i$ will be zero only if there is truly no pressure-wave content in the recorded pressure-difference signal. Moreover, the impact of linear calibration errors

⁸J. Corner, *Theory of the Interior Ballistics of Guns*, John Wiley & Sons, Inc., New York, NY, 1950, pp 339-342.

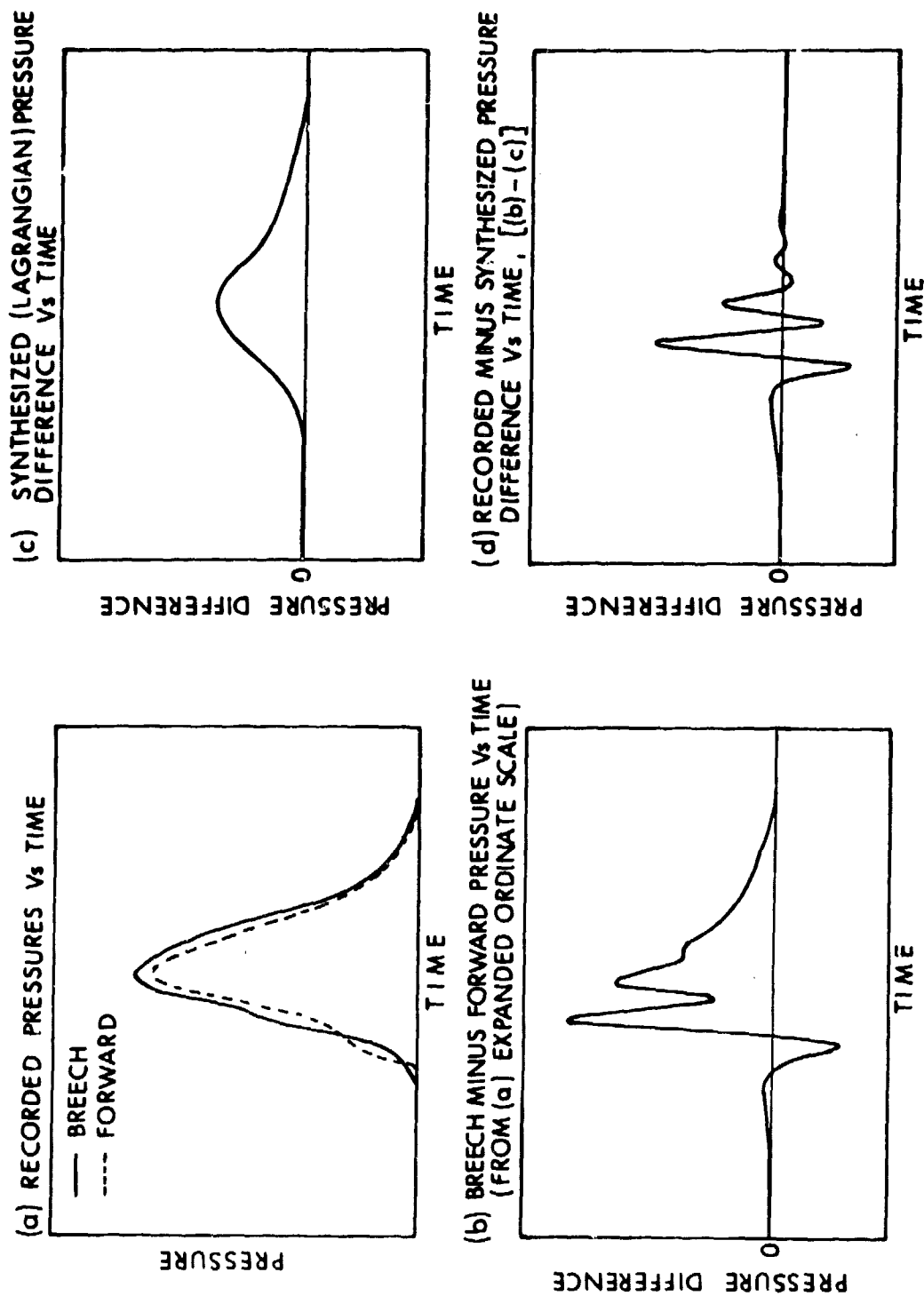


Figure 13. Conceptualized Scheme for Extracting Longitudinal Pressure-Wave Signal

will be limited to that percentage error of the magnitude of the pressure difference rather than of the possibly much greater chamber pressure. This second improvement should allow use of indicators based on events occurring later in the interior ballistic cycle, such as second and third maxima and minima or perhaps ratios of these quantities, should they be motivated by other considerations. To proceed further, however, we must address techniques for extraction of the desired signal from commonly recorded multiple-station pressure-time data.

Simulated Pressure-Difference Profiles. The first attempt made to perform this extraction involved the generation of approximate, ideal pressure-difference-versus-time curves through the use of a classical, lumped-parameter, interior ballistics code. Such codes calculate an interior ballistic trajectory under the assumption of a "well-stirred" gun chamber characterized by uniform thermodynamic parameters at any instant in time. An idealized pressure gradient, such as the Lagrangian (based on a uniform density and a linear velocity profile for the gas), is superimposed on the solution only to provide a more accurate description of the force profile acting on the base of the projectile. One such computerized model, based on the earlier work of Baer and Frankle⁹, was modified to monitor and display pressure differences as a function of time for any two arbitrary axial locations in the gun chamber/bore. Resulting ($\Delta P, t$) pairs were then supplied as input to a program which fit the data to a variety of simple functions, such as $\Delta P = at^{be^{ct}}$, via the method of least squares. The functional description so obtained facilitated removal of the idealized, classical gradient from the measured pressure-difference-versus-time profile. Unfortunately, because of the simplifying assumptions of uniform ignition of the propellant bed and the accompanying absence of any pressure gradient until the projectile starts to move, satisfactory synthetic representations of the classical pressure gradient which closely approximated experimental data for unperturbed environments, particularly for the early portion of the cycle, could not be obtained.

Approximation Using Cubic Splines. A second and similarly unsuccessful attempt to generate a useful, synthetic pressure gradient involved the approximation of experimental pressure-difference-versus-time profiles with a standard cubic spline curve defined by up to 26 user-selectable points. By following this procedure, one could easily approximate a desired profile. The problem, however, was then one of determining just what was the desired curve. Several reasonable schemes were applied to typical problems of interest, but the sensitivity of results to arbitrarily-imposed, systematic differences in procedure was discouraging (see Figure 14). Further, lack of across-the-board success

⁹P.G. Baer and J.M. Frankle, "The Simulation of Interior Ballistic Performance of Guns by Digital Computer Program." BRL R 1183, Ballistic Research Laboratories, Aberdeen Proving Ground, MD, December 1962. (AD #299980)

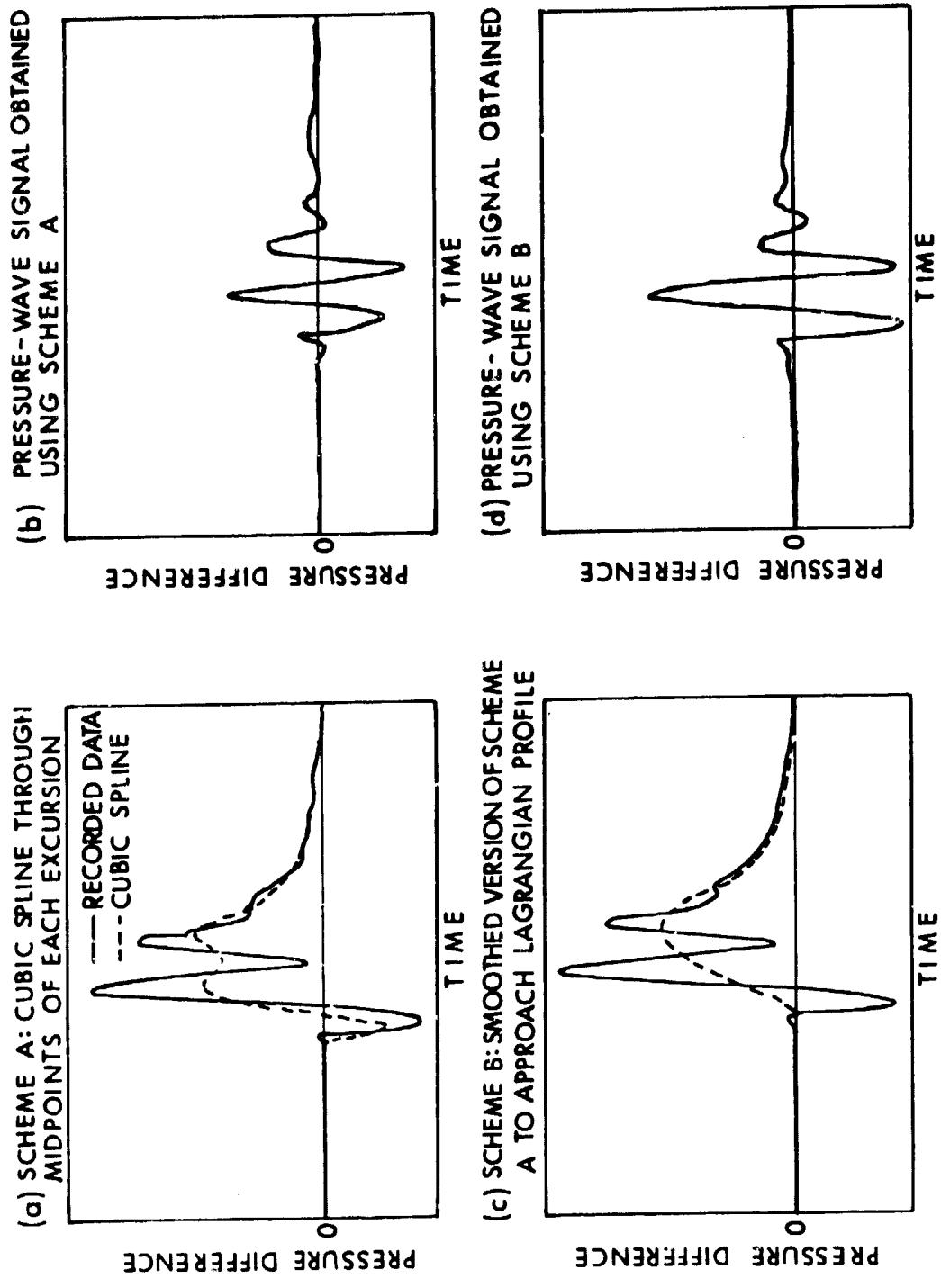


Figure 14. Sensitivity of Detected Pressure-Wave Signal to Alternative Cubic-Spline Techniques for Removal of Lagrangian Profile

for even a small sampling of typical problems with any one procedural scheme for creating the appropriate curve led to abandonment of the technique.

Fourier-Analysis/Digital-Filtering Techniques. As the presence of a longitudinal pressure wave traveling between the breech closure and projectile base is indeed a periodic physical phenomenon (albeit that the period of transit changes with the position of the projectile and thermodynamic and physical states of the propellant/gas mixture), analysis of the pressure-difference signal into component signal frequencies appeared to offer promise. In particular, application of the fast Fourier transform for examination of various features of interest followed by the application of various digital filters for isolation of particular component events was beginning to yield useful results in related ballistic problems¹⁰.

To this end, a computer program was written to process digitized records of experimental pressure-versus-time and pressure-difference-versus-time data using established decomposition and filtering routines in either an interactively-guided or automatic manner. The program is in reality the synthesis of two previous works, coupled and controlled via executive and file-manipulation software. Drawn from IMSL Library 3¹¹ is a subroutine known as FFTR, which computes the fast Fourier transform of a real data sequence - in this case, the digitally-recorded, experimental pressure-difference-versus-time signal. Based on a physical understanding of the problem, the user may then wish to select a frequency domain of interest for further study. McClellan, Parks, and Rabiner had previously written a computer program to establish optimal design parameters for digital filter circuits¹². Their work was modified by Walbert¹³ and a subroutine was added for interactive filter design. Additional algorithms for the application of digital filters to time

¹⁰ A.A. Juhasz, I.W. May, W.P. Aungst, and F.R. Lynn, *Combustion Diagnostics of Very High Burning Rate Propellants*, "17th JANNAF Combustion Meeting, CPIA Publication 329, Vol. 2, pp. 209-240, November 1980.

¹¹ "Subroutine FFTR, Library 3," *International Mathematical and Statistical Libraries, Inc., Sixth Edition, Houston, TX, July 1977.*

¹² J.H. McClellan, T.W. Parks, and L.R. Rabiner, "A Computer Program for Designing Optimum FIR Linear Phase Digital Filters," *IEEE Trans. on Audio and Electroacoustics*, AU-21 (6), 1973, pp 506-526.

¹³ J.N. Walbert, "Computer Algorithms for the Design and Implementation of Linear Phase Finite Impulse Response Digital Filters," *Ballistic Research Laboratory, USA ARRADCOM, Aberdeen Proving Ground, MD, (report in preparation).*

series were developed¹⁴ to allow isolation of various frequency components for further analysis. In the problem of interest to us in this study, the selection may be based either on a quantitative analysis to determine pressure-wave transit frequencies from physical dimensions and wave propagation velocities or on a visual inspection of the frequency power spectrum to identify the frequency domain of interest.

A conceptualized application of this approach is provided in Figure 15. In actuality, there exist a number of potential schemes to conduct the desired filtering, some of which are depicted in Figure 16. The proper selection for a given application will depend on a number of factors, such as data density, number of points in the filter, and frequency domain of the desired portion of the signal. Ideally one wants a narrow transition bandwidth at the cutoff frequencies but a very flat passband (i.e. low ripple), as shown in Figure 17. A thorough analysis of the influence of all available data-digitization and filter-design parameters has not yet been performed. Rather, we have limited ourselves to a feasibility study, the purpose of which has been to determine the applicability of this technique to the problem of pressure-wave analysis. To facilitate accomplishment of this goal, we selected, after only cursory examination of several alternatives, a scheme involving multiple application of a bandpass filter. This choice rendered trivial the selection of cutoff frequencies, and, more importantly, significantly reduced the effective transition bandwidth (see Figure 18).

The next task was to determine the applicability of this technique to a broad class of ballistic environments with respect to pressure waves. Shown in Figures 19 through 25 are the results of double application of a common bandpass filter to seven different experimental pressure-difference-versus-time profiles, all obtained from firings in a 155-mm howitzer but exhibiting a wide range of pressure-wave amplitudes. Power-spectral-density profiles for each of the unfiltered signals reveal significant high-amplitude content in the 200-600-Hz range. Further, for the portion of the ballistic cycle of interest, the physical parameters (e.g., breech to projectile base distance, ~ 90 -120 cm; and gas temperatures, ~ 2500 -3000 K) suggest pressure-wave transit times with corresponding frequencies within this same range (~ 400 -500 Hz). Actual filter-design parameters were selected to provide a flat passband over this range of frequencies within the limits imposed by the available software and digitized data records. No significant problems such as baseline shifts resulting from the low-frequency component of the main pressure-time event are seen to persist after the second application of the bandpass filter. That such a successful filter can be so easily designed for all

¹⁴J.N. Walbert, "Application of Digital Filters and the Fourier Transform to the Analysis of Ballistic Data, "Ballistic Research Laboratory, USA ARADCOM, APG, MD (report in preparation).

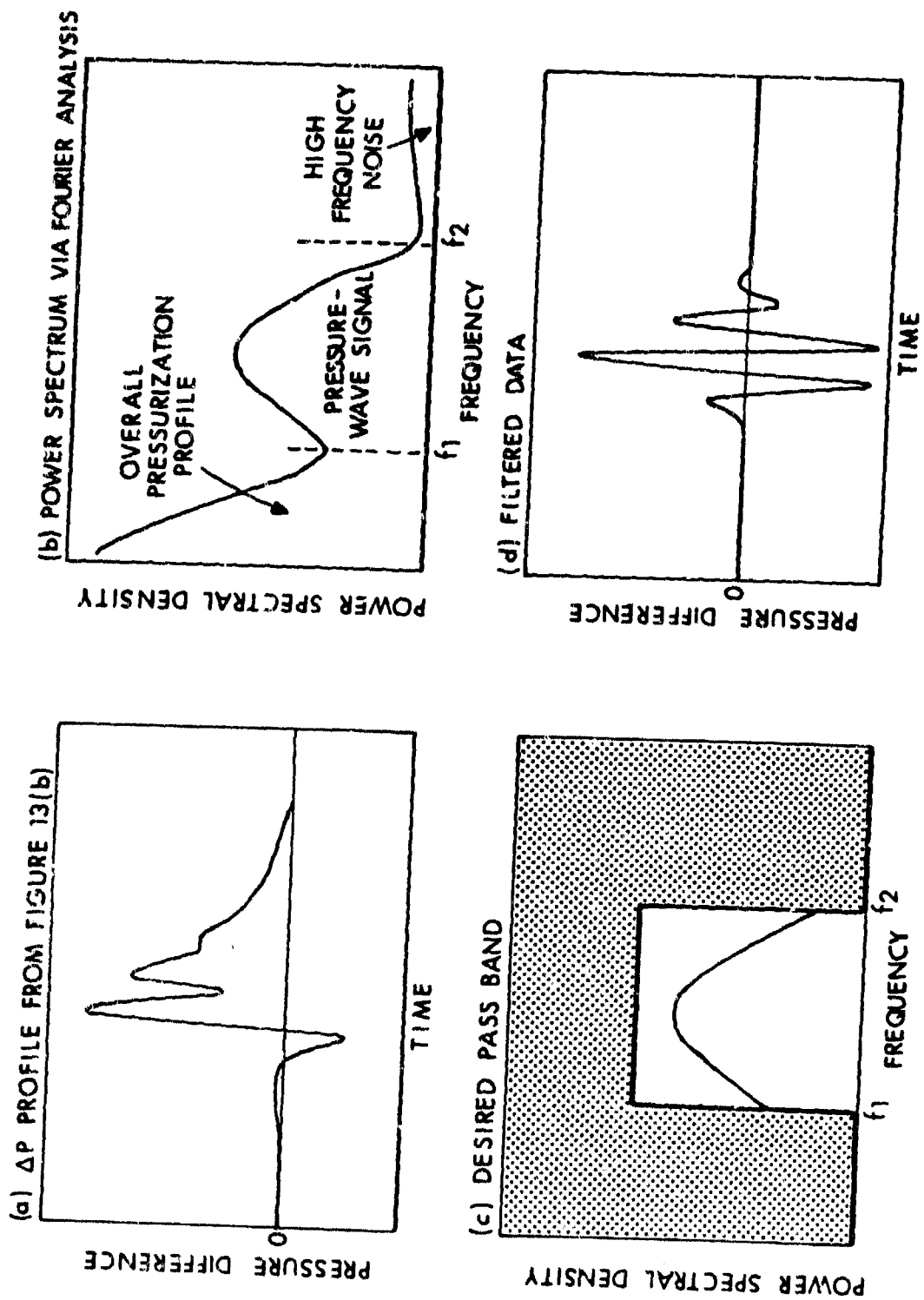


Figure 15. Conceptualized Application of Fourier-Analysis/Digital-Filtering Technique

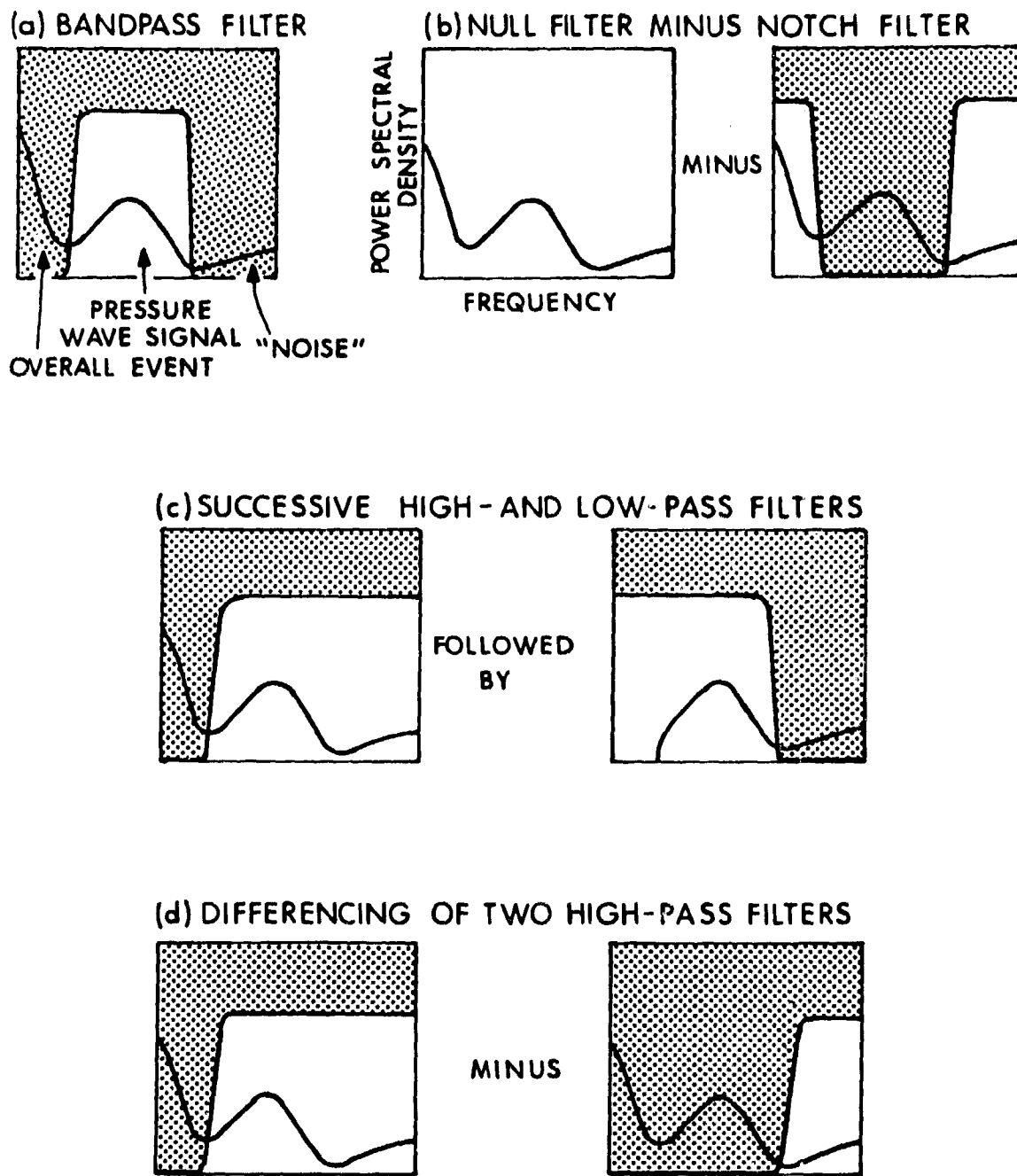


Figure 16. Alternative Schemes for Application of Digital Filters

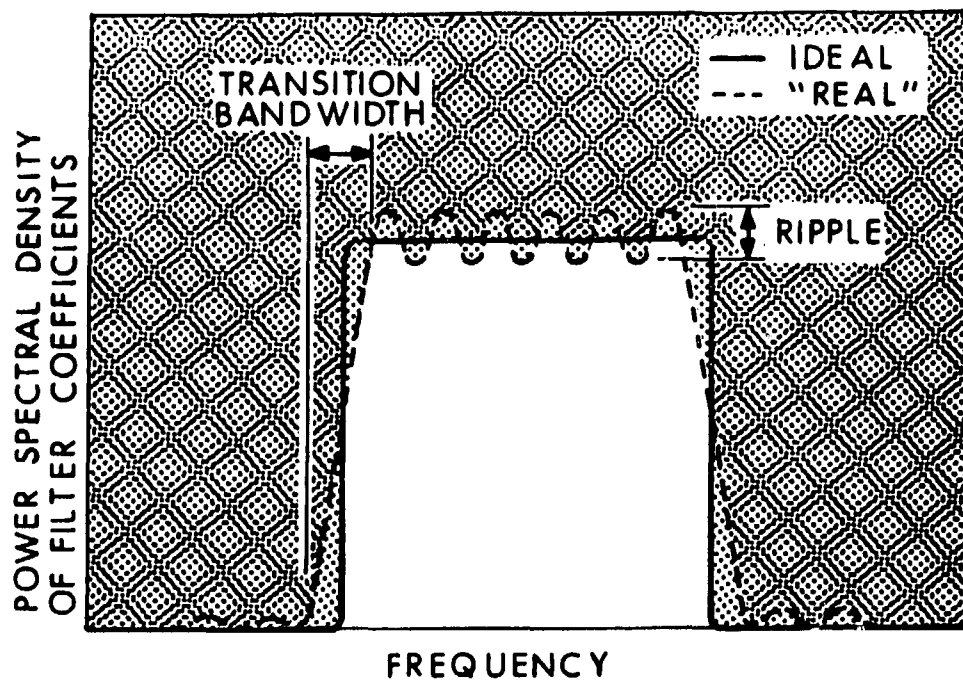


Figure 17. Character of Digital Bandpass Filter

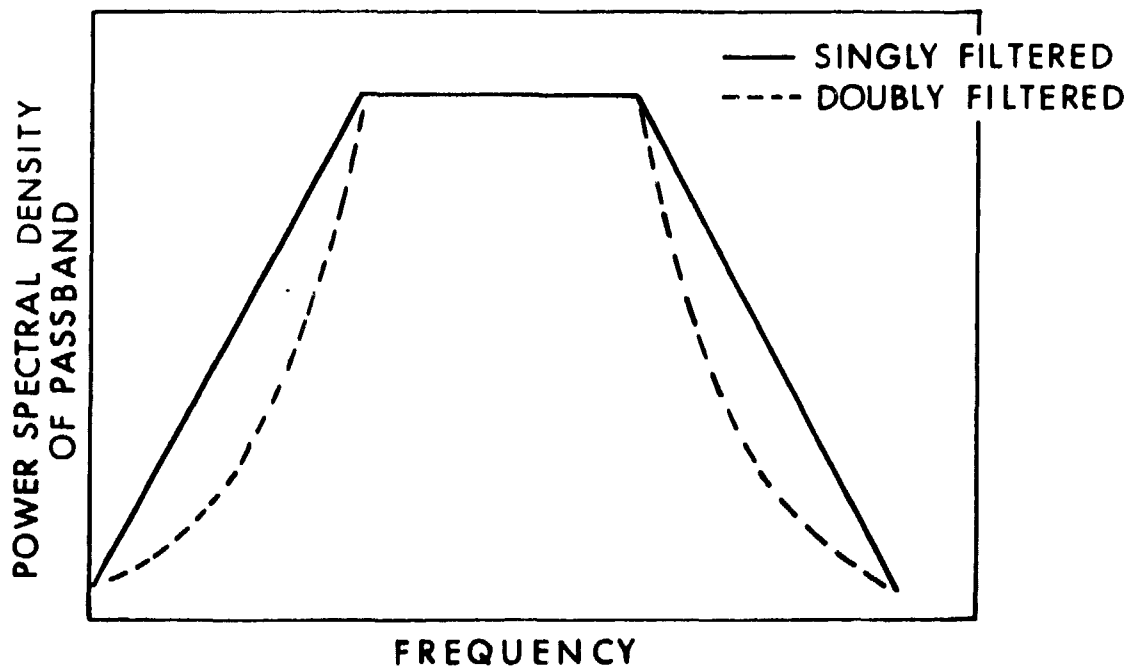


Figure 18. Multiple Application of Bandpass Filter

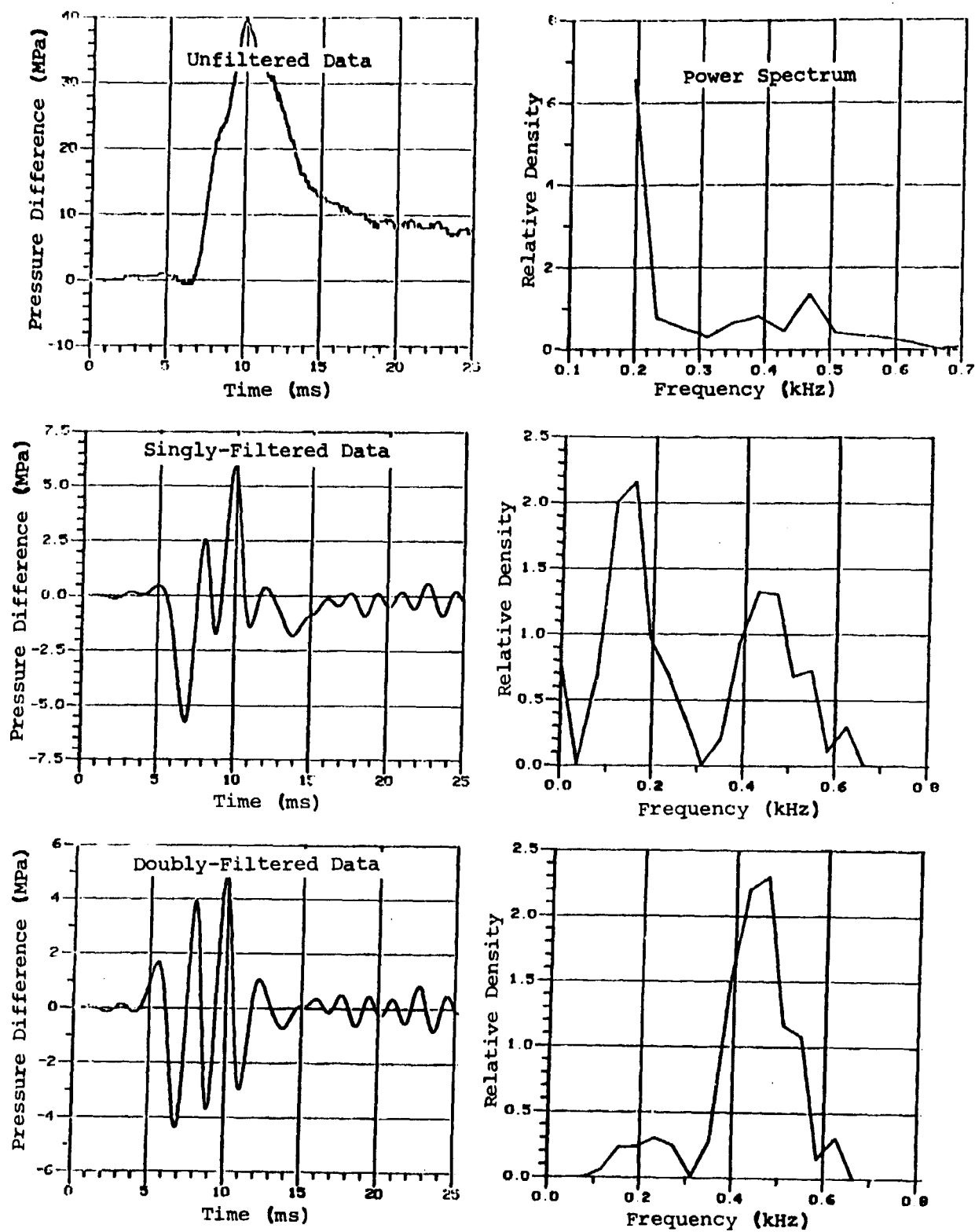


Figure 19. Application of Fourier-Analysis/Digital-Bandpass-Filtering Technique to Experimental 155-mm Howitzer Firing Data - A

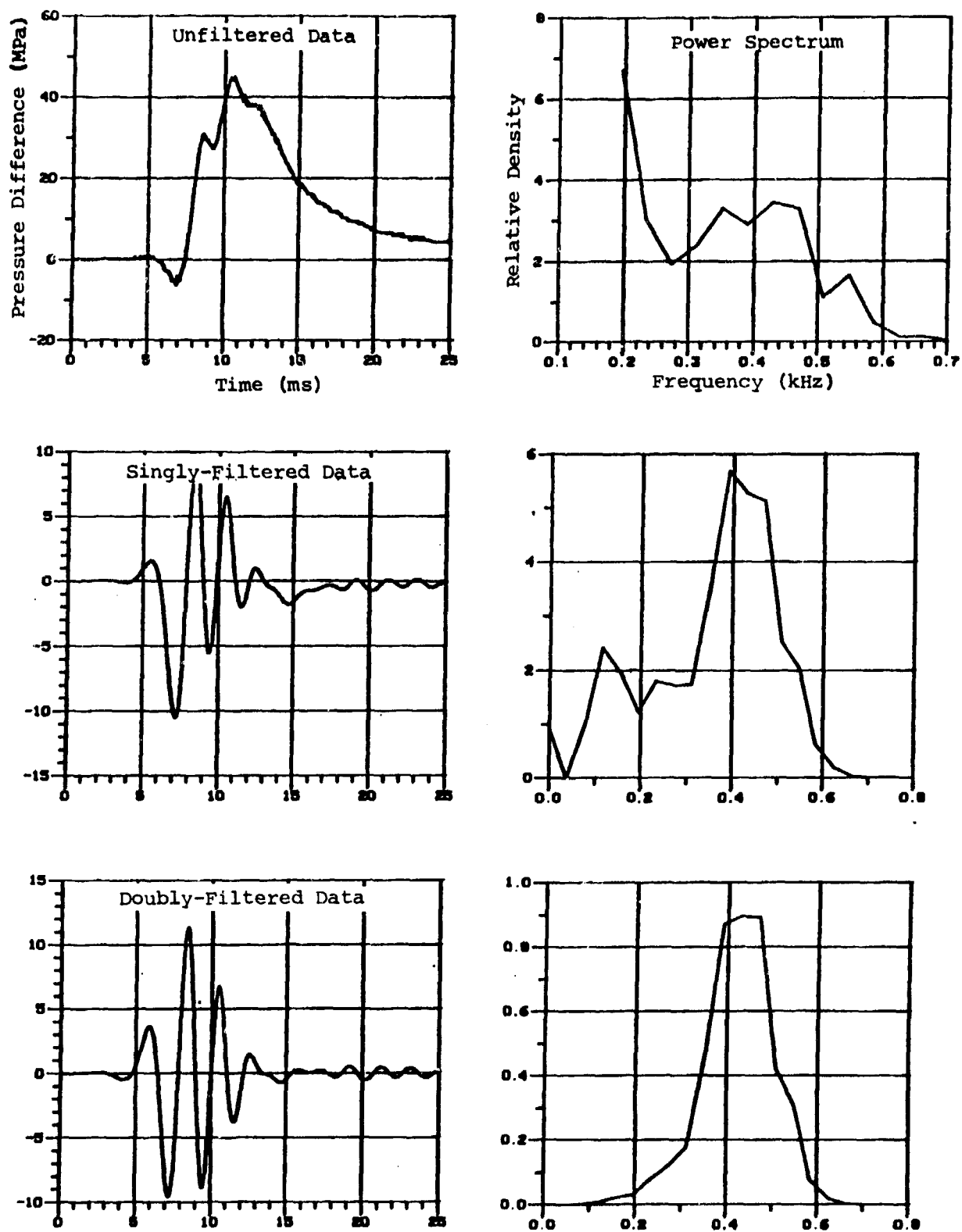


Figure 20. Application of Fourier-Analysis/Digital-Bandpass-Filtering Technique to Experimental 155-mm Howitzer Firing Data - B

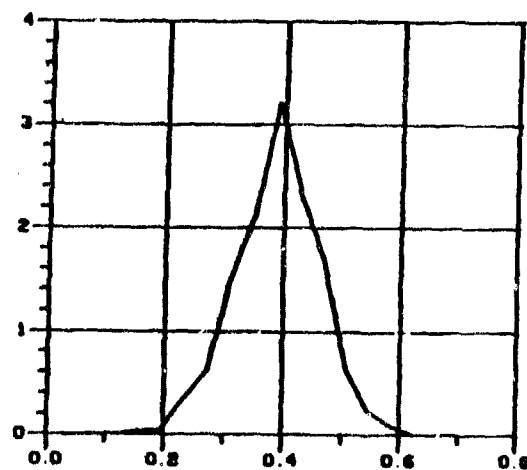
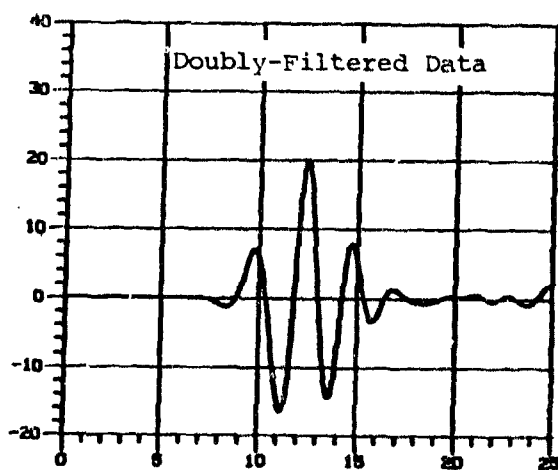
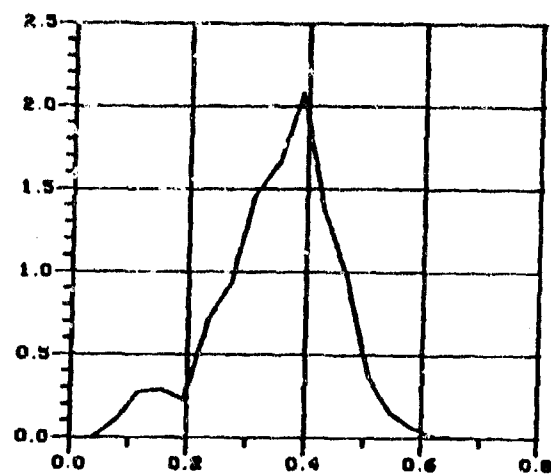
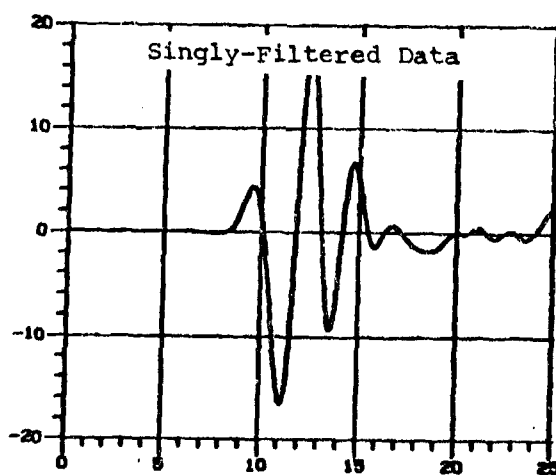
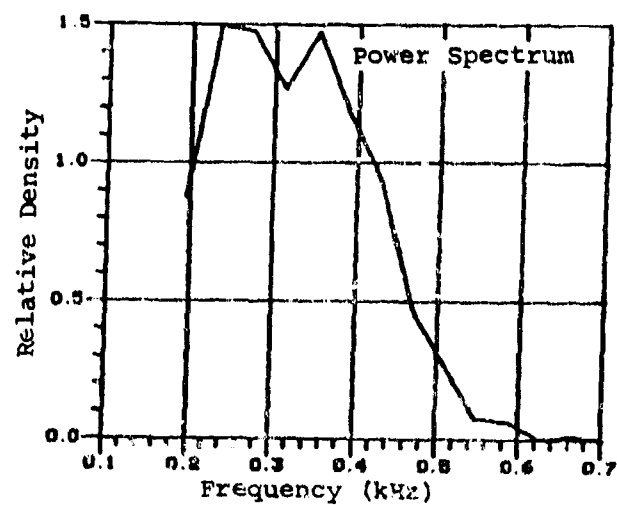
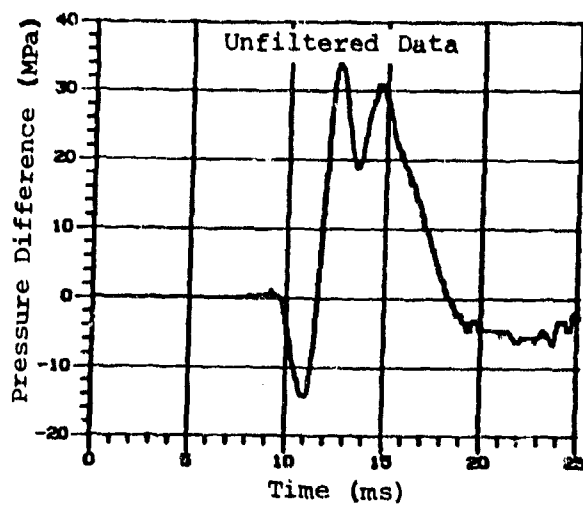


Figure 21. Application of Fourier-Analysis/Digital-Bandpass-Filtering Technique to Experimental 155-mm Howitzer Firing Data - C

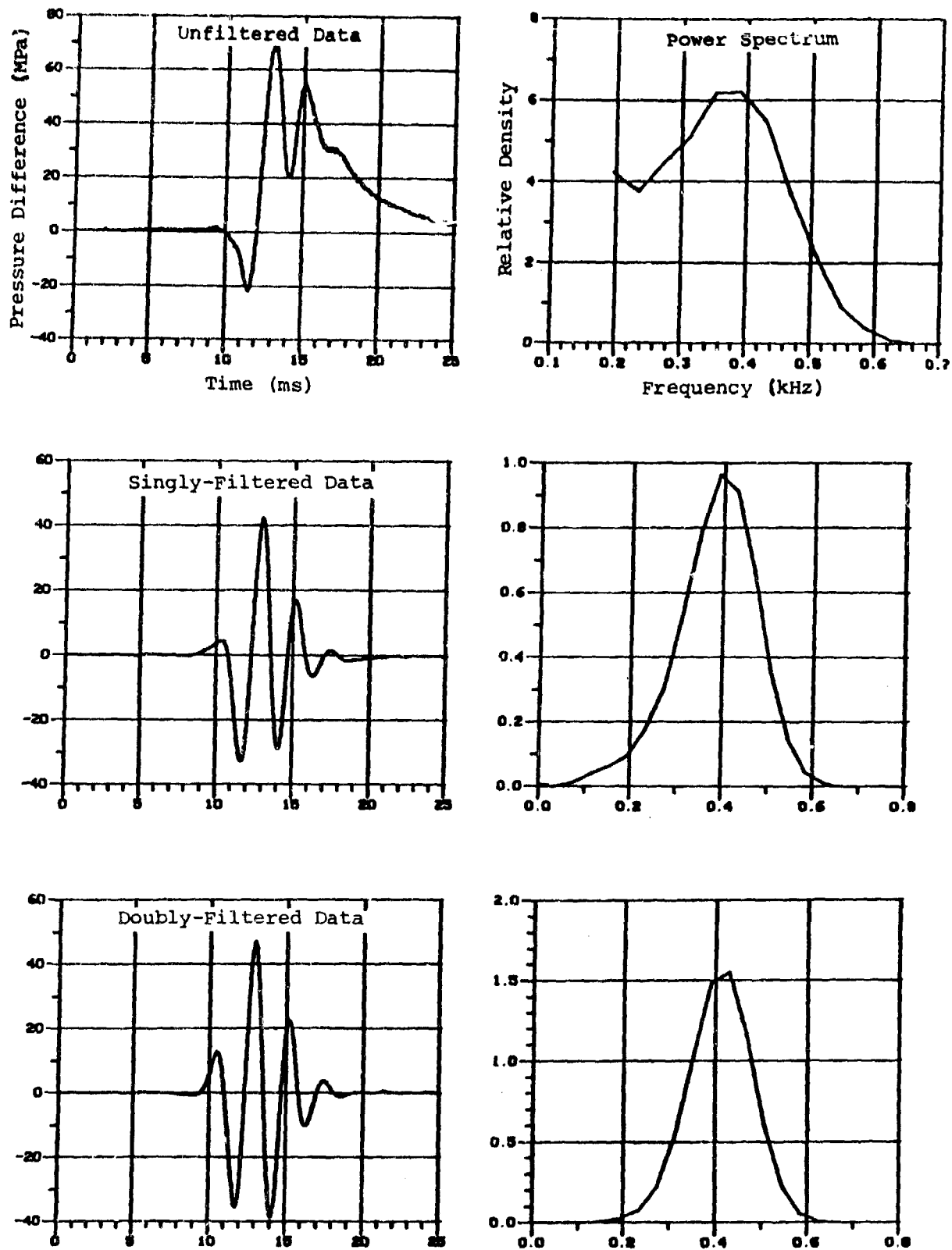


Figure 22. Application of Fourier-Analysis/Digital-Bandpass-Filtering Technique to Experimental 155-mm Howitzer Firing Data - D

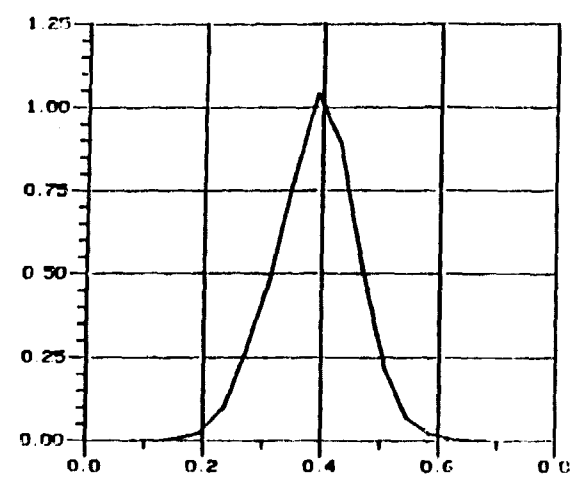
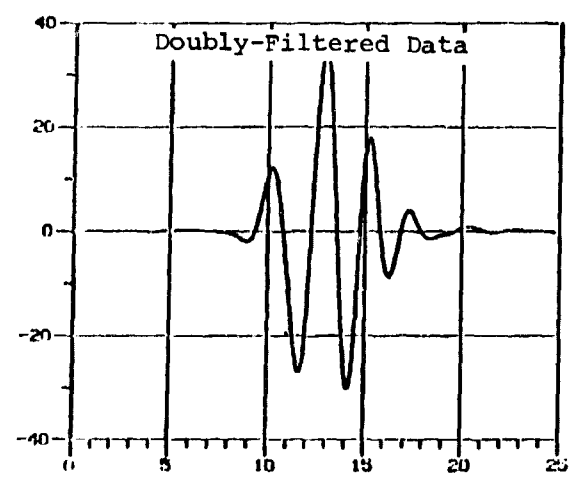
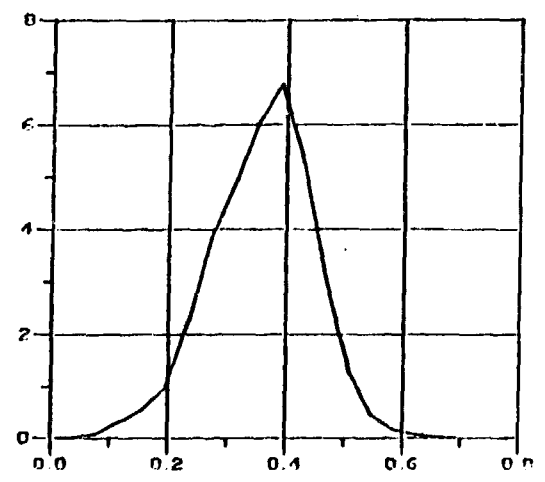
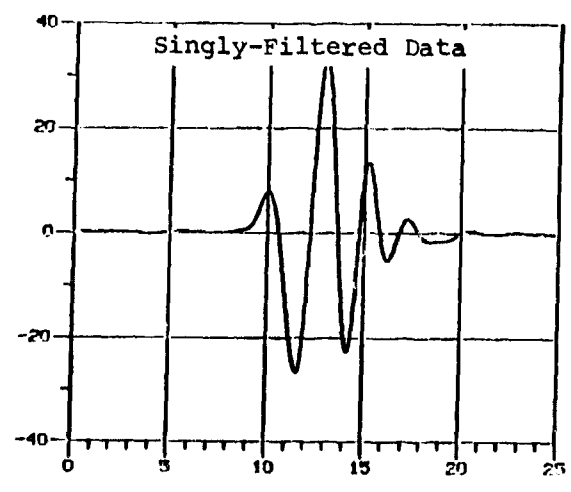
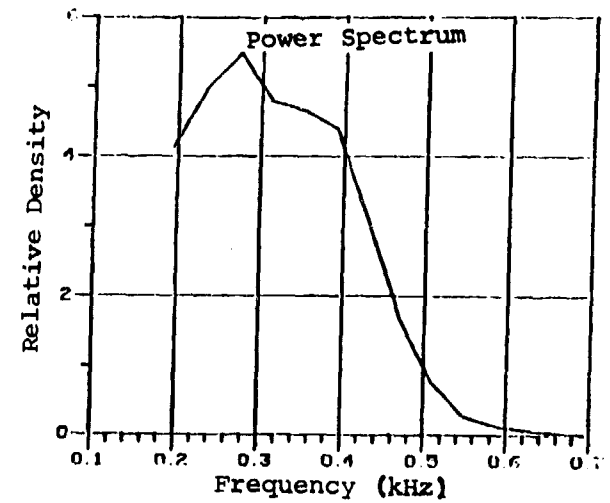
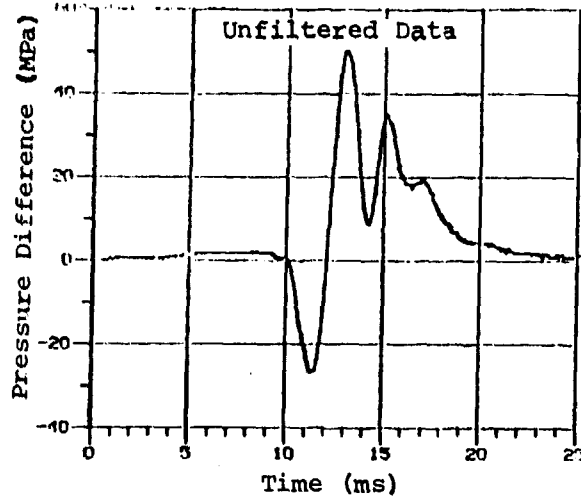


Figure 23. Application of Fourier-Analysis/Digital-Bandpass-Filtering Technique to Experimental 155-mm Howitzer Firing Data - E

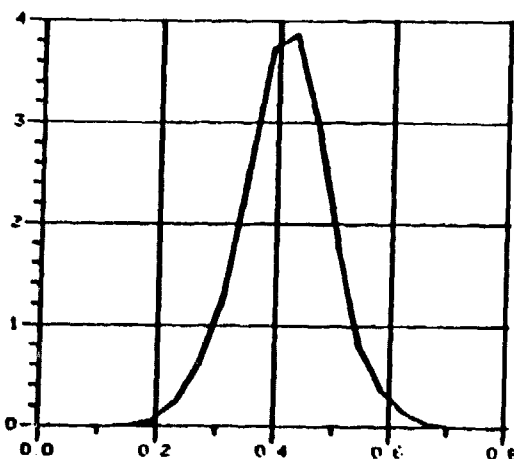
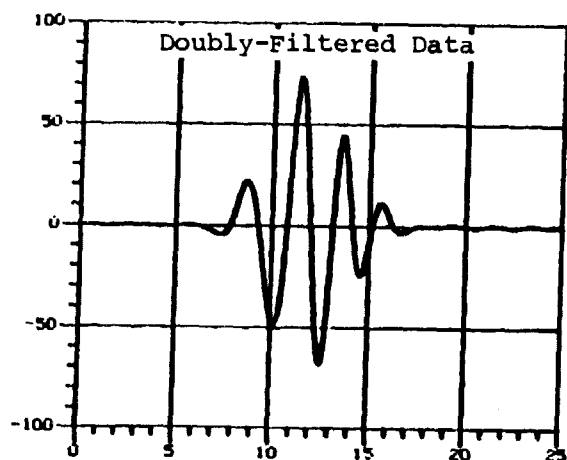
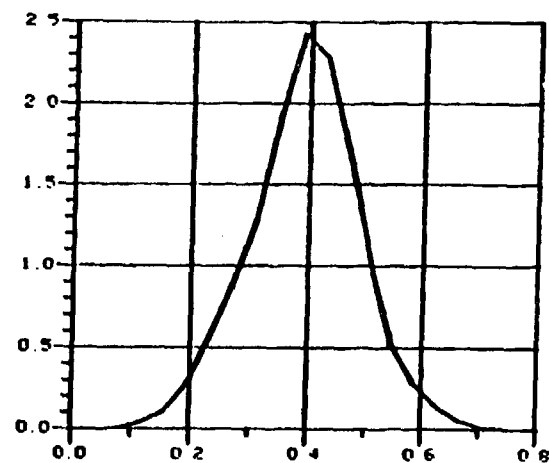
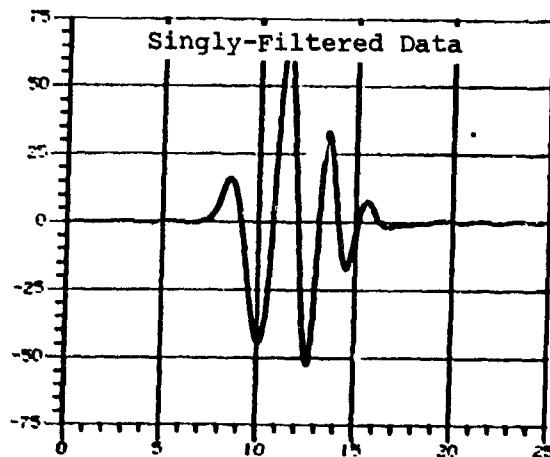
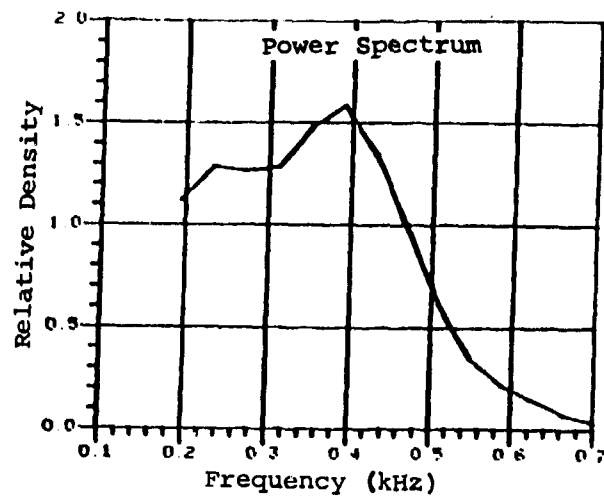
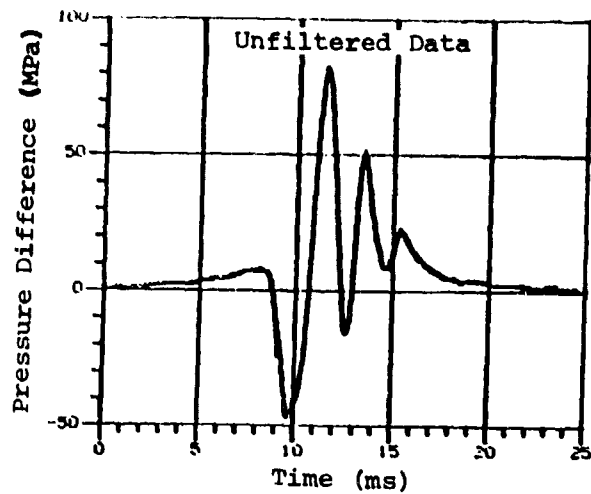


Figure 24. Application of Fourier-Analysis/Digital-Bandpass-Filtering Technique to Experimental 155-mm Howitzer Firing Data - F

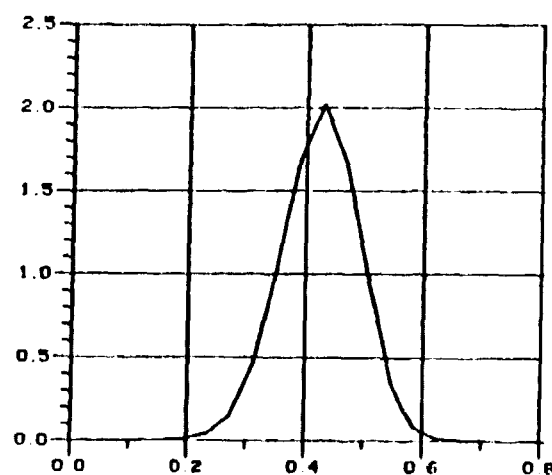
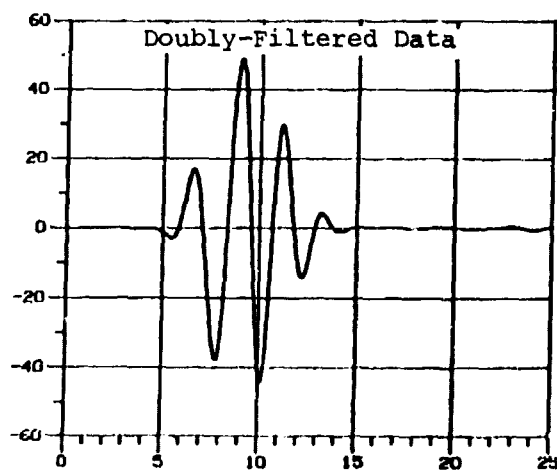
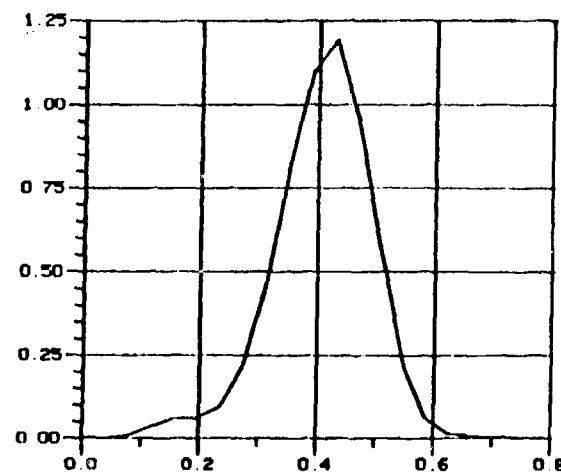
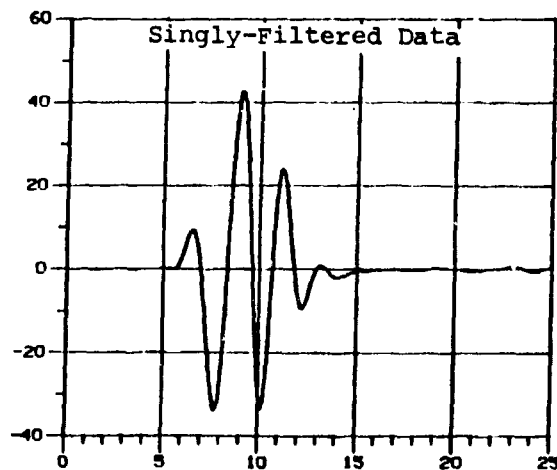
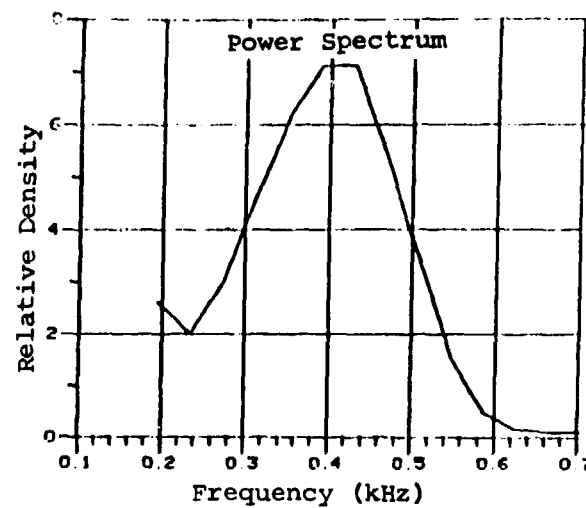
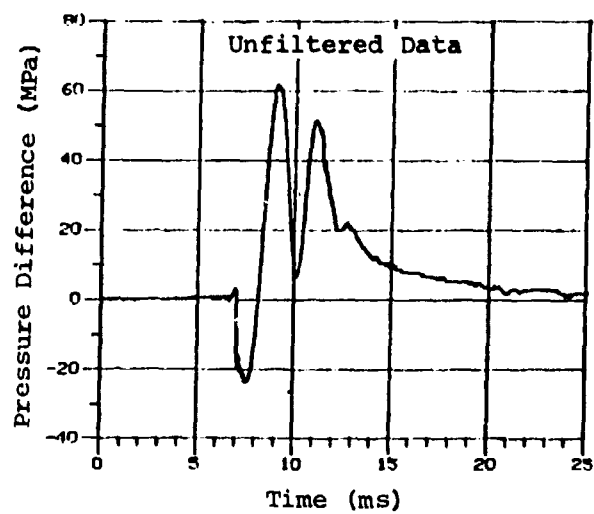


Figure 25. Application of Fourier-Analysis/Digital-Bandpass-Filtering Technique to Experimental 155-mm Howitzer Firing Data - G

ballistic environments is, of course, unproven by this example, though no fundamental problems are seen to exist.

A very limited study was also performed to determine just how sensitive the isolated pressure-wave signal was to the various filter parameters and schemes. Not surprisingly, reproducibility of the final profile was highly dependent on the passband being flat and on the cut-off at the lower edge of the band being sharp enough to avoid low-frequency contamination by that part of the recorded data corresponding to the overall pressure-time curve. As long as these requirements were met, however, results appeared to be acceptable independent of the filtering scheme imposed. The results of Figure 26 demonstrate this feature, though some differences in magnitude are evident since the overall gains of the two filtering schemes were not normalized.

Our real interest, of course, lies more with identifying exploitable advantages associated with any such technique designed to facilitate assessment of pressure waves. It is in this light that we next attempted to study the "ruggedness" of this technique with respect to frequently experienced instrumentation problems. Figures 27 and 28 summarize the results of this study. In the former, we see the recorded pressure-difference-versus-time profile along with companion curves reconstructed from the recorded data by introducing 10% calibration errors in the rear and forward pressure channels, respectively. While a 10% error is excessive, a one-or two-percent error of an approximately linear nature is not uncommon. Moreover, one cannot usually identify the presence of such errors after-the-fact by inspection. Initial $-\Delta P_1$ values for the three curves shown range from -20 to -30 MPa, $(-\Delta P_1 + \Delta P_2)$ values (as defined in Figure 11) from +85 to +105 MPa, and $-\Delta P_2$ values from -8 to +40. However, the corresponding detected profiles after double application of the digital bandpass filter reduce these variations to 3 MPa or less for each of the indicators noted - this for a total calibration-error range of an unrealistically high $\pm 10\%$.

The results of Figure 28, again for the same data round, are even more encouraging. The severe drift shown (associated with the pressure-difference-versus-time curve obtained by differencing the recorded signals from a second set of rear and forward pressure gages for the firing) is of a level which usually renders the data useless. Yet, $-\Delta P_1$, $(-\Delta P_1 + \Delta P_2)$, and $-\Delta P_2$ values for the doubly-filtered data vary by only 1-2 MPa from the corresponding values for all other filtered curves of Figure 27. The high level of success for all test cases must be attributed to the fact that any offset or error associated with that portion of the recorded pressure-difference-versus-time signal outside the passband is removed. Thus, the error factor is applied only in reference to the perturbation level of the pressure wave itself.

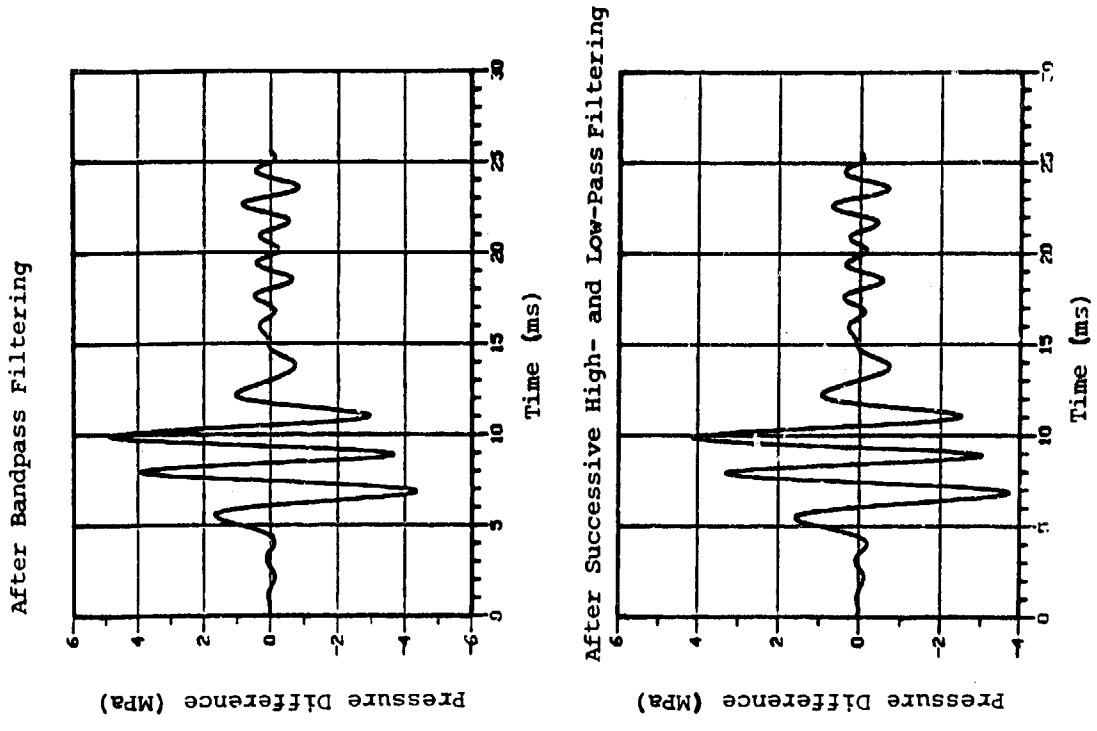


Figure 26. Sensitivity of Detected Pressure-Wave Profile to Two Alternative Digital-Filtering Schemes

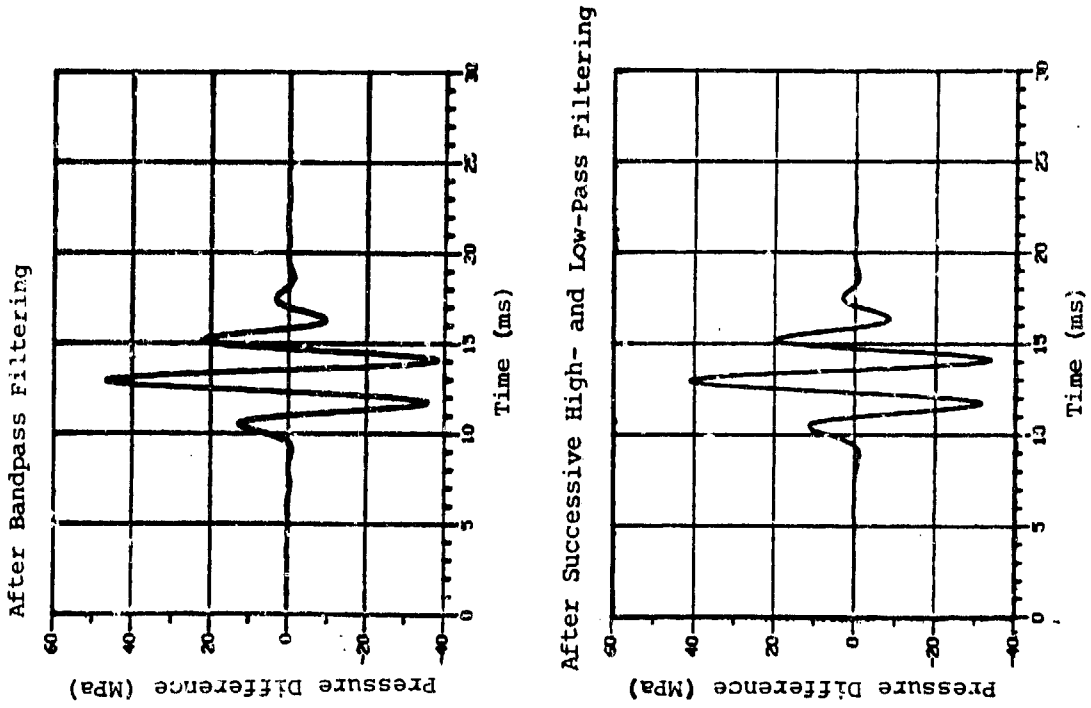


Figure 26 (continued). Sensitivity of Detected Pressure-Wave Profile to Two Alternative Digital-Filtering Schemes

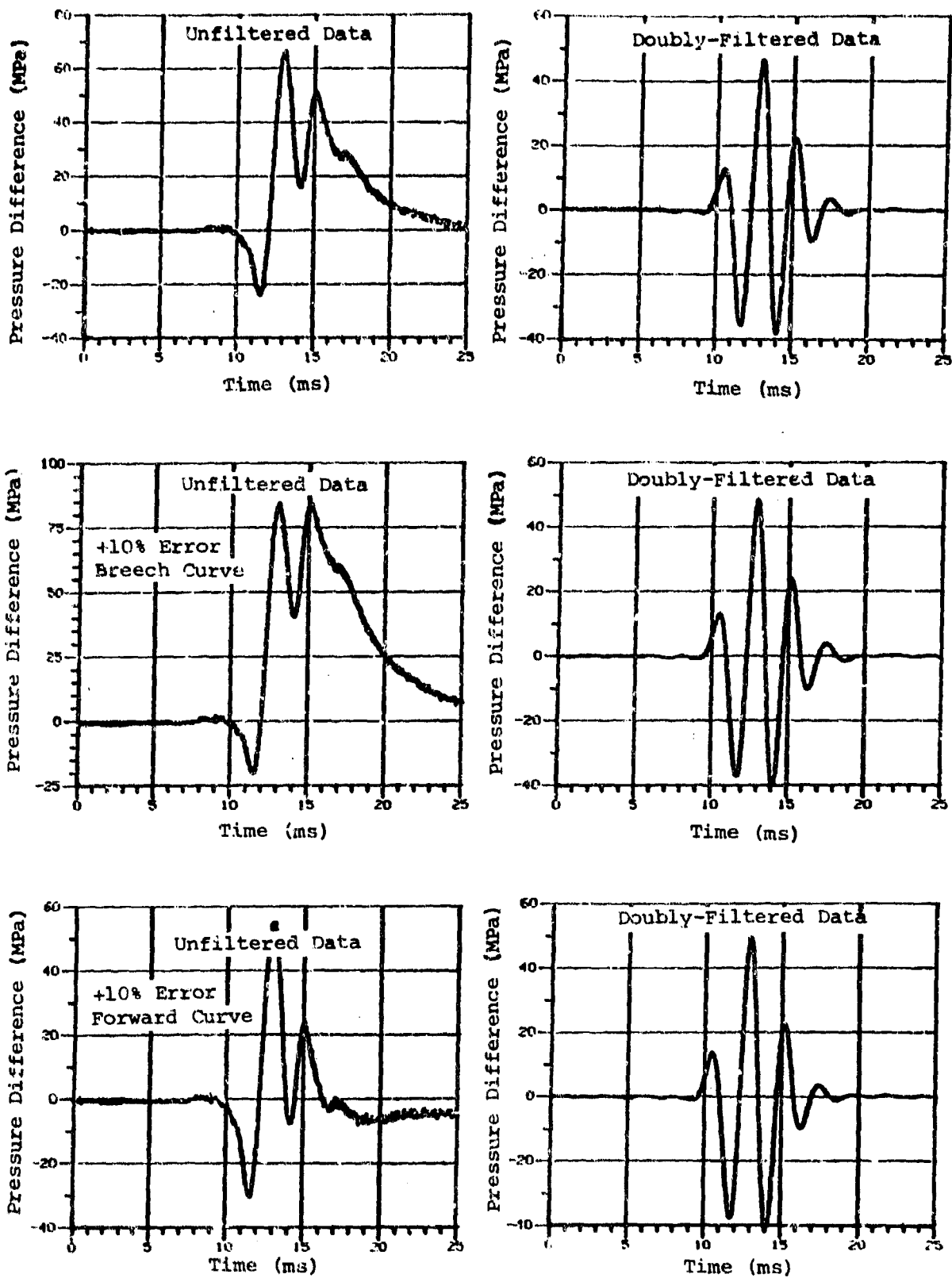


Figure 27. Sensitivity of Detected Pressure-Wave Profile to 10% Linear Calibration Errors

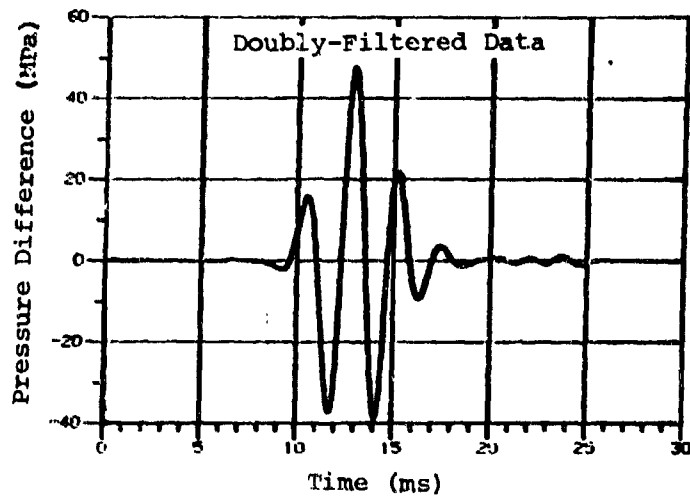
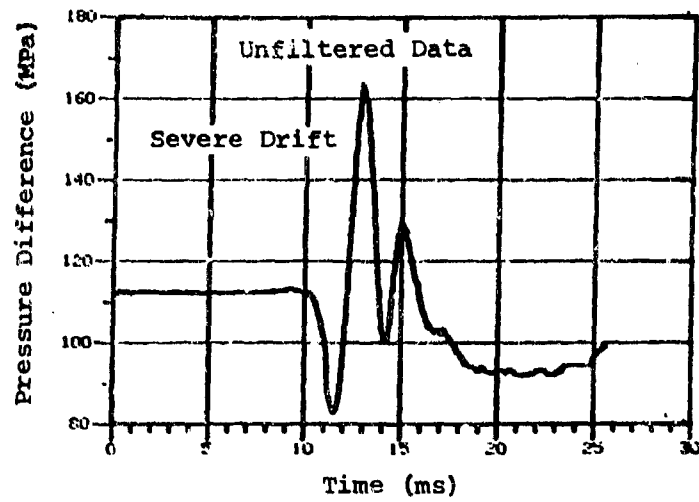


Figure 28. Sensitivity of Detected Pressure-Wave Profile to Severe Signal Drift

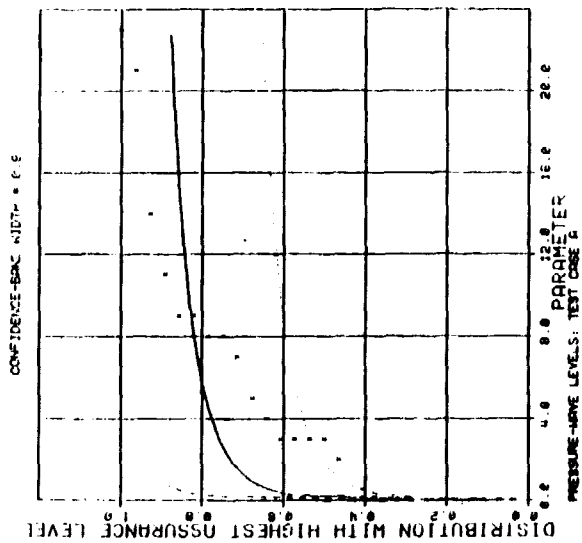
Finally, improvements were sought in respect to our ability to provide a statistical description of a population of experimental pressure-wave amplitudes in order to facilitate the projection of failure rates, as described early in this report. We recall that the use of $-\Delta P_1$ as a measure of the magnitude of pressure waves had associated with it the practice of assigning arbitrary zero values to all curves, such as that shown in Figure 8(b), for which the initial, lower extremum (associated with the stagnation of the ignition front at the projectile base) fell above the baseline. Thus, in many cases a piece of quantitative information reflecting the physical nature of the pressure wave associated with such rounds was forfeited, altering the apparent population of pressure-wave amplitudes and often degrading the statistical fit which was achievable. Again, only a limited study could be performed to assess any improvement in this area; however, the results are encouraging.

Appendix A is composed of a series of pressure-difference-versus-time profiles for 155-mm, Zone 8, Propelling Charges fired at the Ballistic Research Laboratory's Sandy Point Firing Facility. Included for each firing is the recorded breech-minus-forward pressure-difference-versus-time profile along with the resulting profile after processing with the previously described double application of a digital bandpass filter. Values for $-\Delta P_1$ and $(-\Delta P_1 \rightarrow \Delta P_2)$ were measured for both sets of curves, and an attempt was made to describe statistically the resulting sample populations with exponential or two- or three-parameter Weibull distribution functions. Since a well defined $+\Delta P_2$ often could not be identified on the unprocessed curves, the diminished, available population of $(-\Delta P_1 \rightarrow \Delta P_2)$ data based on the unfiltered curves was not felt to be representative of the overall physical body of data and was dropped from the study. Plots of the cumulative distribution functions with the highest assurance level for the remaining three sets of data are presented in Figure 29. Perhaps owing to the fact that it was composed of firings of 155-mm, Zone 8, Propelling Charges from a number of different production lots, our body of data was difficult to describe with any of the available distribution functions. However, we do observe an improvement in fit accompanying use of the filtered data, most significantly manifested in the 2-parameter Weibull description of the $(-\Delta P_1 \rightarrow \Delta P_2)$ population.

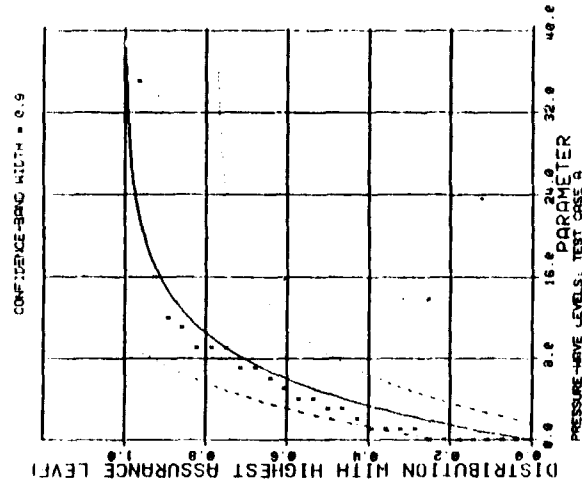
III. CONCLUSIONS AND RECOMMENDATIONS

Quantitative assessment of the safety of new propelling charges with respect to the presence of longitudinal pressure waves is essential. The existing procedure for assessing the influence of pressure waves on maximum chamber pressures and associating a projected catastrophic failure (breechblow) rate with a given propelling charge/weapon combination carries with it concerns of both fundamental and practical natures. The causal connection between pressure waves and increases in peak pressures has been addressed in a separate study⁶; we have herein limited ourselves to other aspects of the problem.

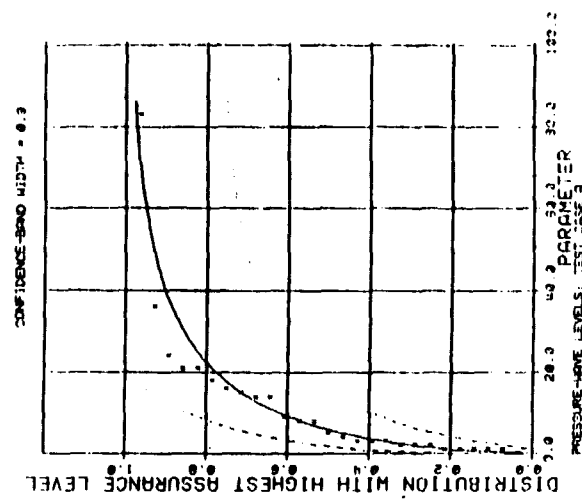
UNFILTERED $-\Delta P_i$



FILTERED $-\Delta P_i$



FILTERED $(-\Delta P_1 \rightarrow +\Delta P_2)$



Assurance Level:

0.0079

0.0588

0.4416

Figure 29. Best-Fit Cumulative Distribution for Populations Based on Three Alternative Indicators of Pressure-Wave Magnitude

With reference to the currently employed pressure-difference-versus-time profile, a number of alternative indicators of the level of pressure waves have been investigated. Use of the standard $-\Delta P_i$ parameter was shown to suffer from a problem of arbitrarily assigned zeros when the $-\Delta P_i$ minimum falls above the baseline, from a sensitivity to instrumentation calibration errors (i.e., error is proportional to pressure rather than to pressure difference), and, in some cases, from a fundamental shortcoming associated with it being a measure of the pressure gradient supportable in the gun chamber too early in the cycle. Use of a $(-\Delta P_1 \rightarrow \Delta P_2)$ parameter removed the problem of zeros, but substituted another in that the local maximum associated with $+\Delta P_2$ was not always readily identifiable. Further, its sensitivity to calibration problems was increased over that of $-\Delta P_i$. However, this same feature of extending further in time into the interior ballistic cycle rendered $(-\Delta P_1 \rightarrow \Delta P_2)$ free from the fundamental concern mentioned for $-\Delta P_i$. Additional indicators based on subsequent minima and maxima or their ratios were similarly encumbered with problems.

Extraction of the unperturbed pressure-difference-versus-time signal, associated only with motion of the projectile, from the recorded breech-minus-forward pressure-difference profile was shown to remove the problem of arbitrary zeros, reduce the sensitivity to instrumentation calibration errors (i.e., error becomes proportional to the pressure-difference signal, not overall pressure), and facilitate selection and measurement of a physically well-motivated indicator of pressure-wave magnitude. Such "detection" of a true pressure-wave signal was most easily effected through decomposition of the digitally recorded pressure-difference-versus-time signal into its various frequency components via Fourier analysis, separation of the desired portion of the spectrum via digital filtering, and reconstruction of the resulting pressure-wave profile. While extensive study was not conducted, a doubly-applied bandpass filter was shown to be applicable to a broad class of profiles, obtained from firings of experimental charges designed to provide a wide range of pressure-wave amplitudes. The passband itself was definable either from a thermo-physical analysis of the gun/charge configuration or via visual inspection of the power spectrum of the Fourier coefficients corresponding to the recorded profile. Further, insensitivity of the filtered signal to instrumentation problems (e.g., calibration errors, signal drift) was demonstrated. Finally, use of a $(-\Delta P_1 \rightarrow \Delta P_2)$ indicator measured after application of the double bandpass filter was shown to lead to substantial improvements in terms of "goodness-of-fit" for statistical description of populations of the pressure-wave parameter.

Based on these results, it is recommended that, at the time of the next requested propelling charge safety assessment, the Ballistic Research Laboratory also perform a parallel assessment of the same body of data employing, as an indicator of pressure waves, $(-\Delta P_1 \rightarrow \Delta P_2)$, subjected to appropriate bandpass filtering. Substitution of this parameter for $-\Delta P_i$ would be the only substantial change; procedures for determination of sensitivity of peak pressure to the parameter and statistical projection

of the probability of reaching the failure level would remain unchanged. A further recommendation for adoption of the new indicator may be made at that time, based on the trade-off between any improvements in the confidence of the prediction and the added burden of digital-filter processing.

We note further that while substantial improvements may result from adoption of the proposed scheme, a "cookbook procedure" is not anticipated. A responsible safety assessment will always include careful consideration of all background and otherwise-related data. In addition, it is not immediately obvious that the results of this study are, in all cases, applicable to the problem of multiple-increment charges. The more complex sequencing of flame propagation and increment separation may well lead to safety problems not directly correlative to the indicators mentioned. We caution the reader, in particular, with respect to catastrophic failures associated with transient, solid-phase loads on the projectile base, a subject which has received much study in recent years^{15,16}.

¹⁵C.T. Boyer, Jr., "Significant Early-Time Transient Projectile Acceleration with Concomitant Minimal Pressure Waves," NSWC/DL-TR-3913, Naval Surface Weapons Center, Dahlgren Laboratory, Dahlgren, VA, November 1978.

¹⁶T.C. Minor, "Characterization of Ignition Systems for Bagged Artillery Charges," 17th JANNAF Combustion Meeting, CPIA Publication 329, Vol. 2, pp. 45-68, November 1980.

REFERENCES

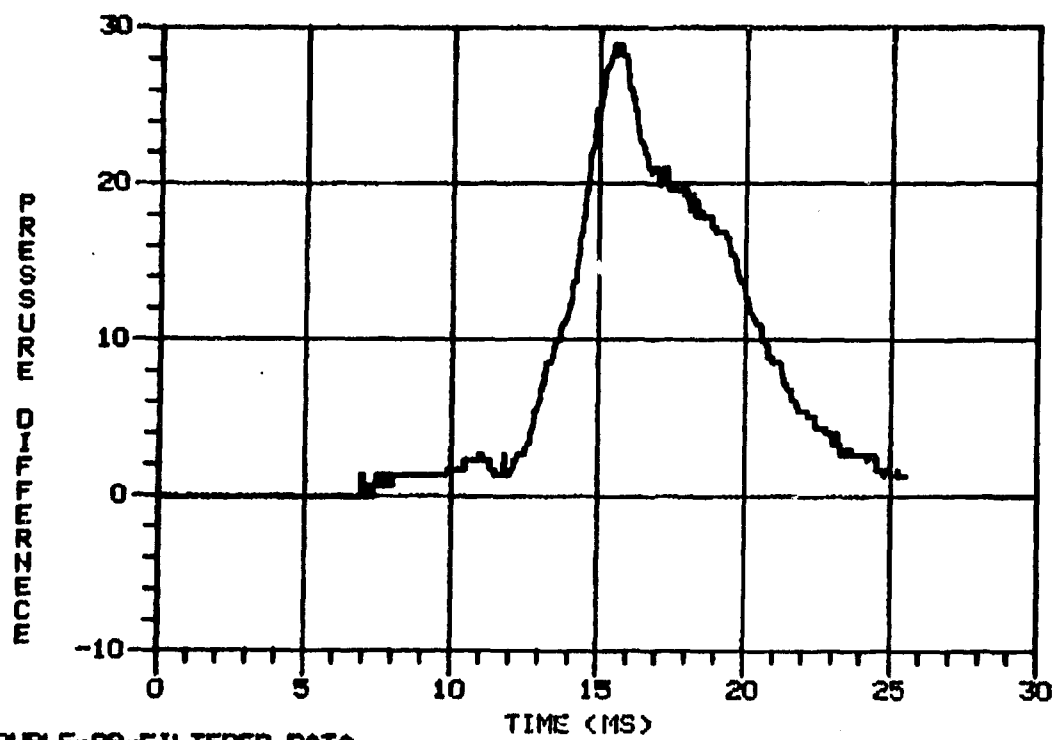
1. A.J. Budka and J.D. Knapton, "Pressure Wave Generation in Gun Systems: A Survey," BRL MR 2567, USA Ballistic Research Laboratories, Aberdeen Proving Ground, MD, December 1975. (AD #B008893L)
2. D.W. Culbertson, M.C. Shamblen, and J.S. O'Brasky, "Investigation of 5"/38 Gun In-Bore Ammunition Malfunctions," NWL-TR-2624, Naval Weapons Laboratory, Dahlgren, VA, December 1971.
3. L. Kell, "The 5-Inch Illuminating Projectile Dud Investigation," NSWL/DL-TR-3792, Naval Surface Weapons Center, Dahlgren Laboratory, Dahlgren, VA, January 1979.
4. E.V. Clarke, Jr. and I.W. May, "Subtle Effects of Low-Amplitude Pressure Wave Dynamics on the Ballistics Performance of Guns," 11th JANNAF Combustion Meeting, CPIA Publication 261, Vol. 1, pp. 141-156, December 1974.
5. N. Lockett, "British Work on Solid Propellant Ignition," Bulletin of the First Symposium on Solid Propellant Ignition," Solid Propellant Information Agency, Silver Spring, MD, October 1956.
6. C.R. Ruth and A.W. Horst, "Experimental Validation for the Uniqueness of the Differential Pressure-Maximum Pressure Sensitivity Curves Used for Charge Safety Assessment," Ballistic Research Laboratory, USA ARRADCOM, Aberdeen Proving Ground, MD, (report in preparation).
7. I.W. May and A.W. Horst, "Charge Design Considerations and Their Effect on Pressure Waves in Guns," Interior Ballistics of Guns, H. Krier and M. Summerfield, Editors, Progress in Astronautics and Aeronautics, Vol. 66, AIAA, New York, NY, 1979, pp. 197-227.
8. J. Corner, Theory of the Interior Ballistics of Guns, John Wiley & Sons, Inc., New York, NY, 1950, pp 339-342.
9. P.G. Baer and J.M. Frankle, "The Simulation of Interior Ballistic Performance of Guns by Digital Computer Program." BRL R 1183, Ballistic Research Laboratories, Aberdeen Proving Ground, MD, December 1962. (AD #299980)
10. A.A. Juhasz, I.W. May, W.P. Aungst, and F.R. Lynn, "Combustion Diagnostics of Very High Burning Rate Propellants," 17th JANNAF Combustion Meeting, CPIA Publication 329, Vol. 2, pp. 209-240, November 1980.
11. "Subroutine FFTR, Library 3," International Mathematical and Statistical Libraries, Inc., Sixth Edition, Houston, TX, July 1977.

REFERENCES (continued)

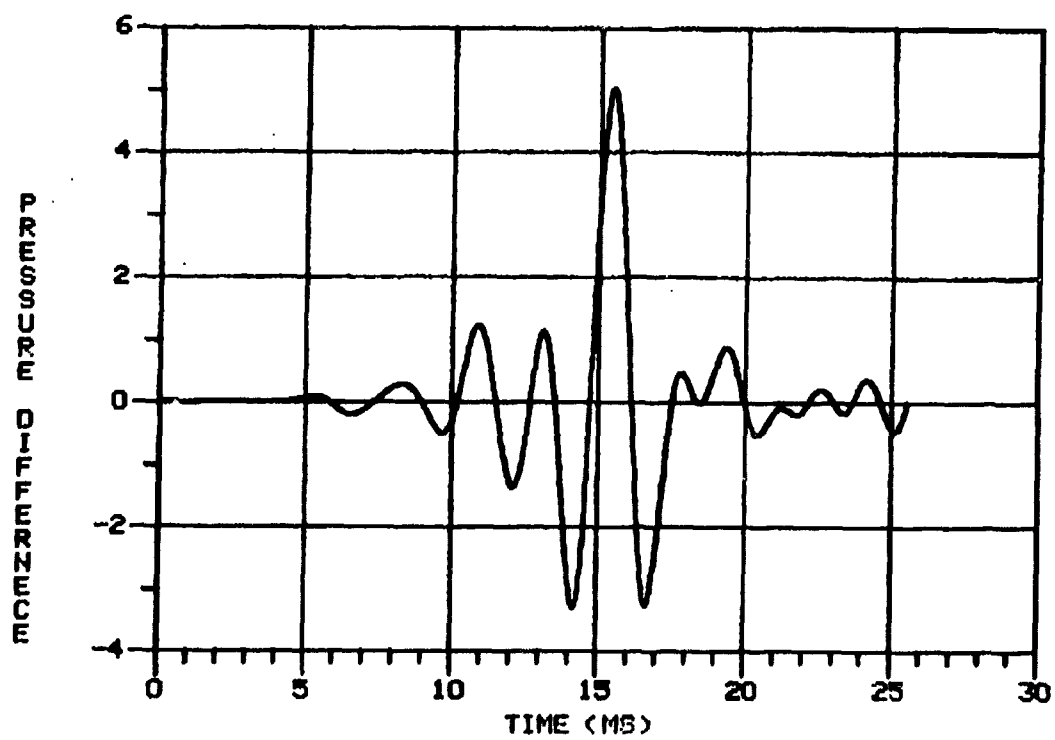
12. J.H. McClellan, T.W. Parks and L.R. Rabiner, "A Computer Program for Designing Optimum FIR Linear Phase Digital Filters," IEEE Trans. on Audio and Electroacoustics, AU-21 (5), 1973, pp. 506-526.
13. J.N. Walbert, "Computer Algorithms for the Design and Implementation of Linear Phase Finite Impulse Response Digital Filters," Ballistic Research Laboratory, USA ARRADCOM, Aberdeen Proving Ground, MD (report in preparation).
14. J.N. Walbert, "Application of Digital Filters and the Fourier Transform to the Analysis of Ballistic Data," Ballistic Research Laboratory, USA ARRADCOM, APG, MD (report in preparation).
15. C.T. Boyer, Jr., "Significant Early-Time Transient Projectile Acceleration with Concomitant Minimal Pressure Waves," NSWC/DL-TR-3913, Naval Surface Weapons Center, Dahlgren Laboratory, Dahlgren, VA, November 1978.
16. T.C. Minor, "Characterization of Ignition Systems for Bagged Artillery Charges," 17th JANNAF Combustion Meeting, CPIA Publication 329, Vol. 2, pp. 45-68, November 1980.

APPENDIX

PRESSURE-DIFFERENCE-VERSUS-TIME PROFILES
FOR 155-mm, ZONE 8, PROPELLING CHARGES

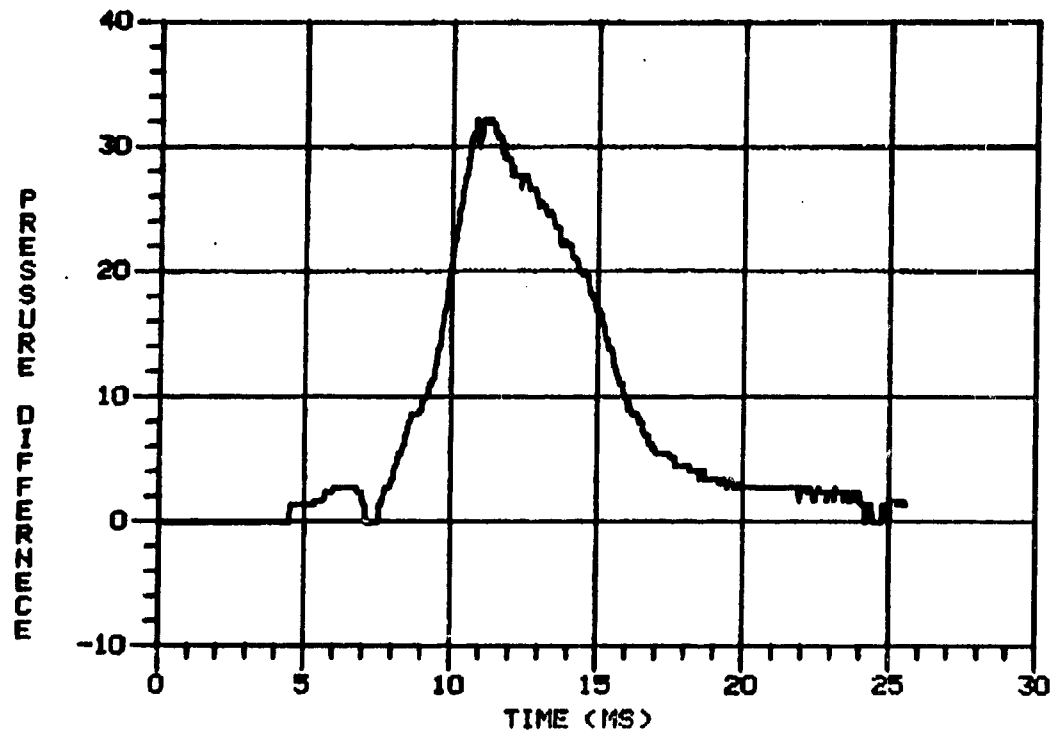


DOUBLE-BP-FILTERED DATA

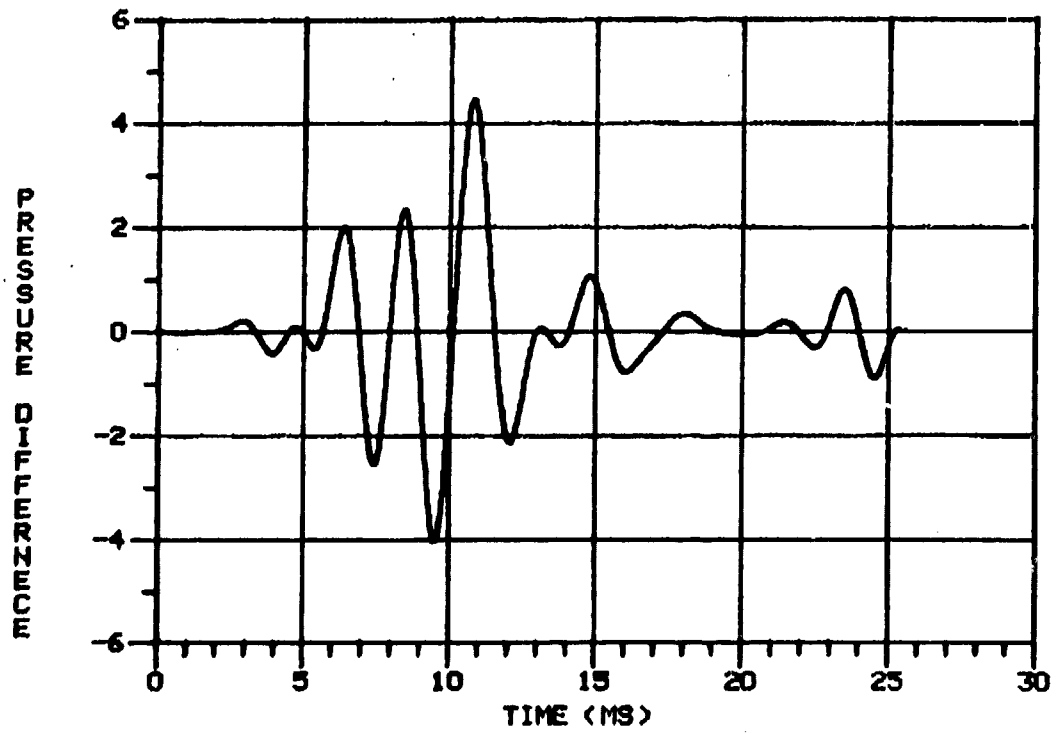


DELTA P STUDY

8

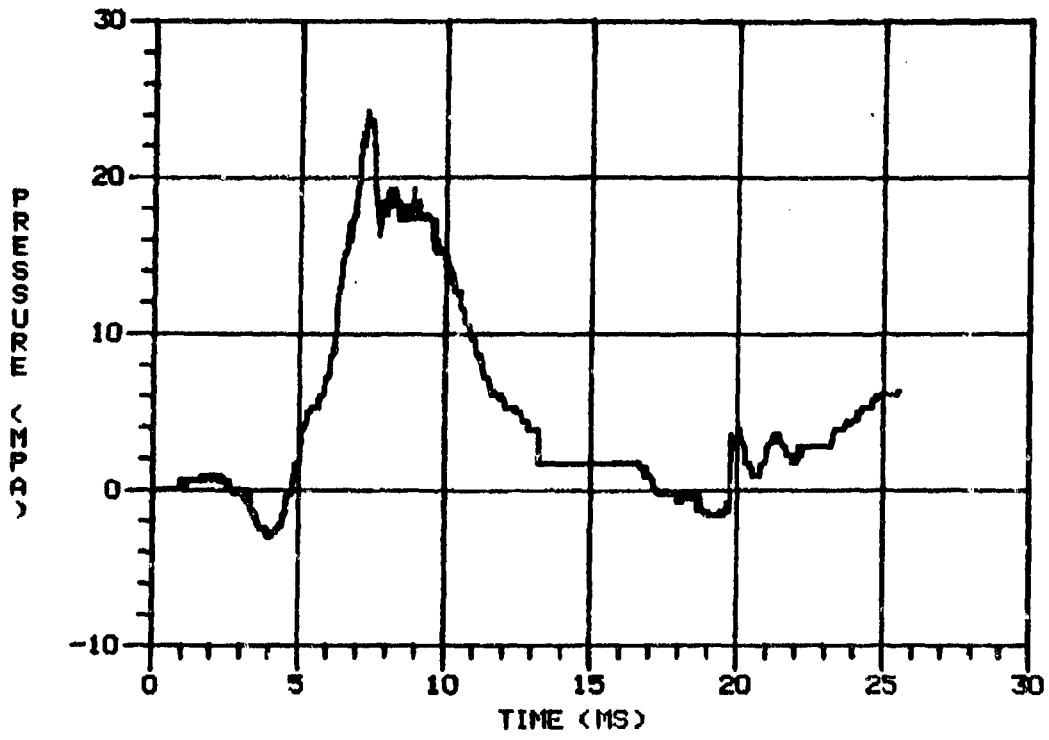


DOUBLE-BP-FILTERED DATA

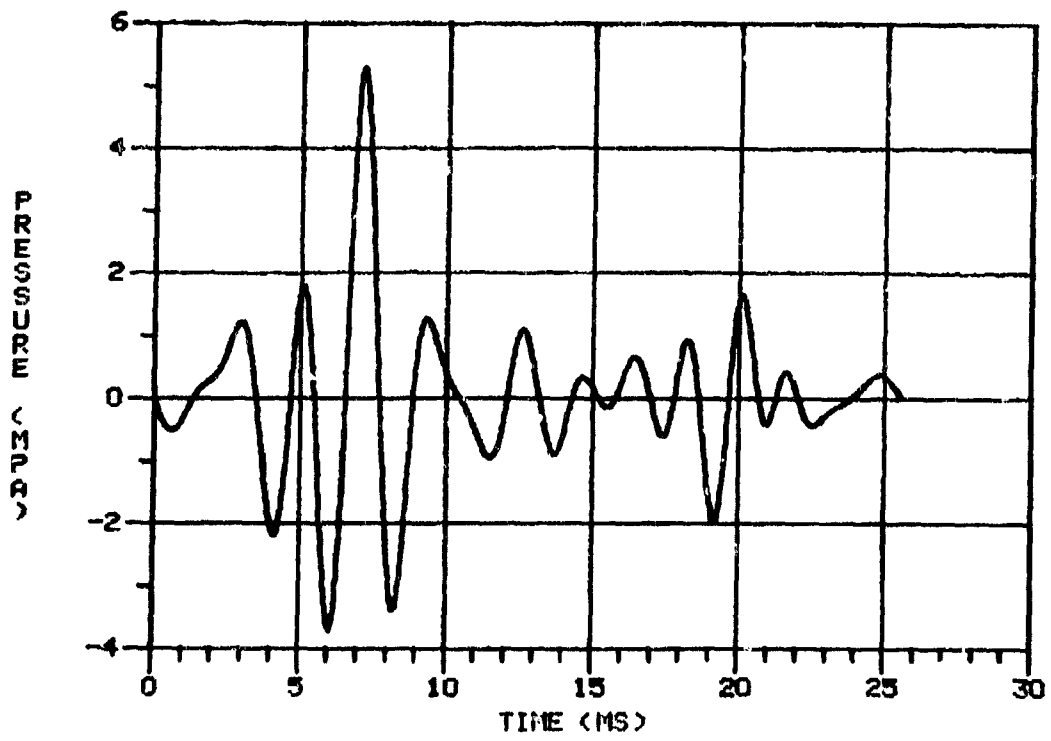


NOVEL GRAIN GEOMETRY

5

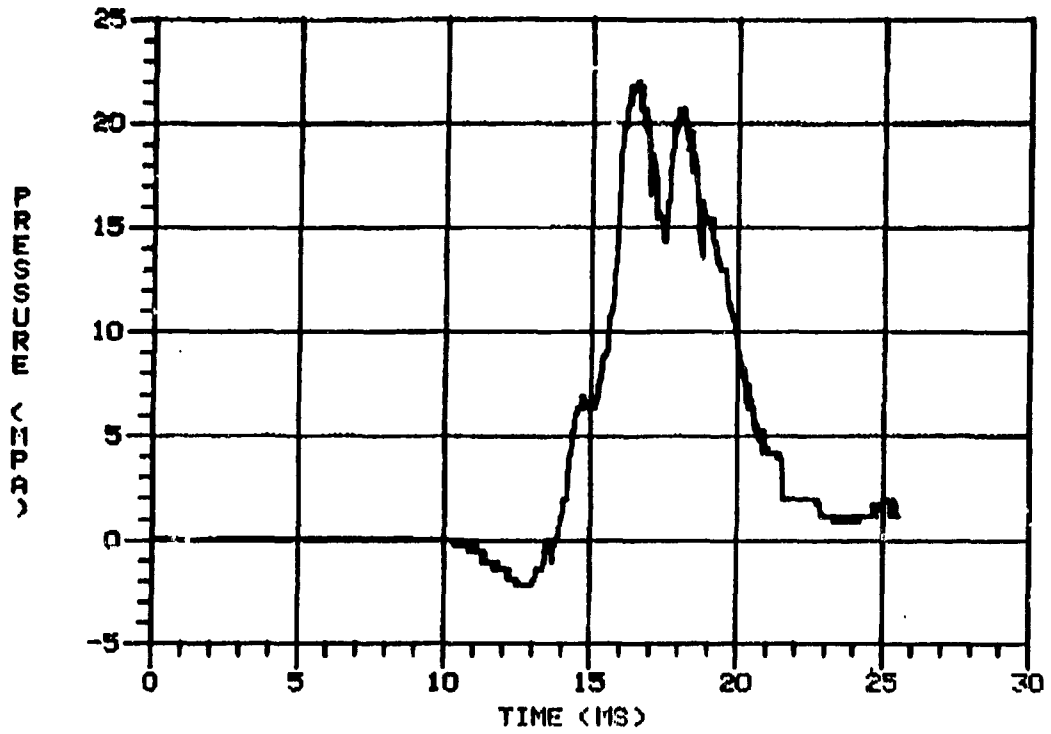


DOUBLE-BP-FILTERED DATA

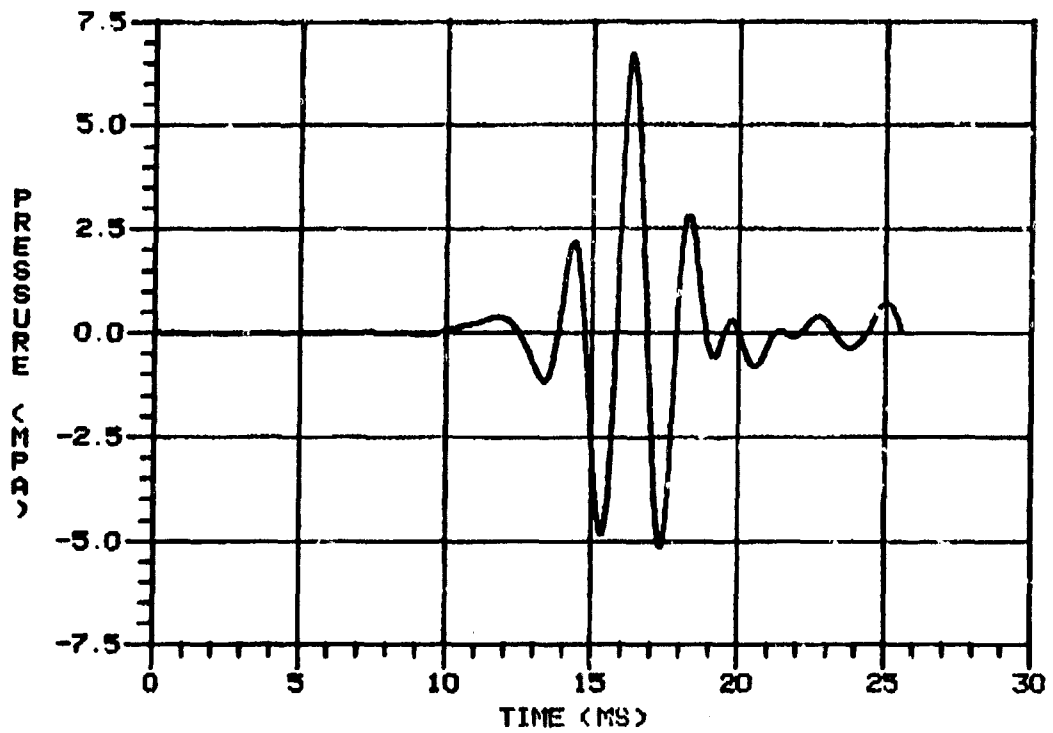


NOVEL GRAIN GEOMETRY

6

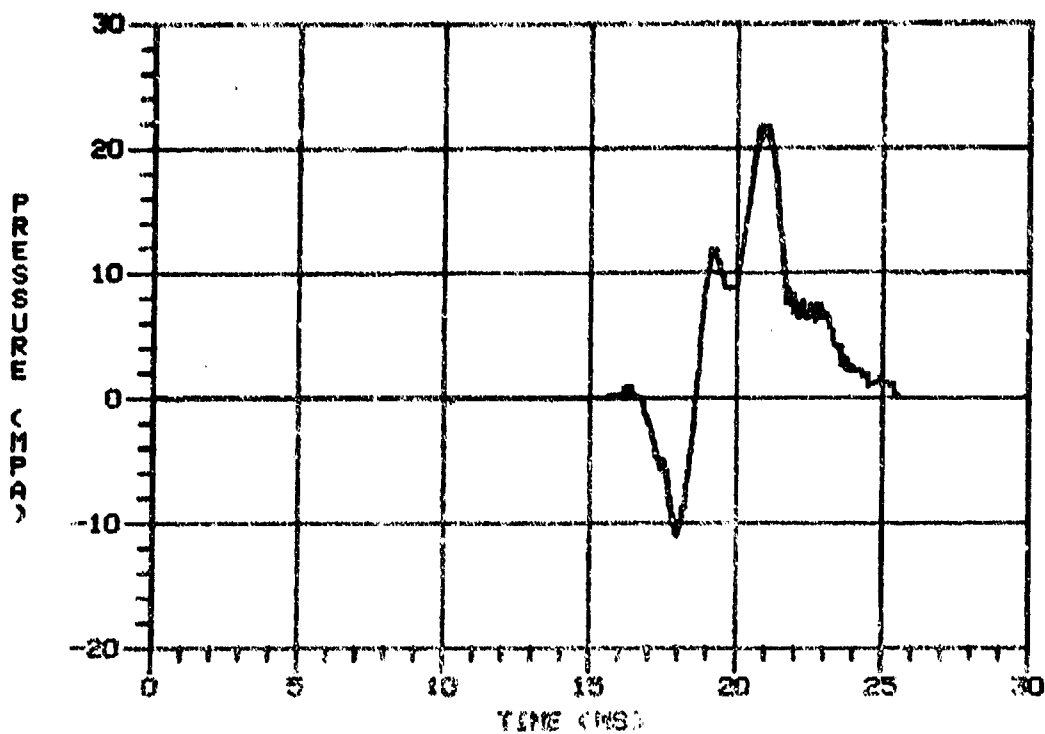


DOUBLE-BP-FILTERED DATA

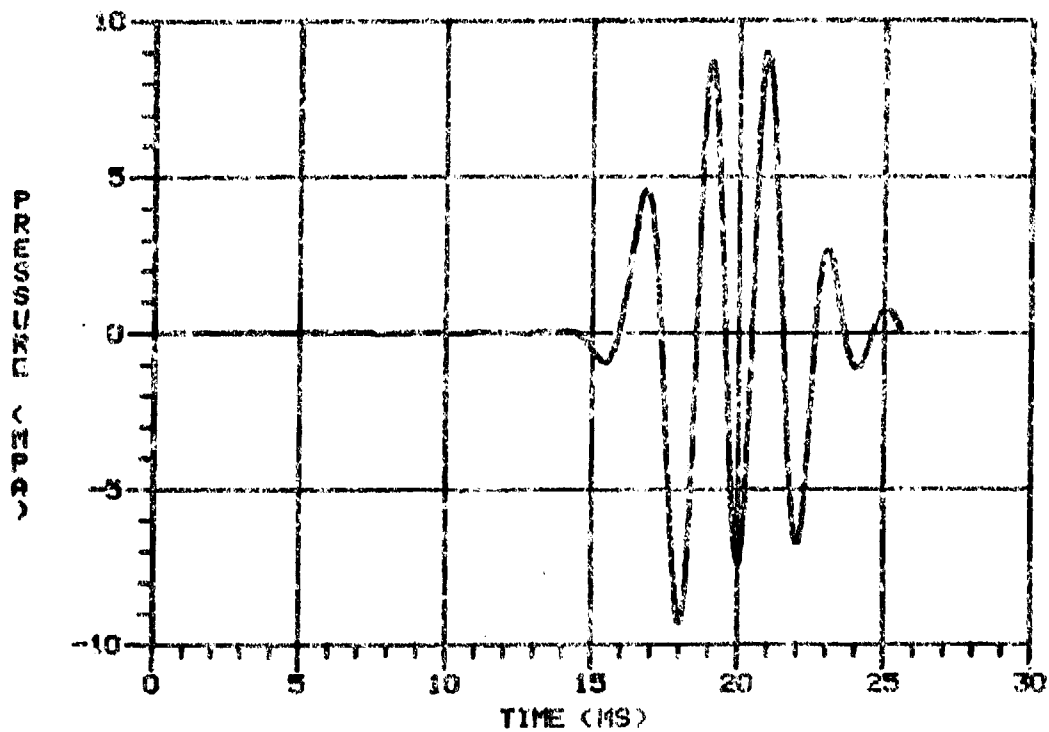


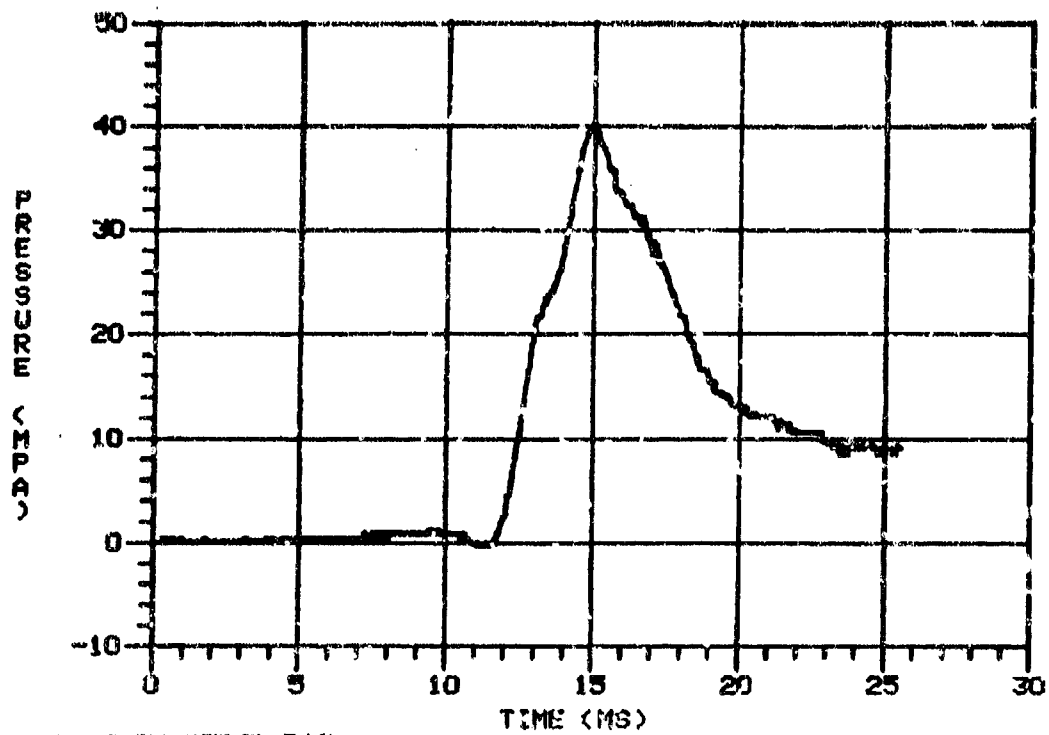
NOVEL GRAIN GEOMETRY

10

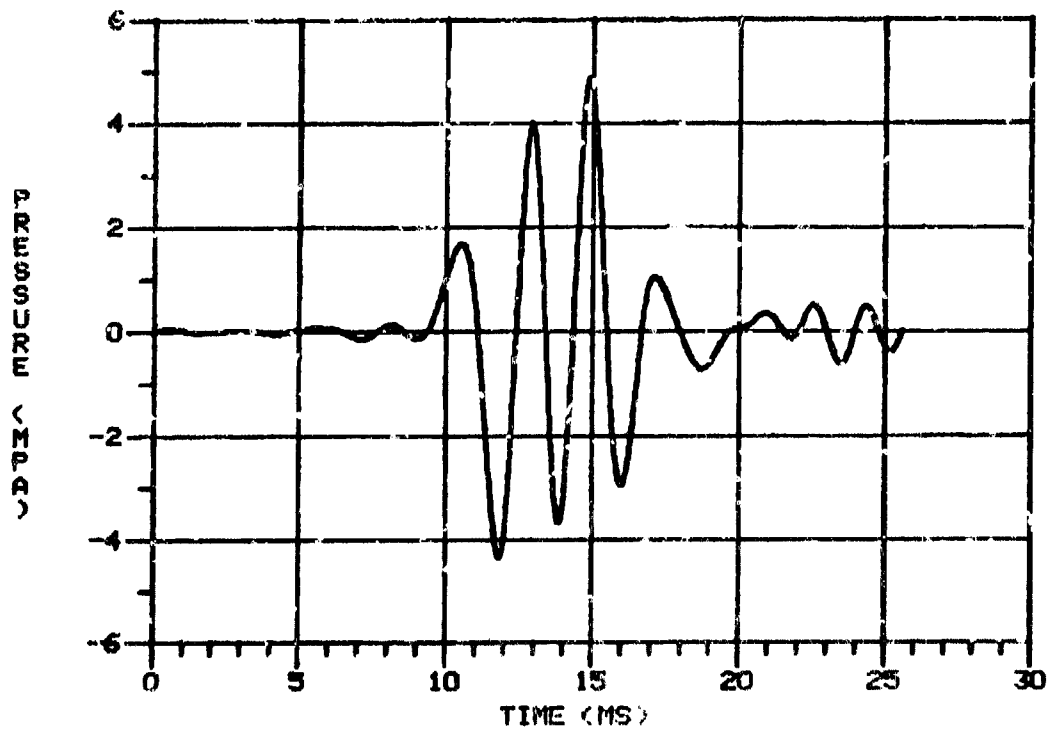


DOUBLE-BP-FILTERED DATA



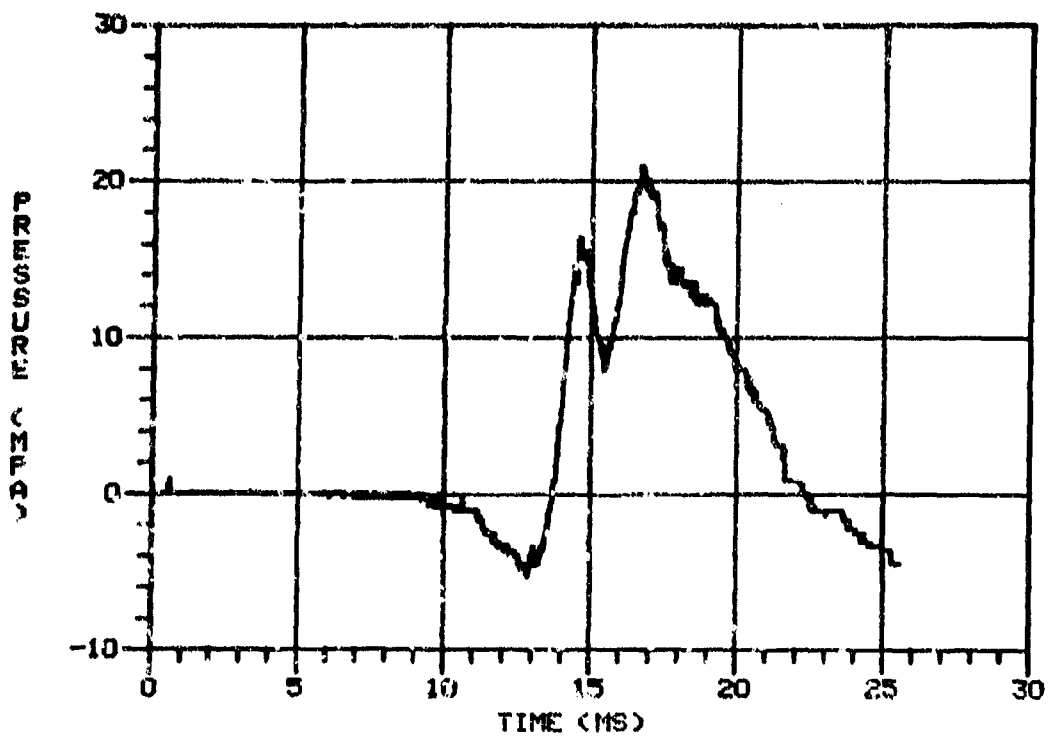


DOUBLE-OF-FILTERED DATA

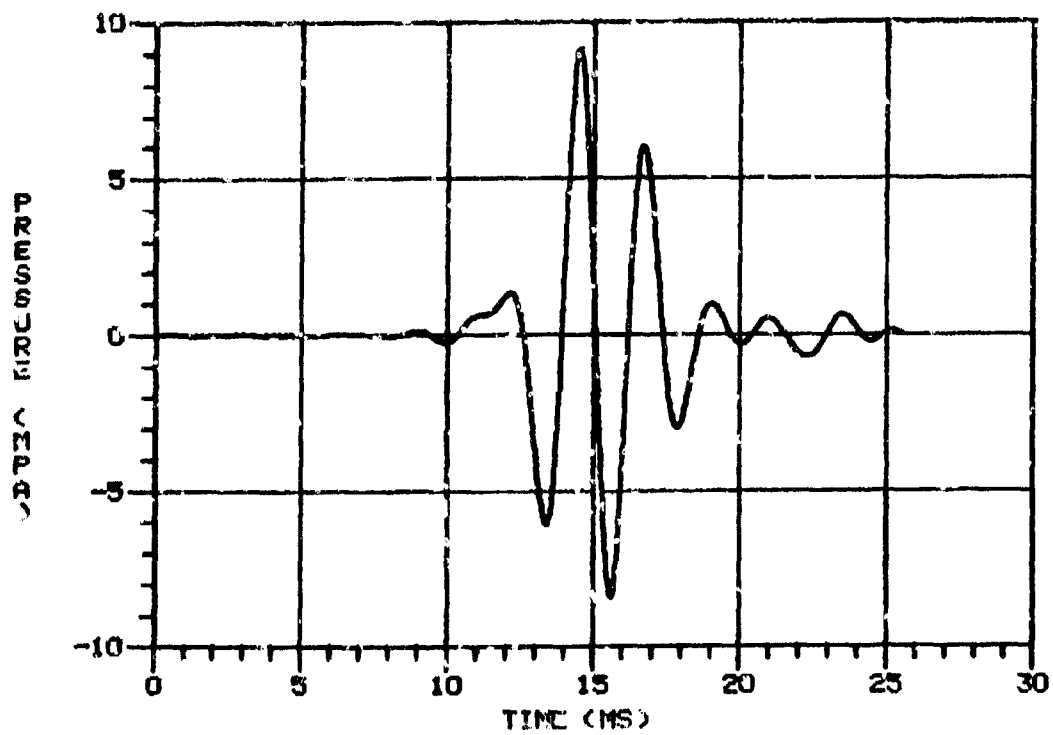


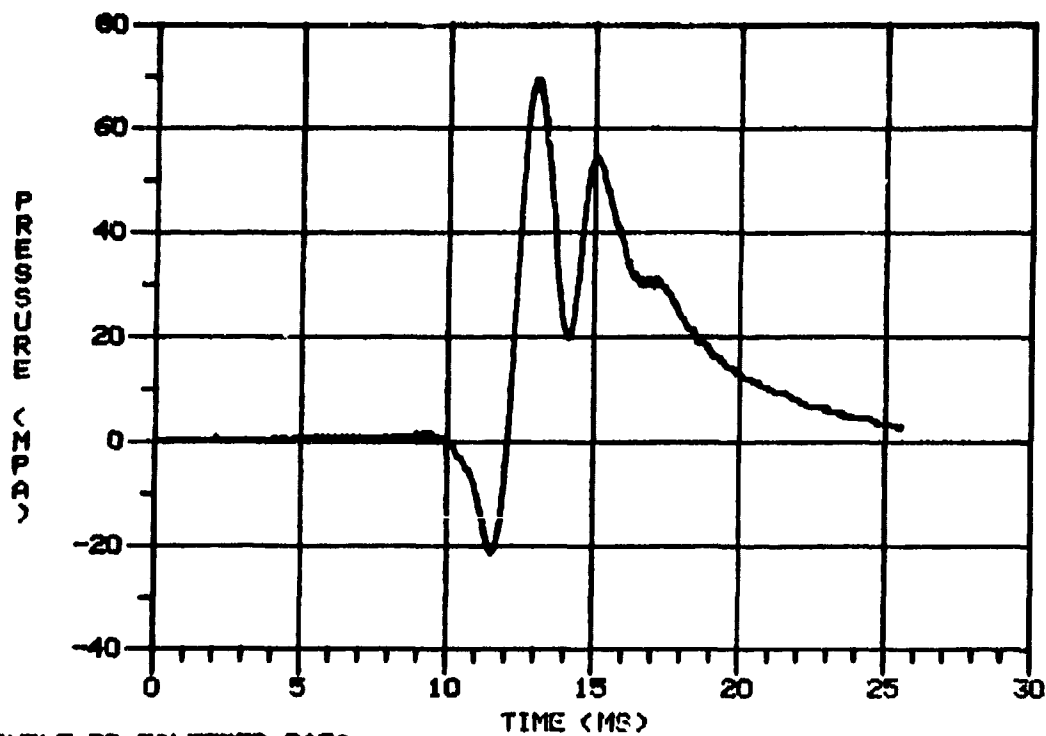
NOVEL GRAIN GEOMETRY

15

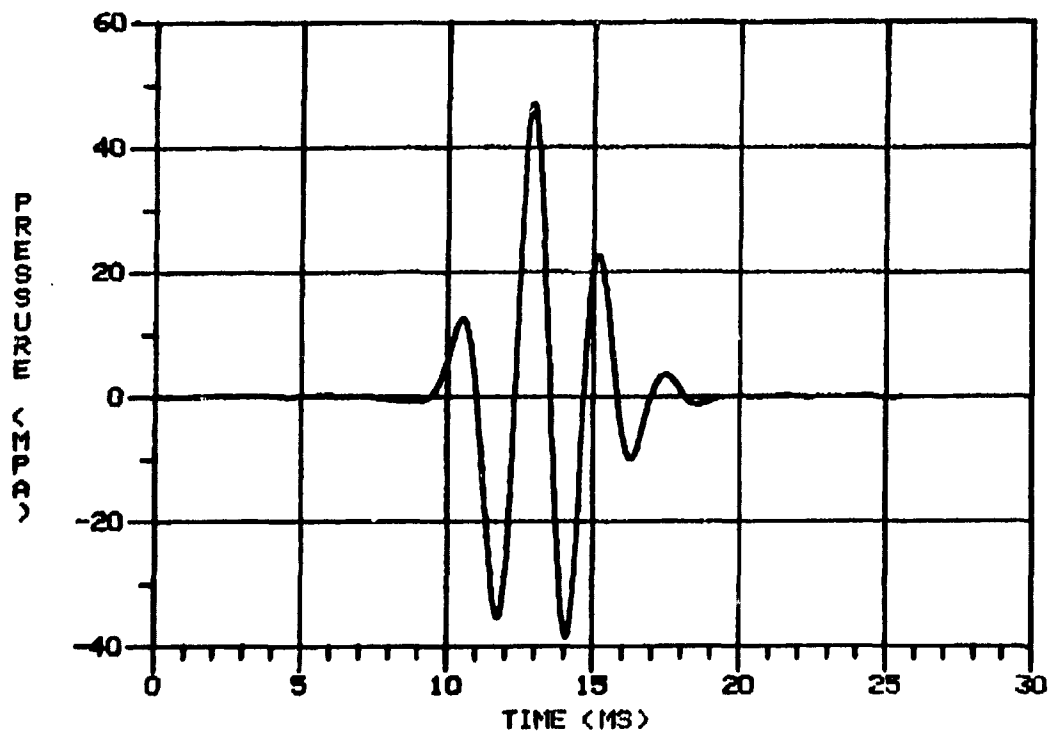


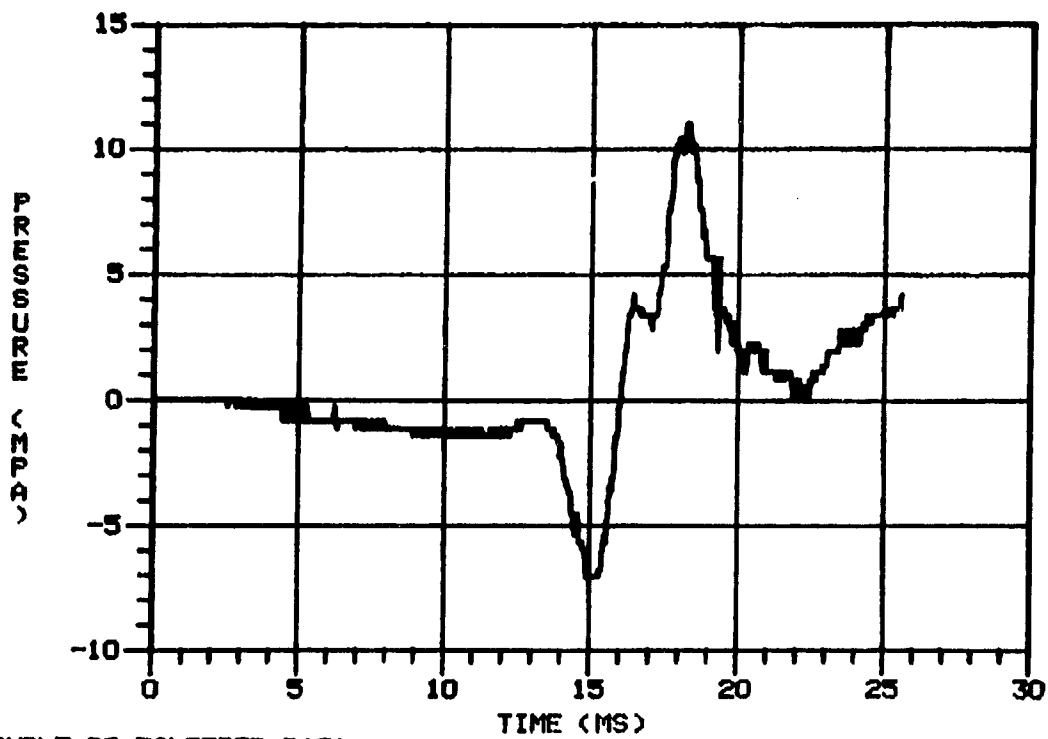
DOUBLE-BP-FILTERED DATA



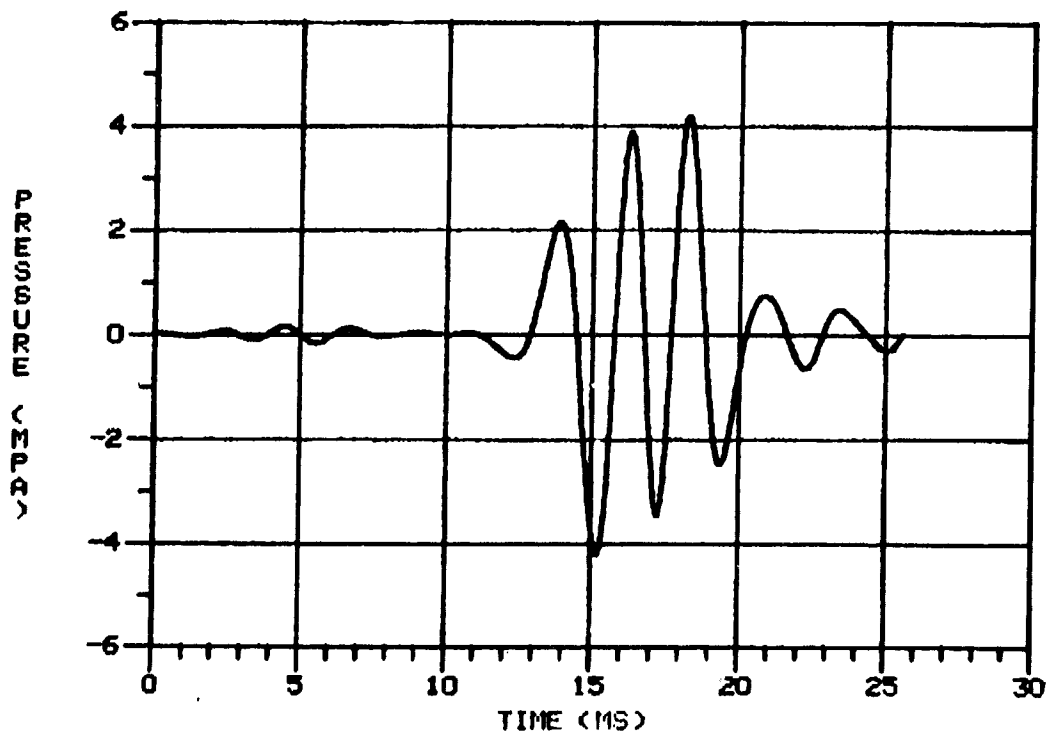


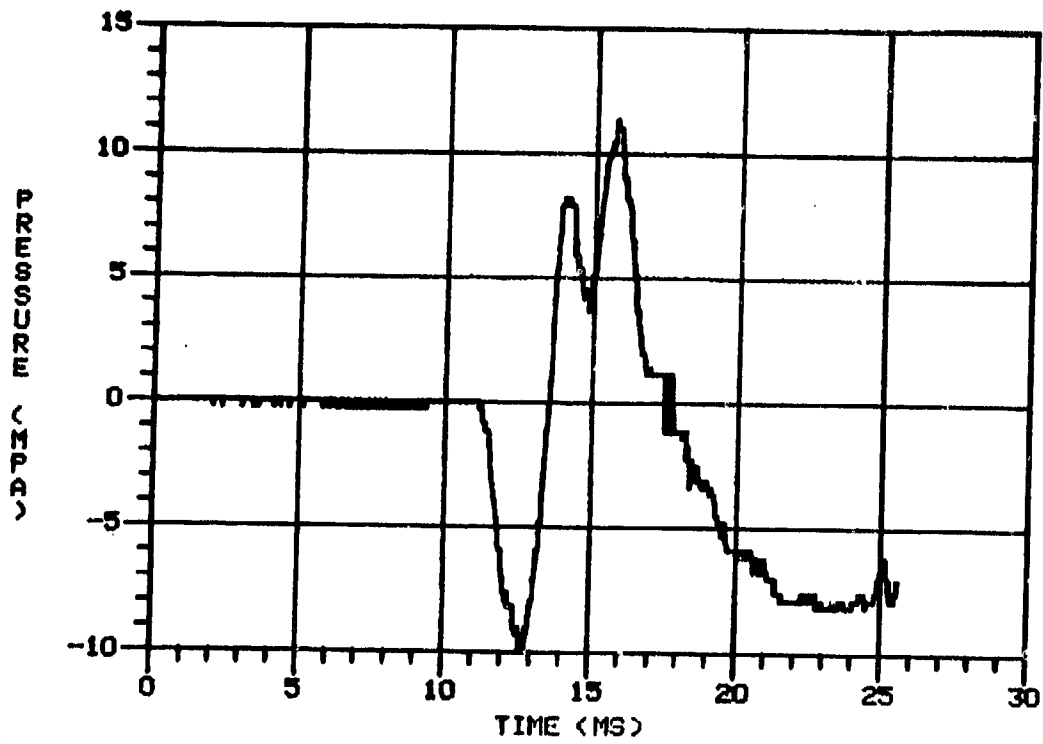
DOUBLE-BP-FILTERED DATA



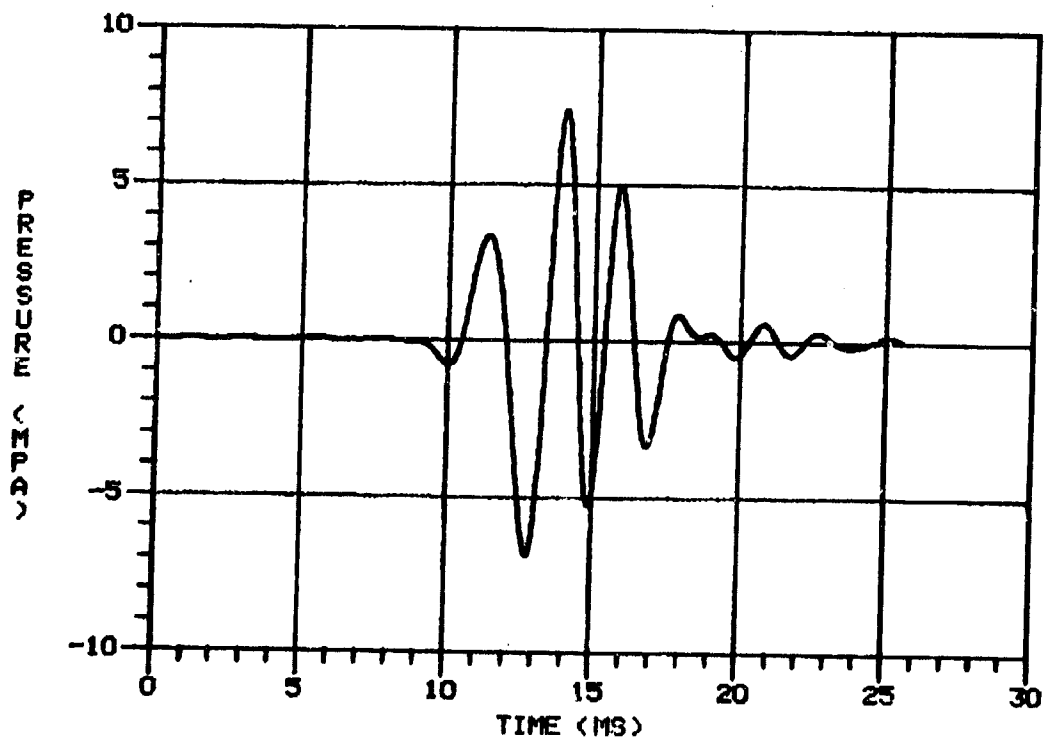


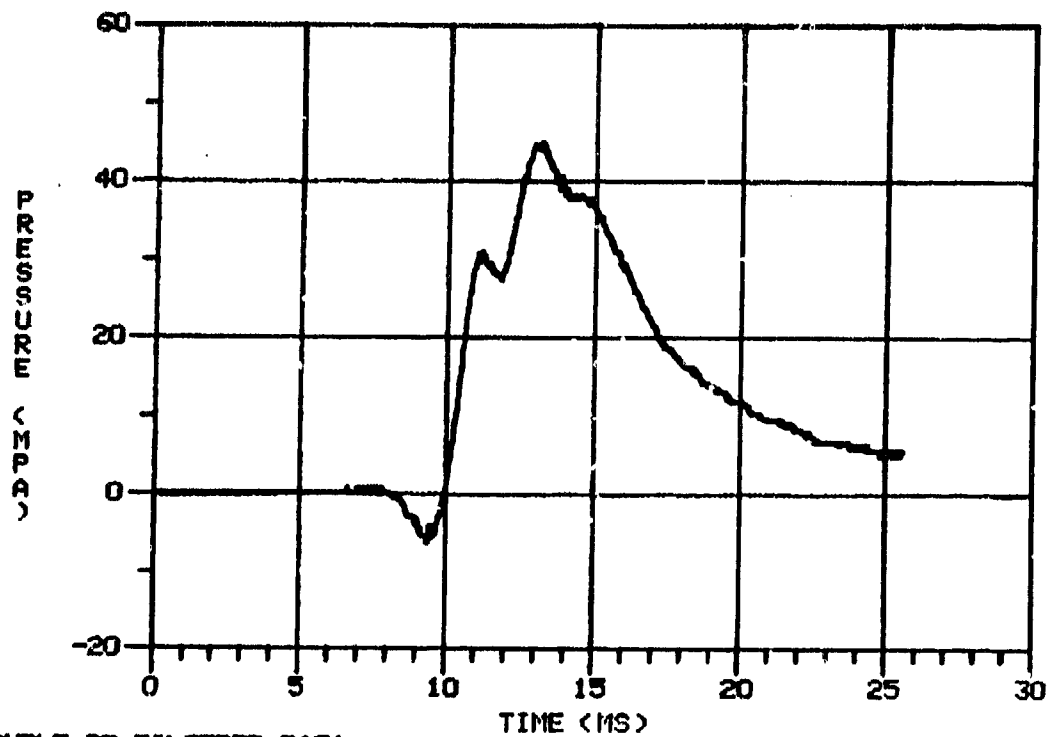
DOUBLE-BP-FILTERED DATA



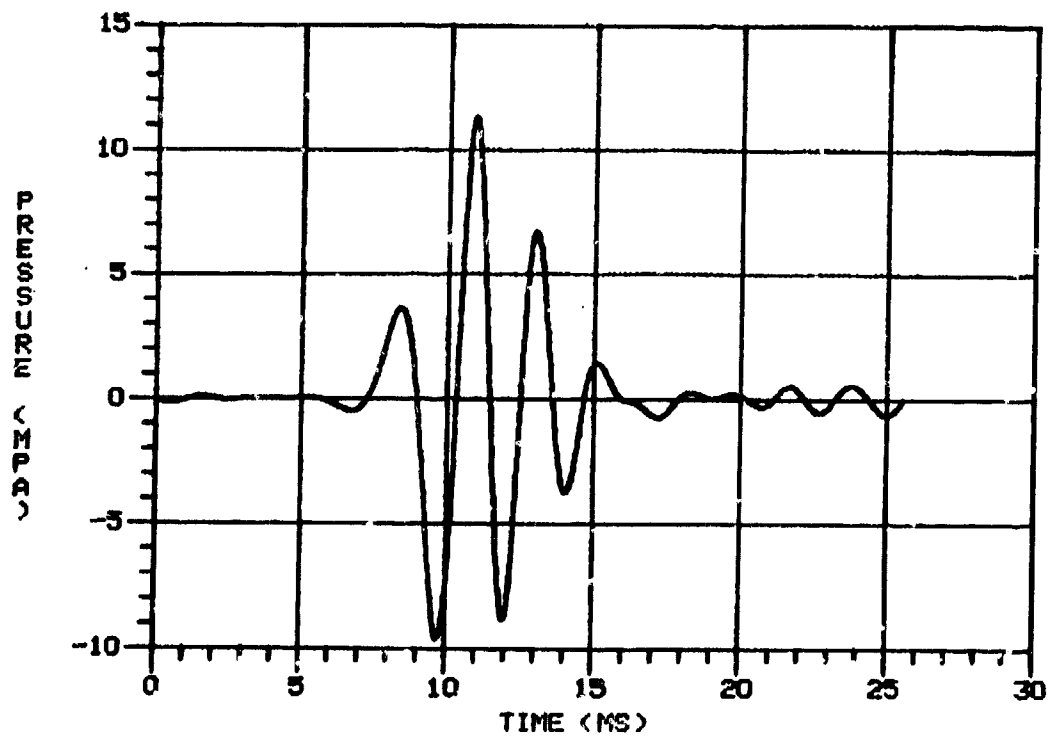


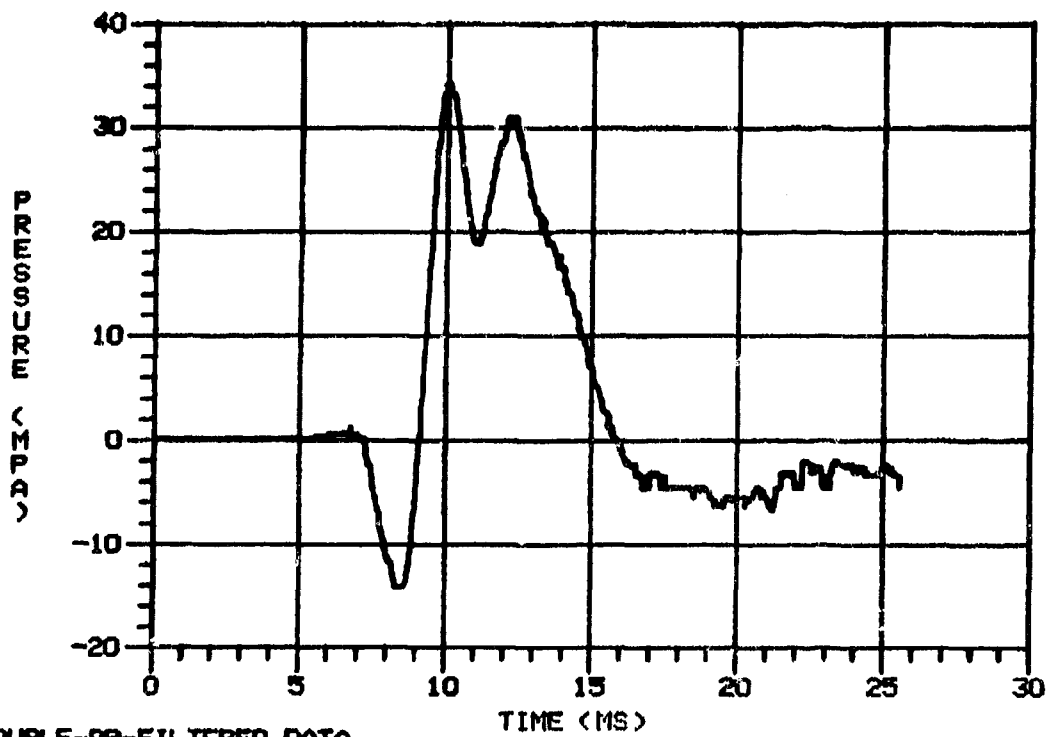
DOUBLE-BP-FILTERED DATA



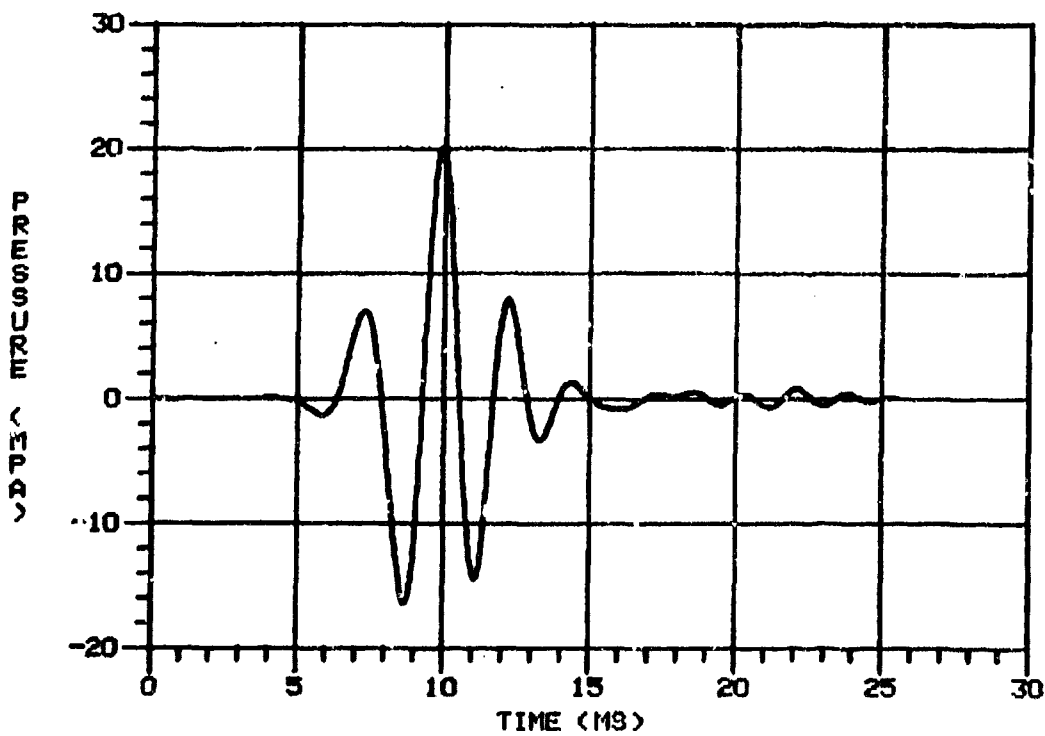


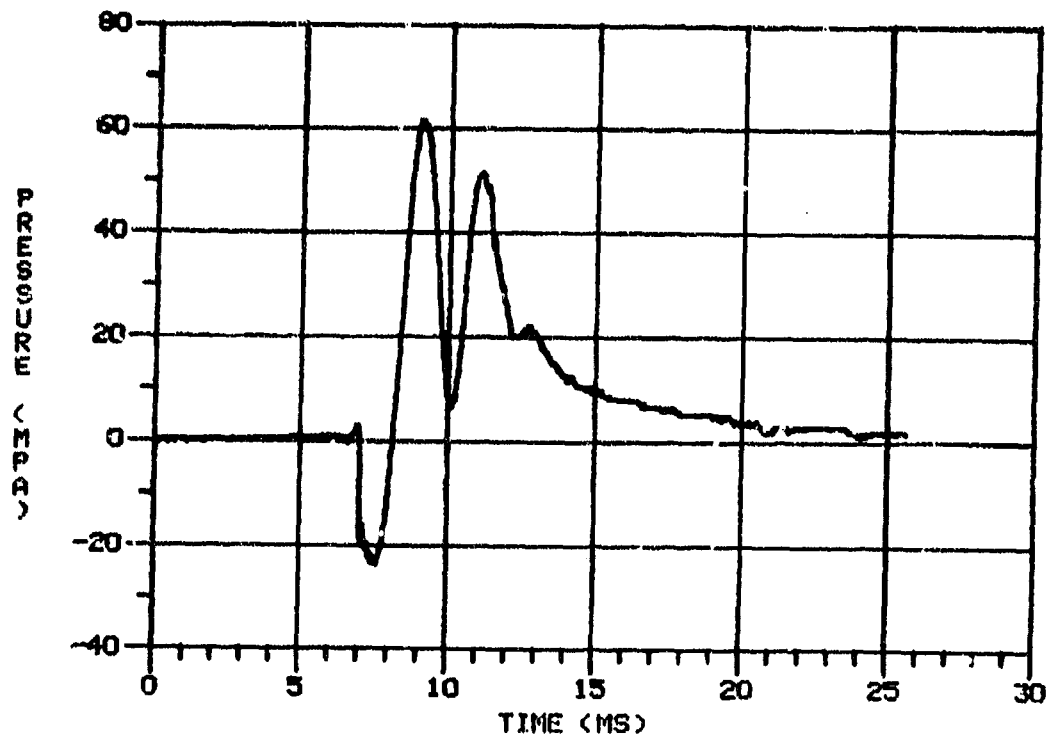
DOUBLE-BP-FILTERED DATA



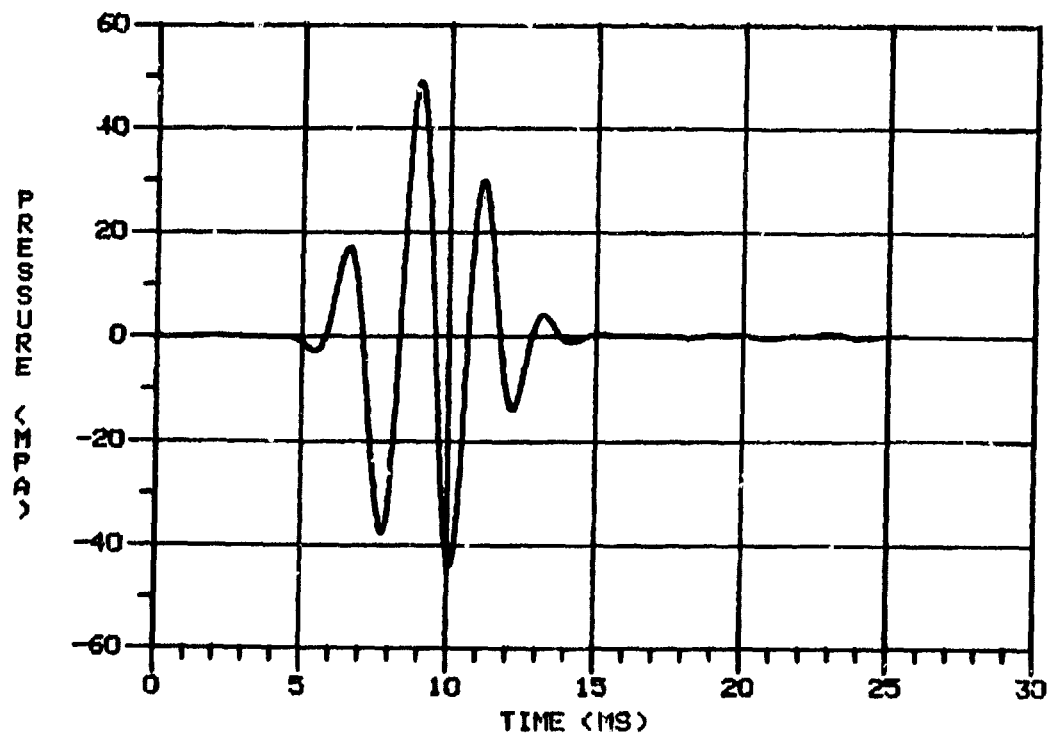


DOUBLE-BP-FILTERED DATA



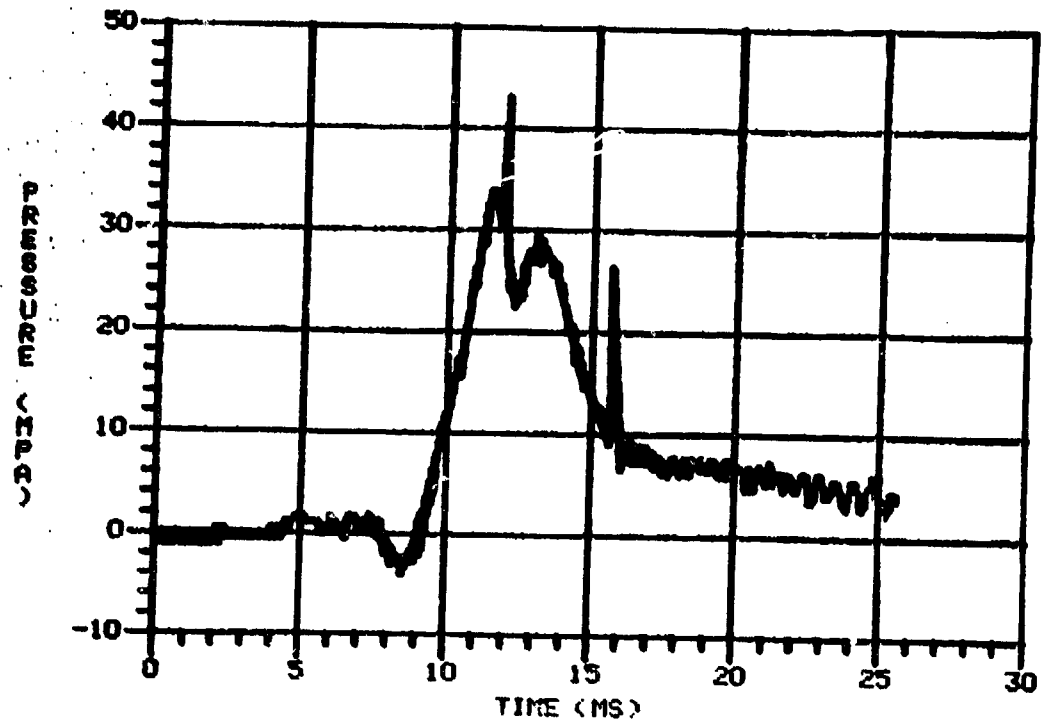


DOUBLE-BP-FILTERED DATA

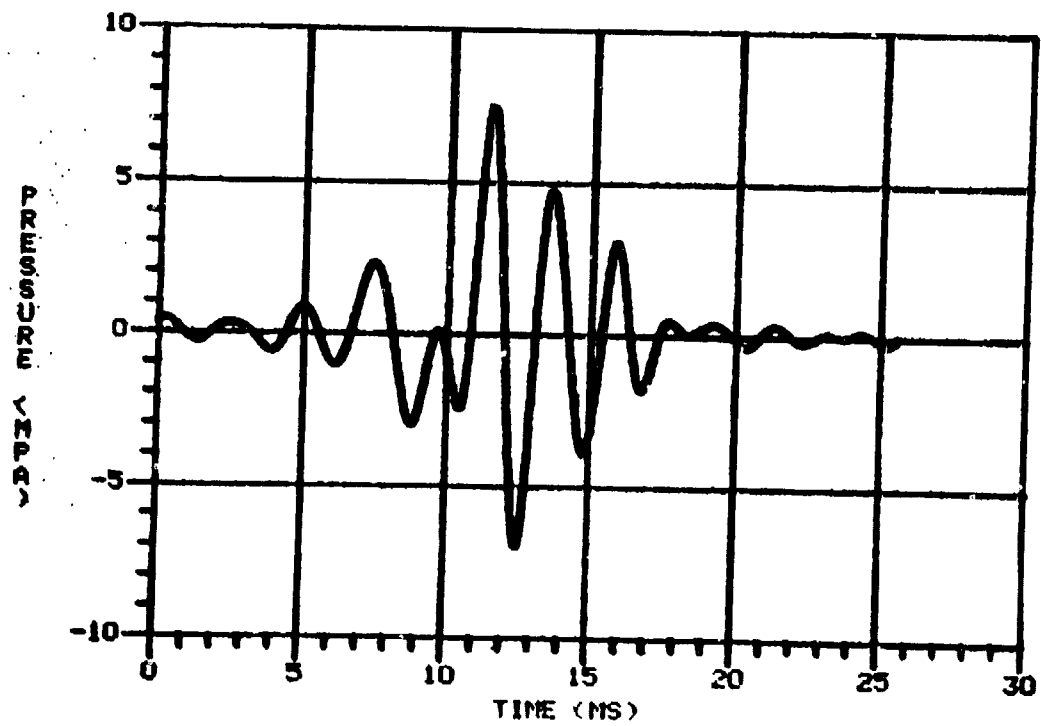


RAW PRESSURE: CHANNEL 1 LESS CHANNEL 5

STICK 004

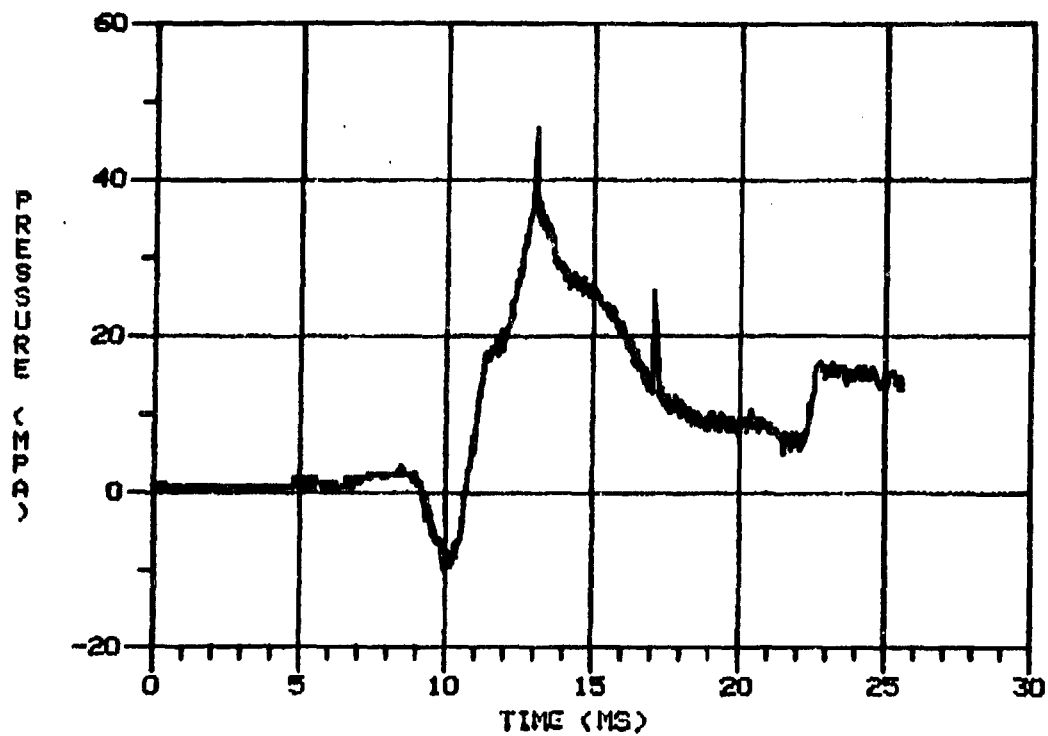


DOUBLE-BP-FILTERED DATA

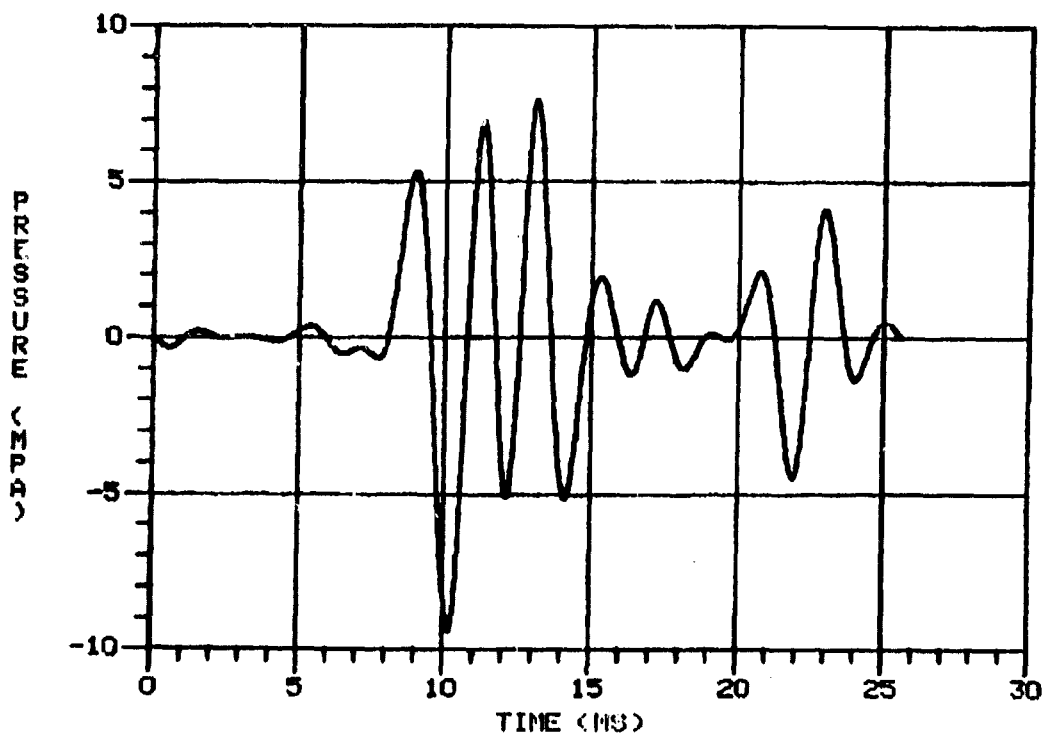


RAW PRESSURE CHANNEL 1 LESS CHANNEL 5

STICK 040

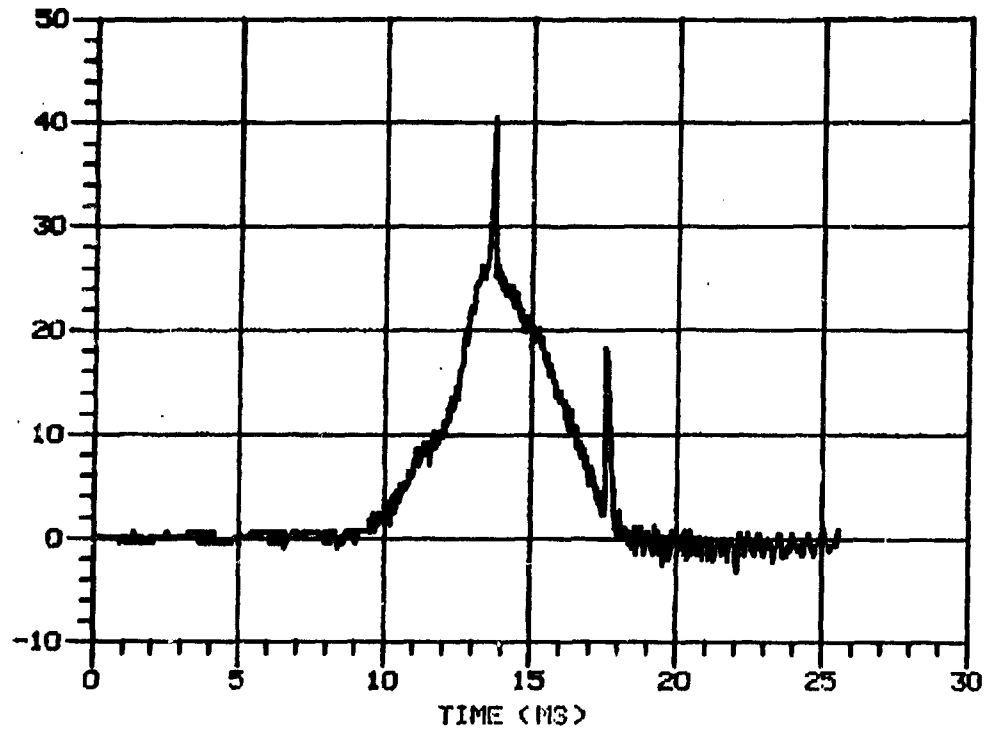


DOUBLE-BP-FILTERED DATA

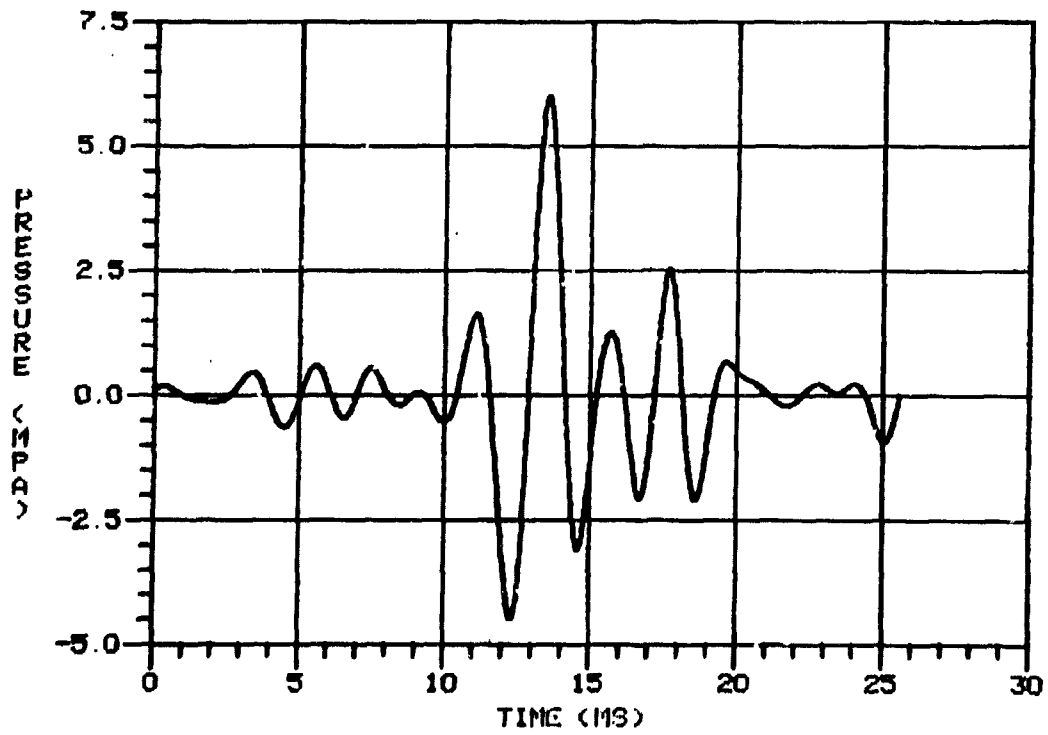


RAW PRESSURE: CHANNEL 1 LESS CHANNEL 5

STICK 053

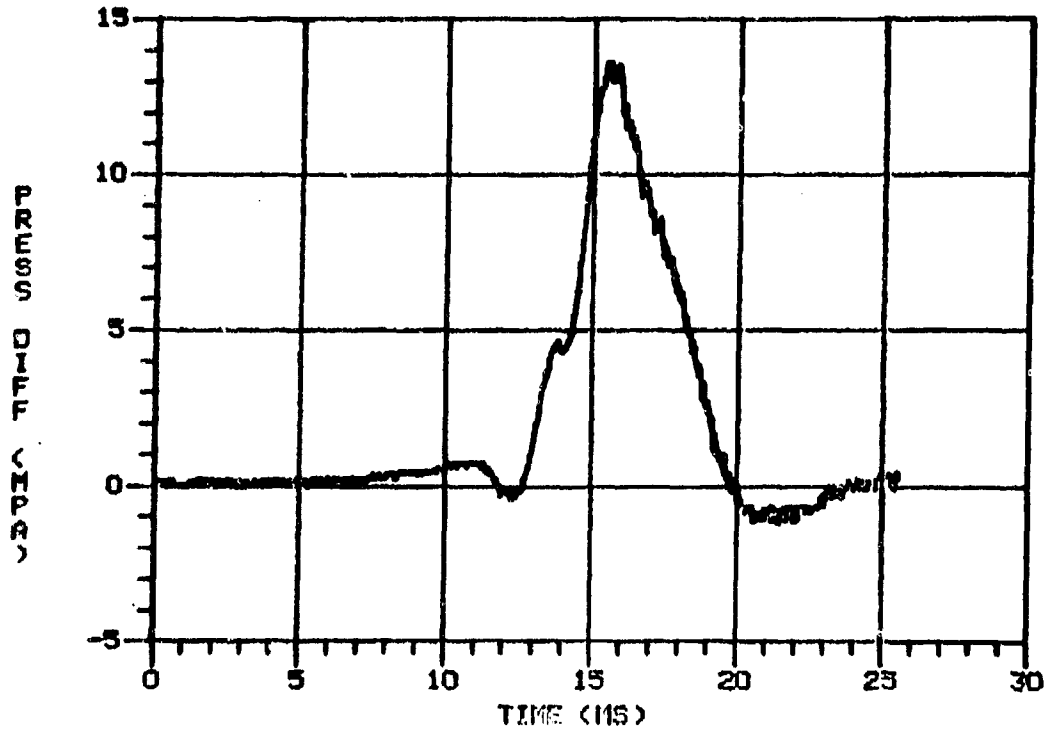


DOUBLE-BP-FILTERED DATA

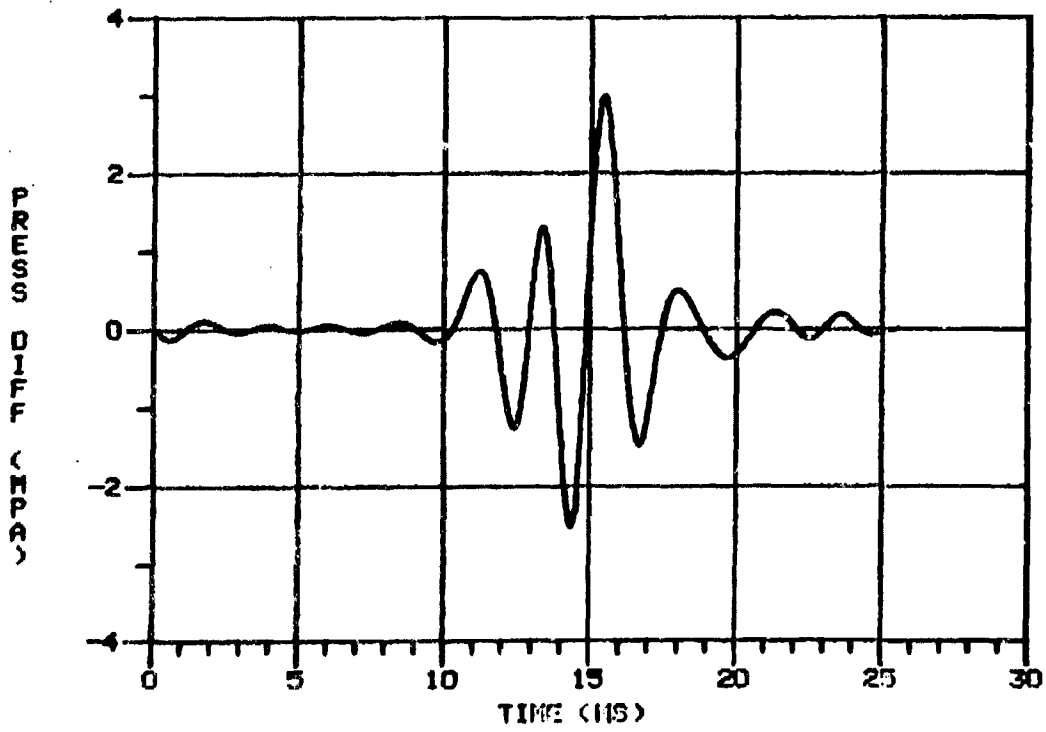


INCREASED LOAD DENSITY STICK

145

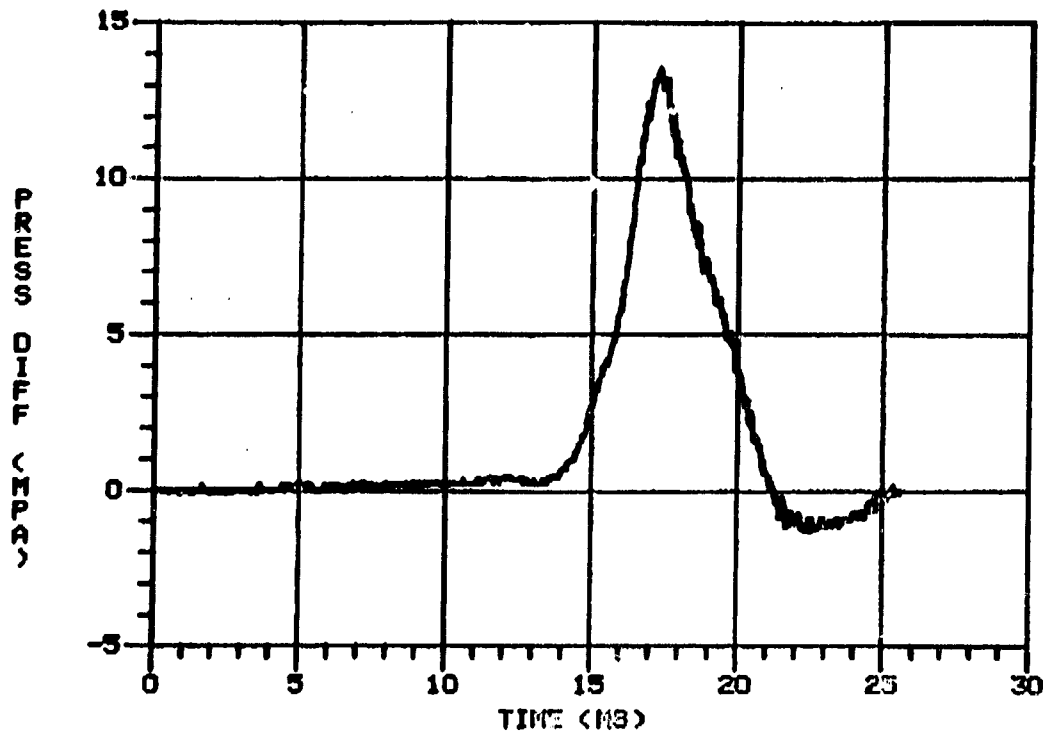


DOUBLE-BP-FILTERED DATA

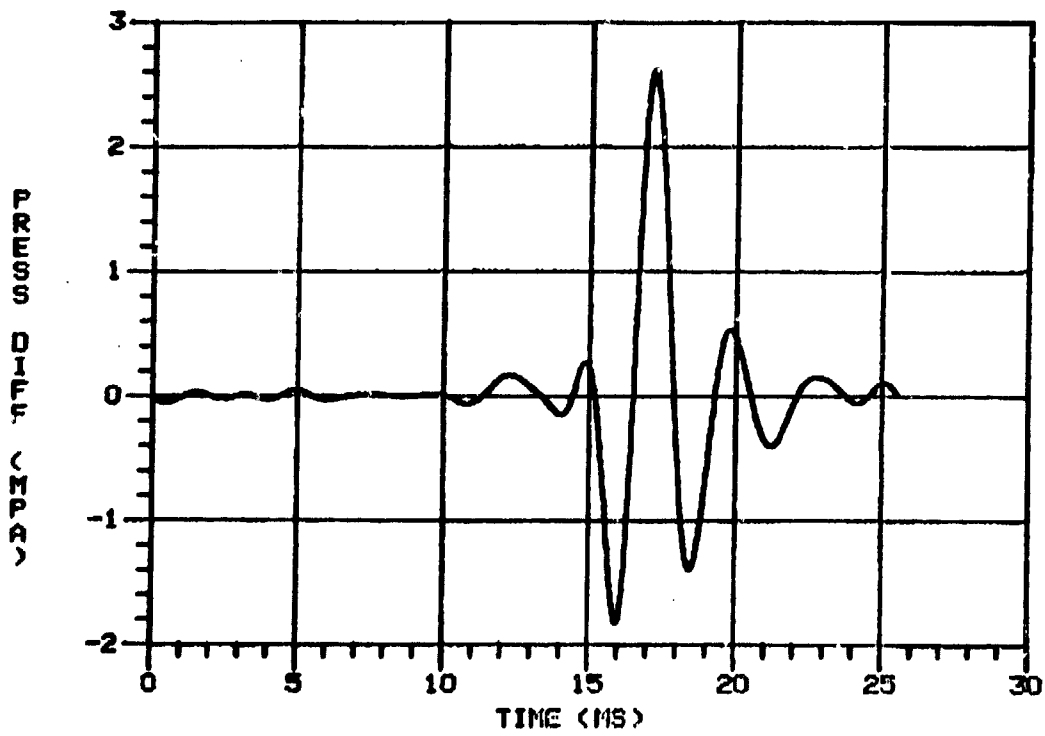


INCREASED LOAD DENSITY STICK

146

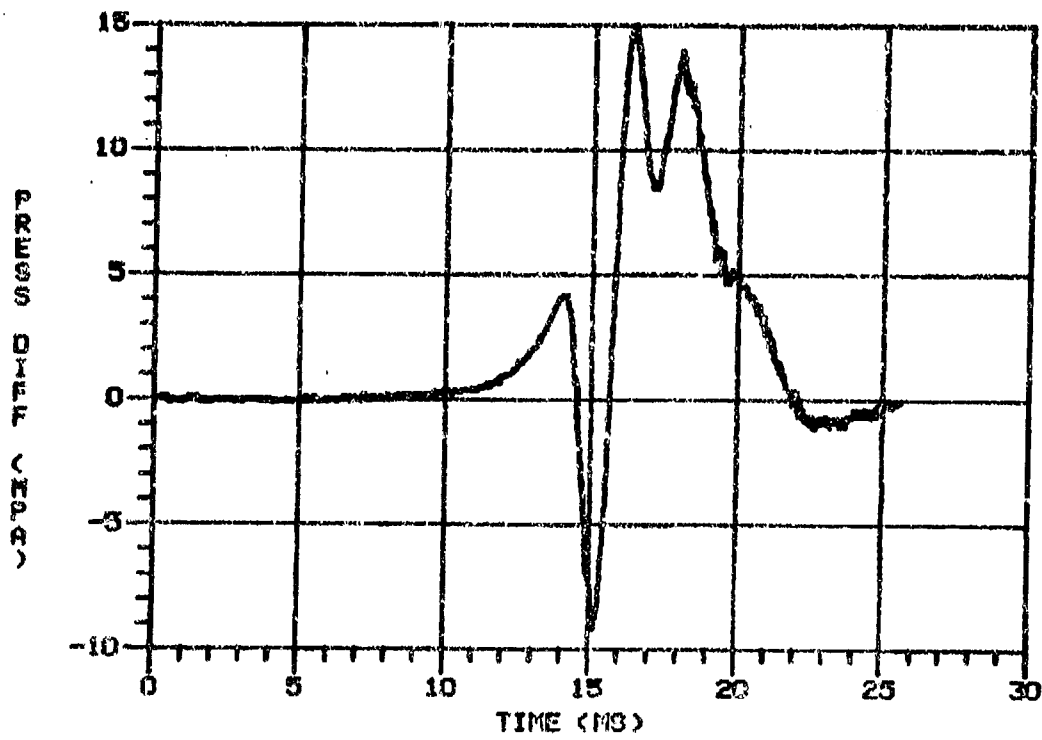


DOUBLE-BP-FILTERED DATA

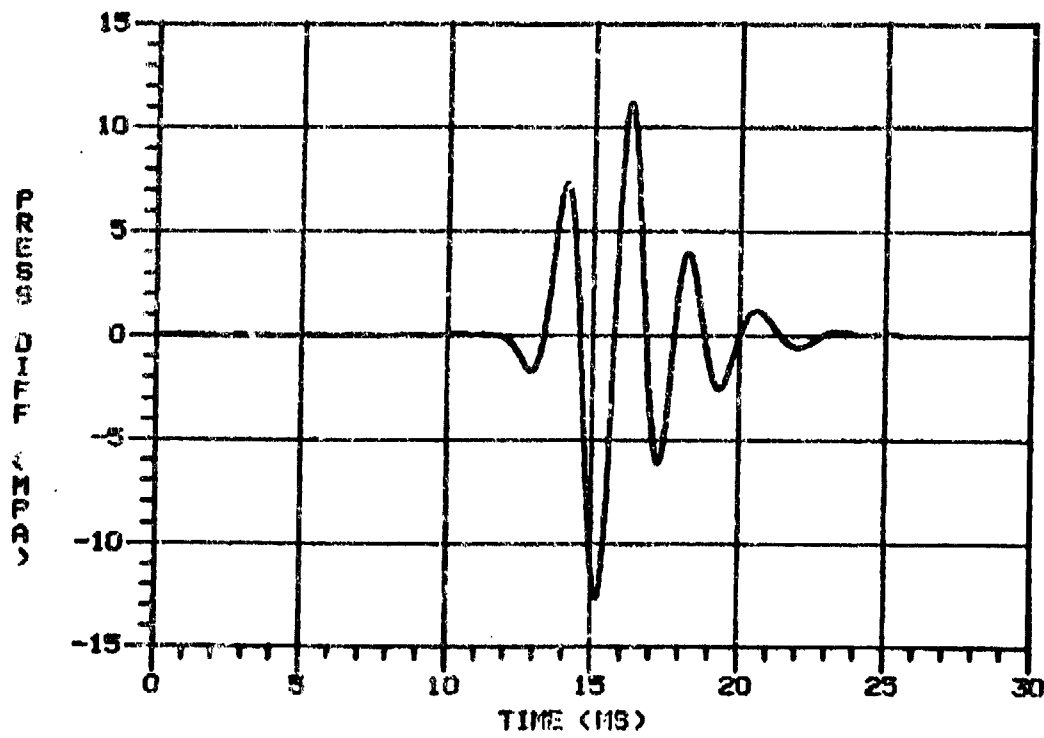


INCREASED LOAD DENSITY STICK

147

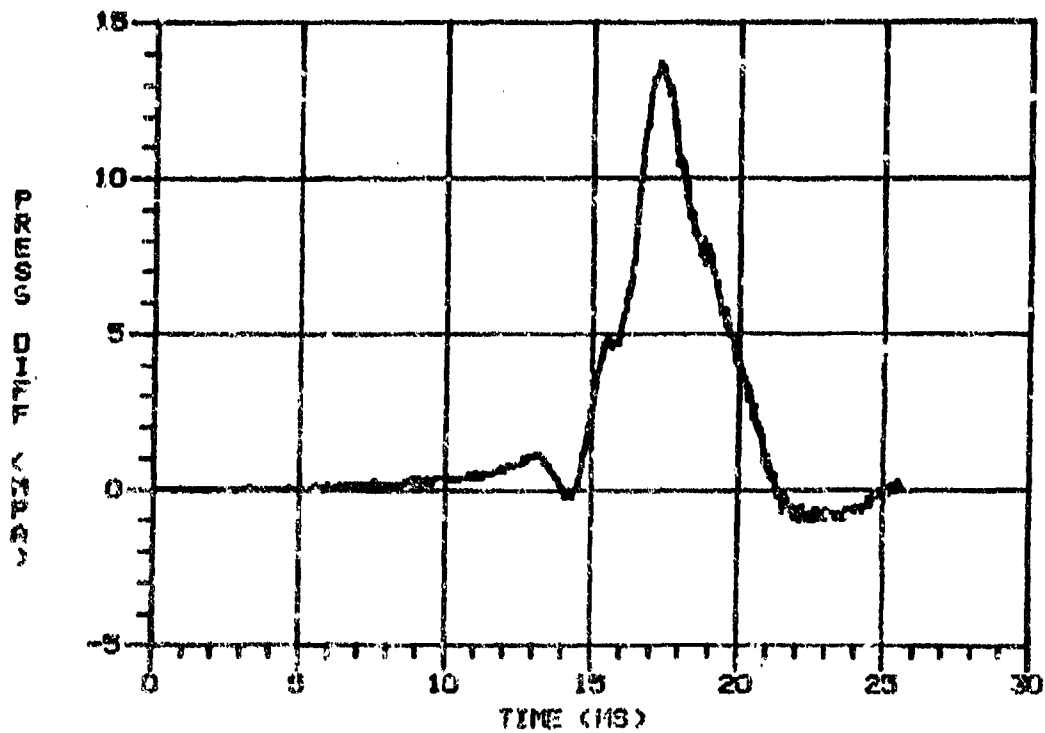


DOUBLE-BP-FILTERED DATA

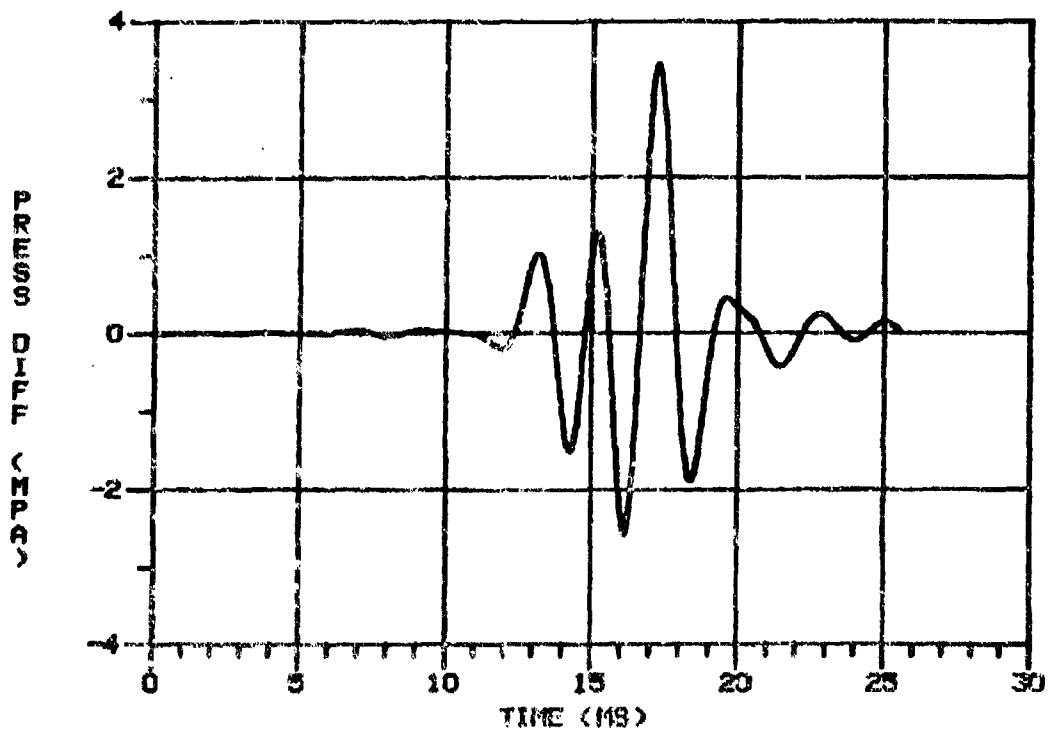


INCREASED LOAD DENSITY STICK

148

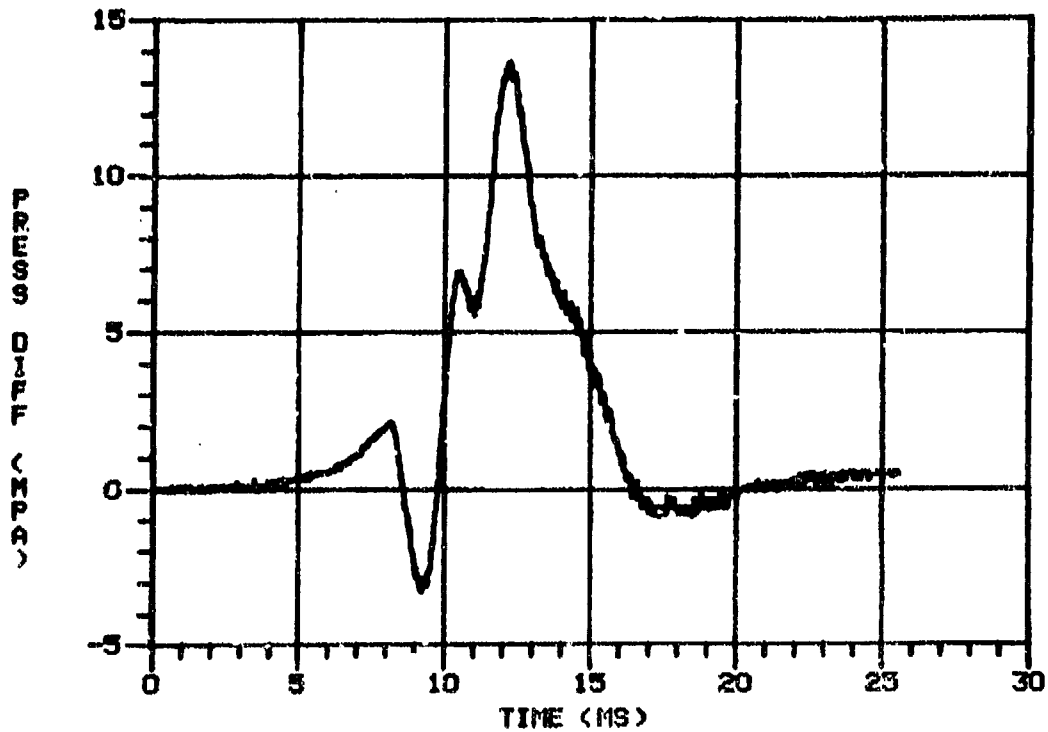


DOUBLE-BP-FILTERED DATA

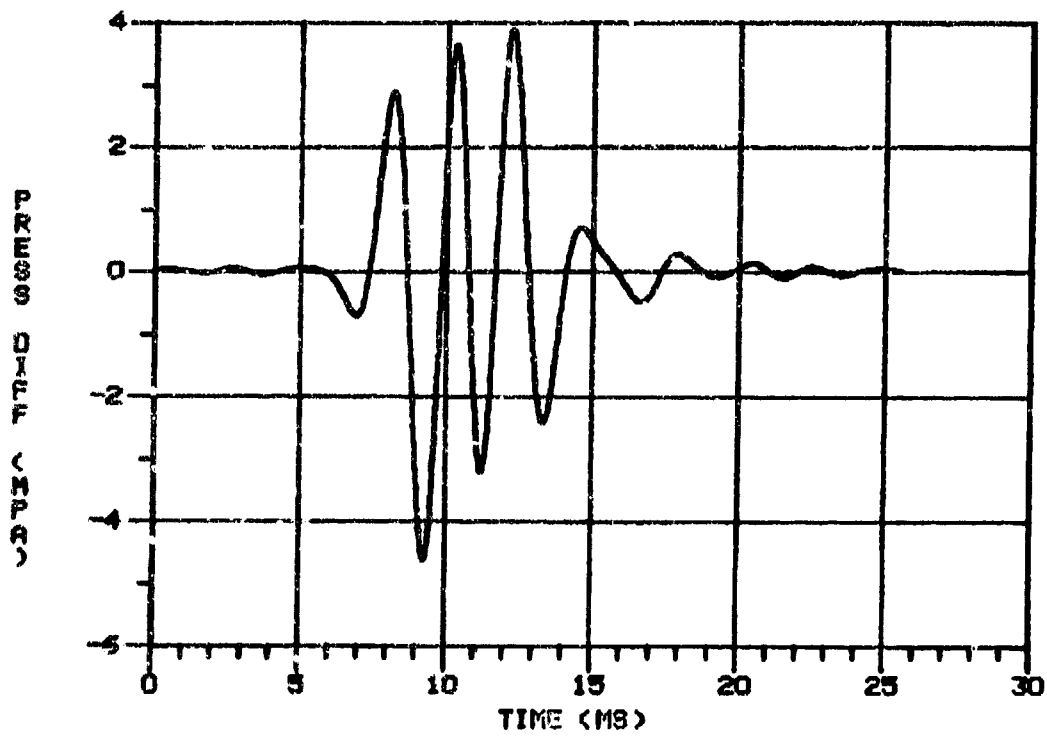


INCREASED LOAD DENSITY STICK

149

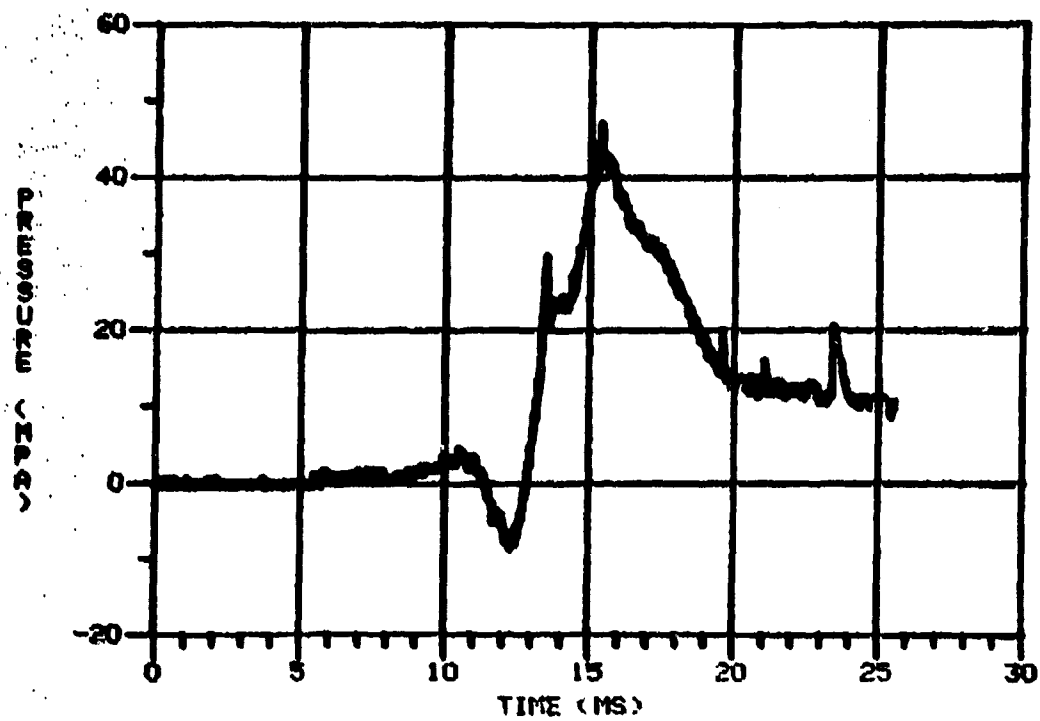


DOUBLE-BP-FILTERED DATA

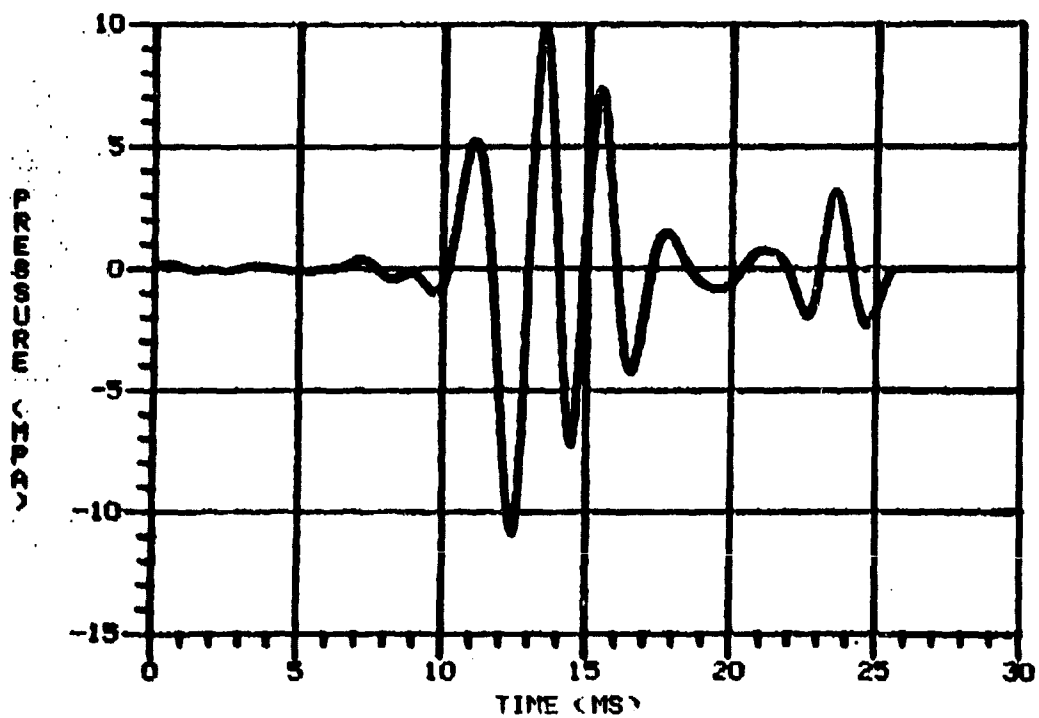


RAW PRESSURE CHANNEL 1 LESS CHANNEL 5

CCASE003

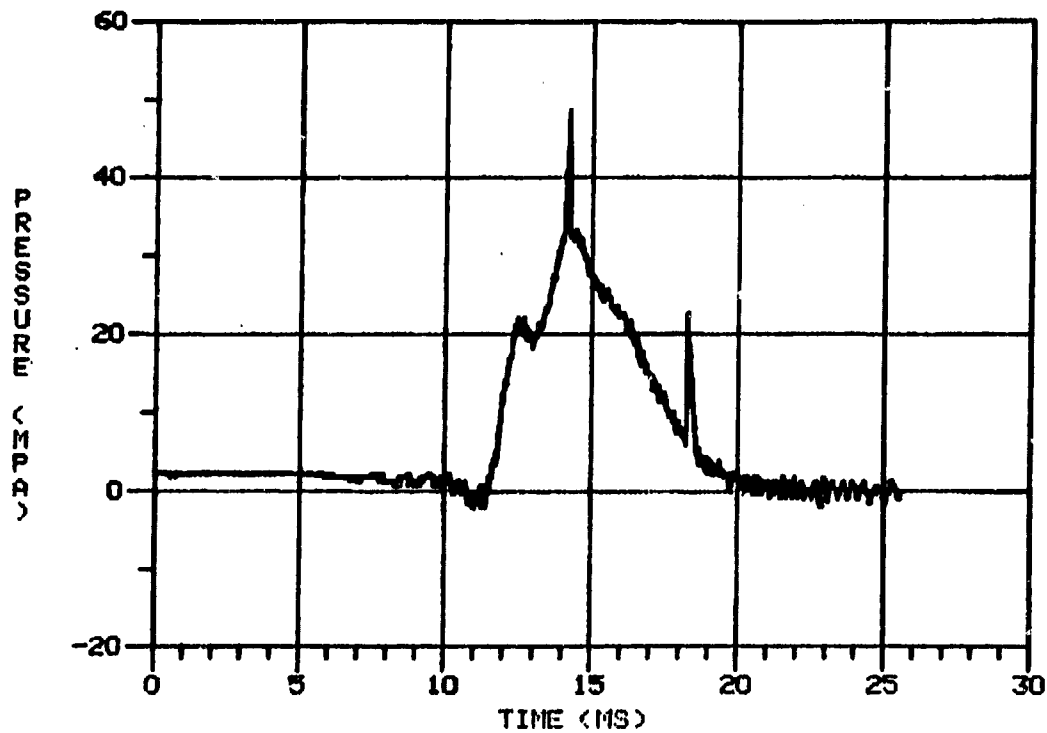


DOUBLE-BP-FILTERED DATA

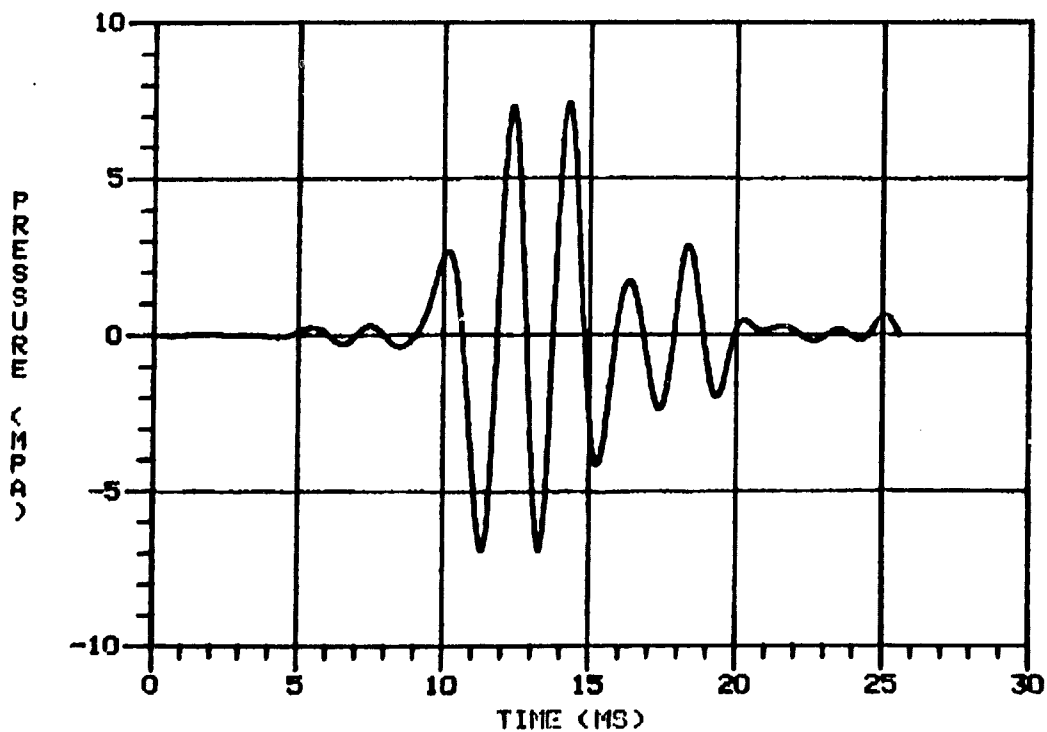


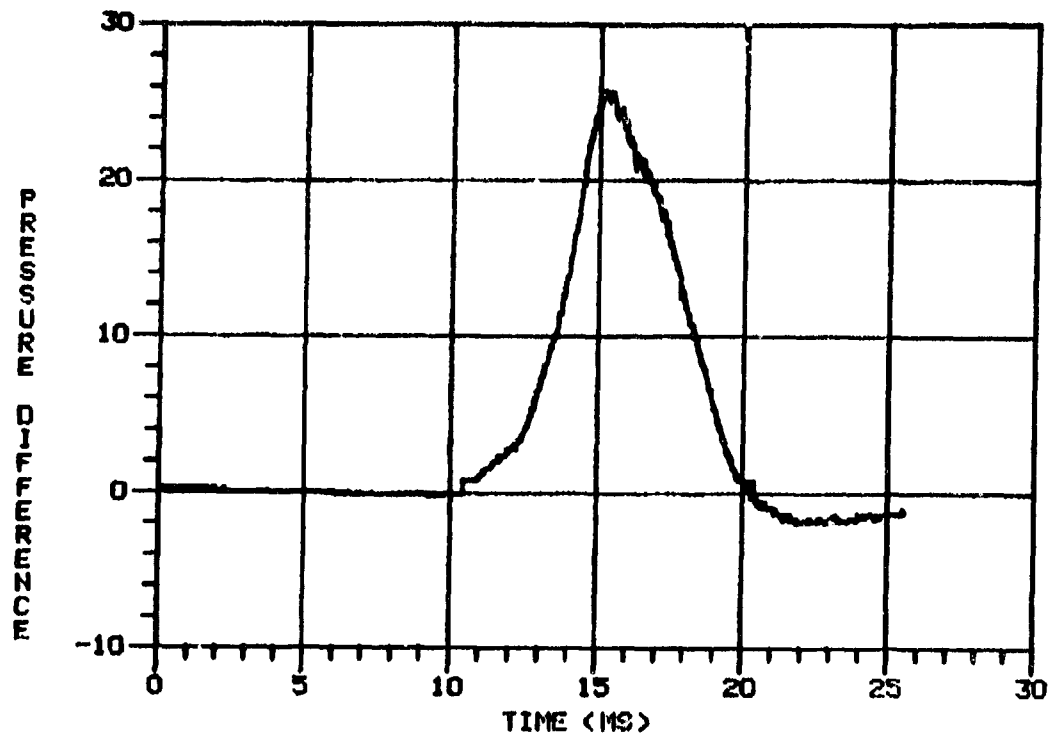
RAW PRESSURE: CHANNEL 1 LESS CHANNEL 5

CASE T14

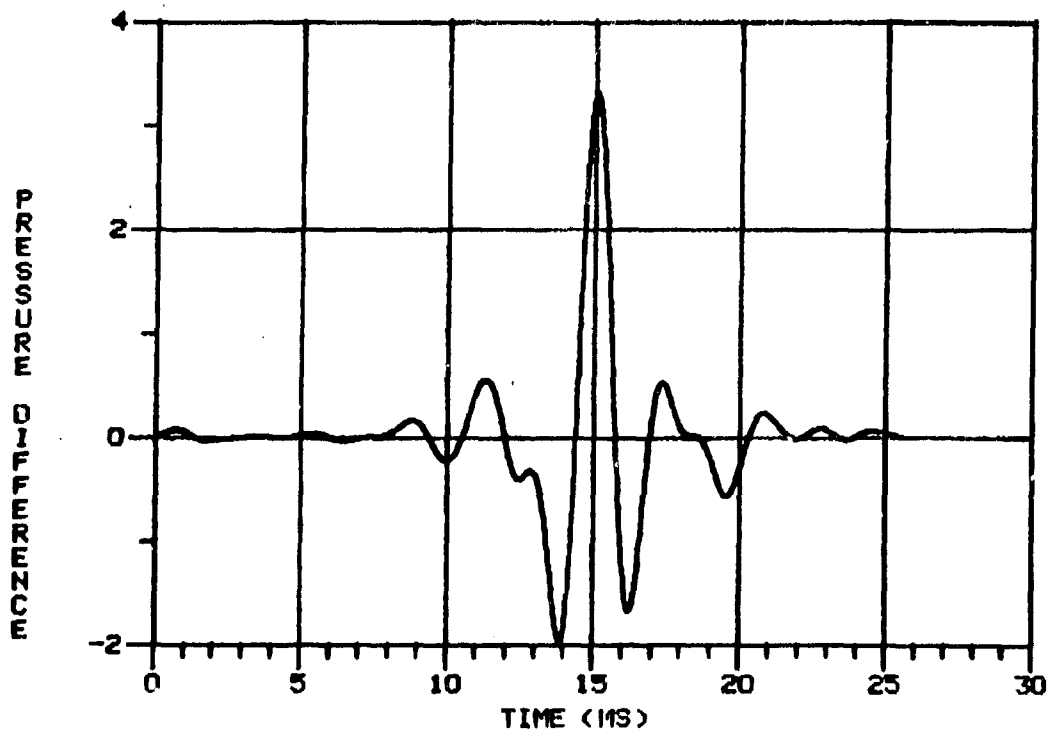


DOUBLE-BP-FILTERED DATA



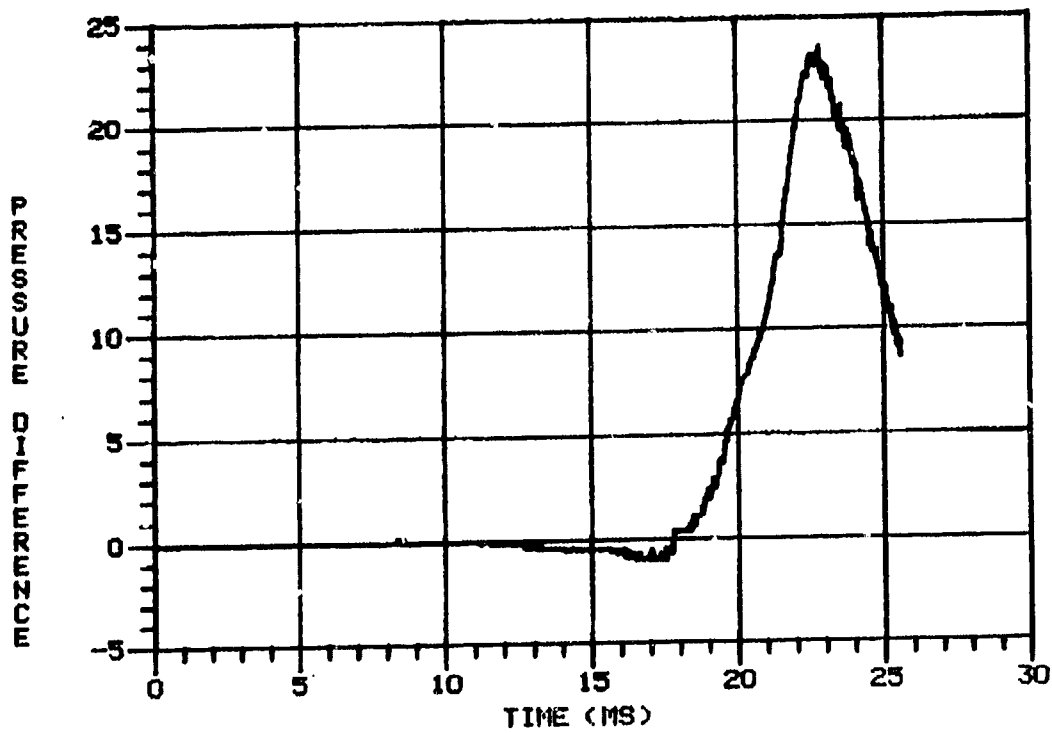


DOUBLE-BP-FILTERED DATA

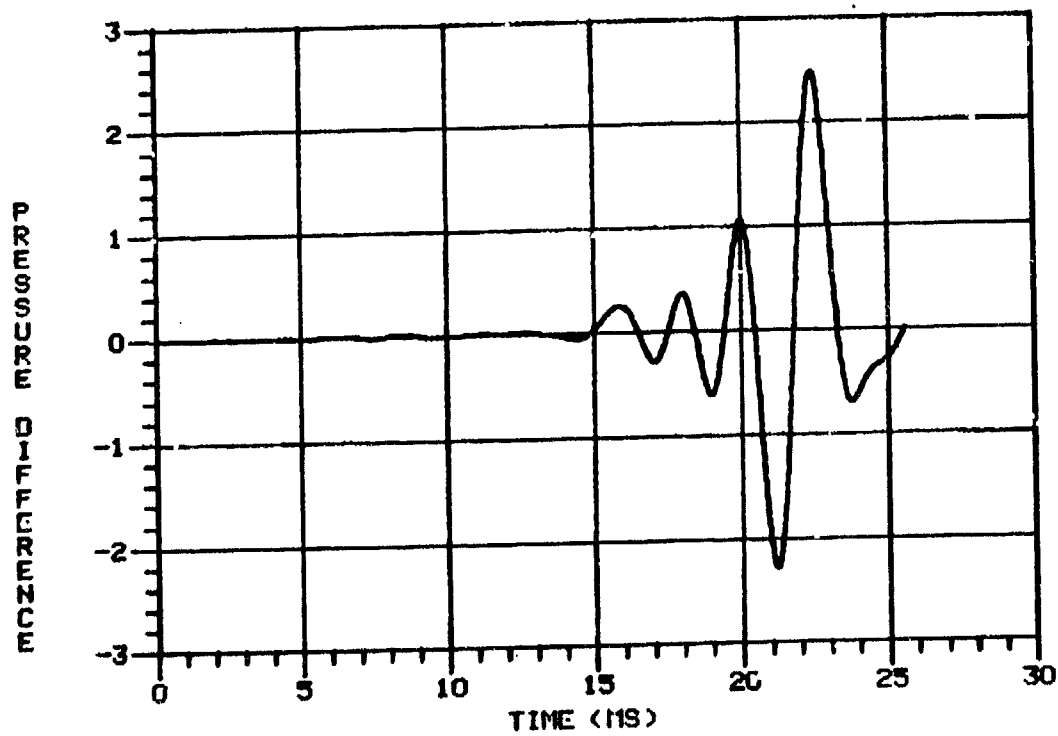


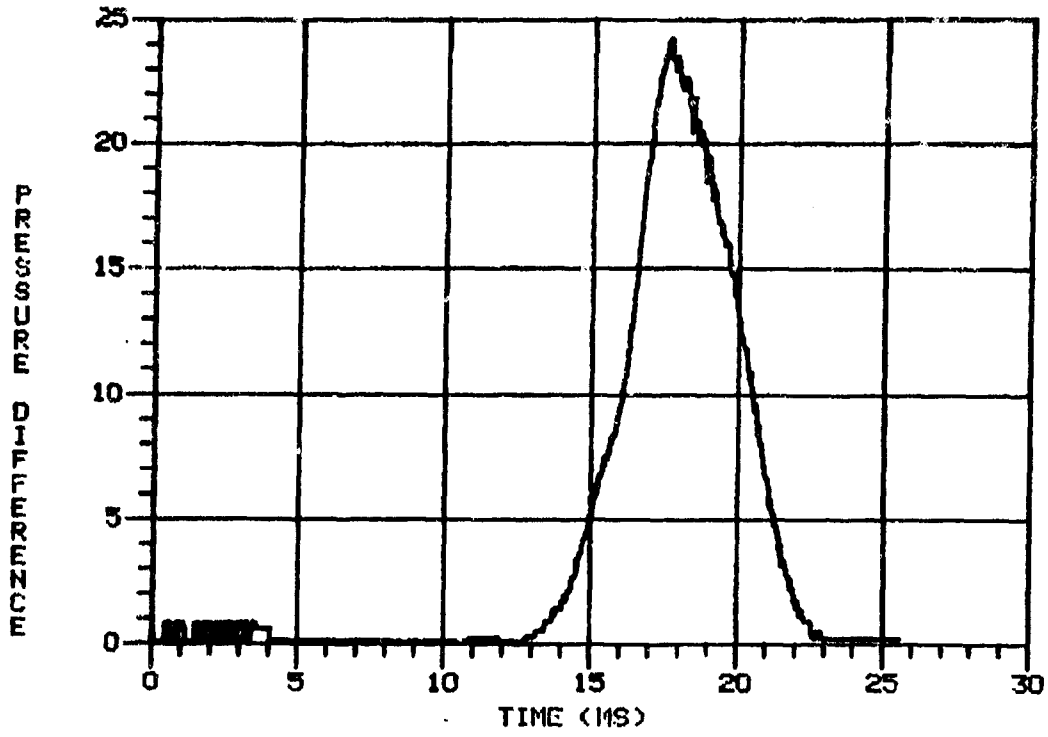
COMBUSTIBLE CASES

32

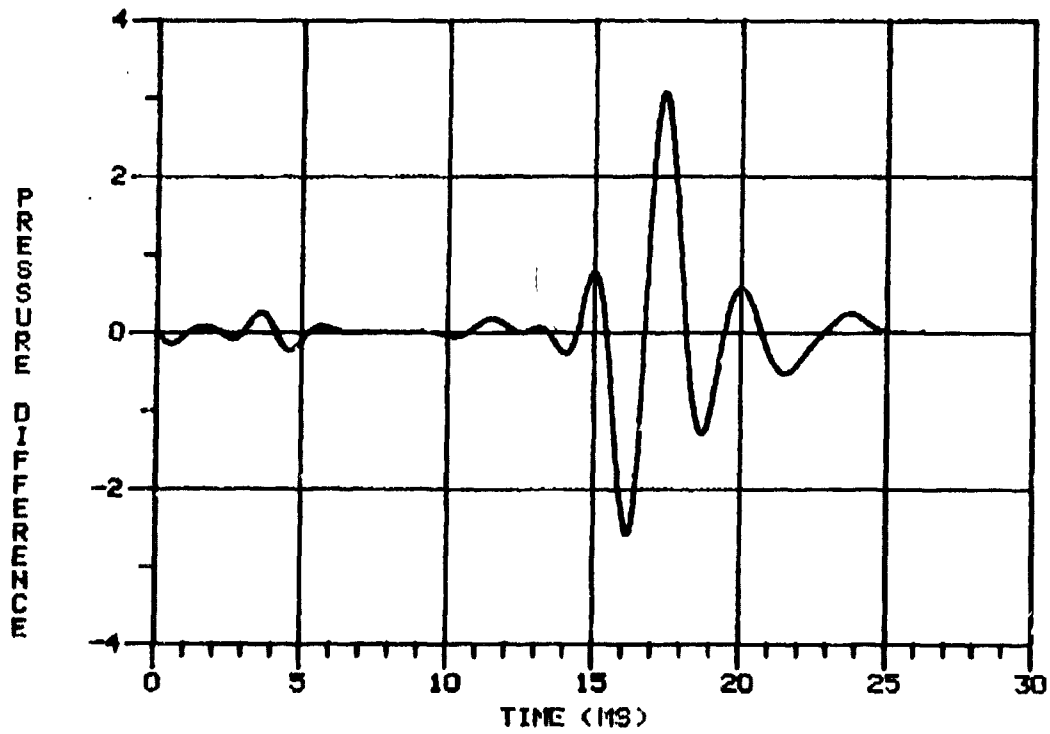


DOUBLE-BP-FILTERED DATA



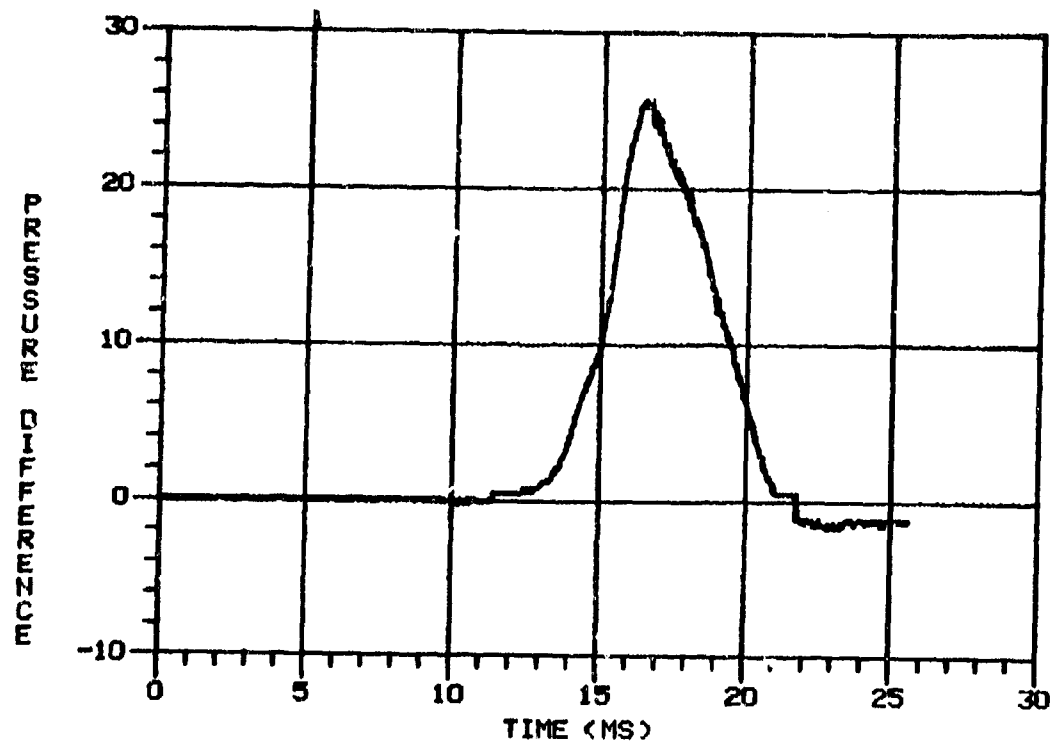


DOUBLE-BP-FILTERED DATA

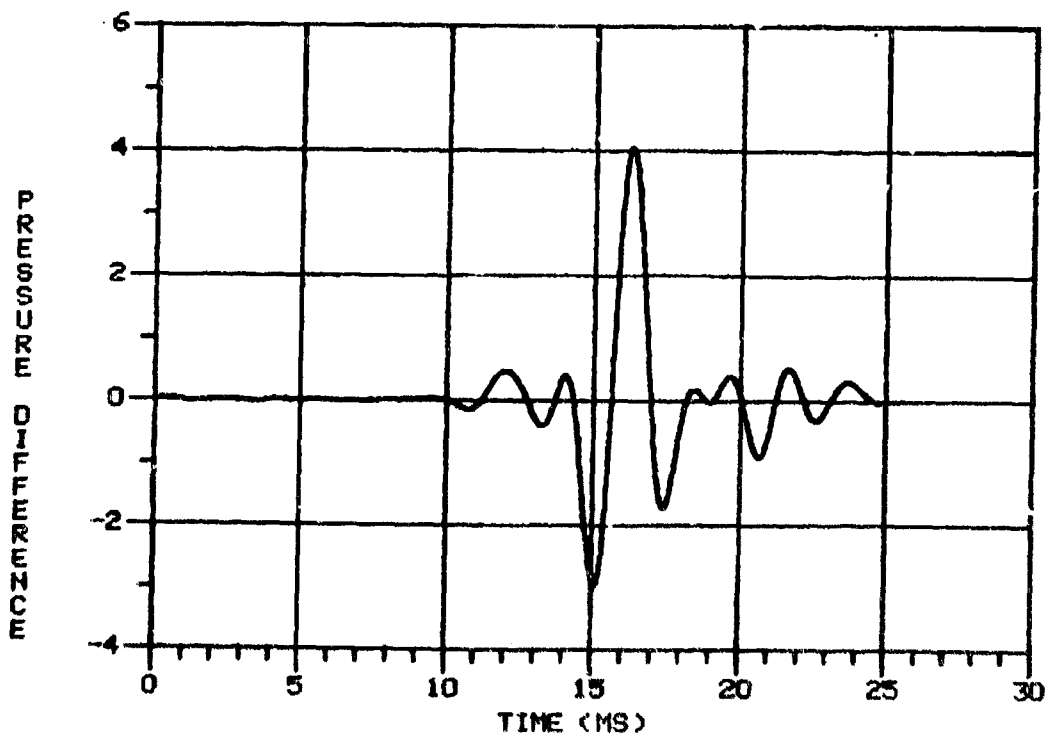


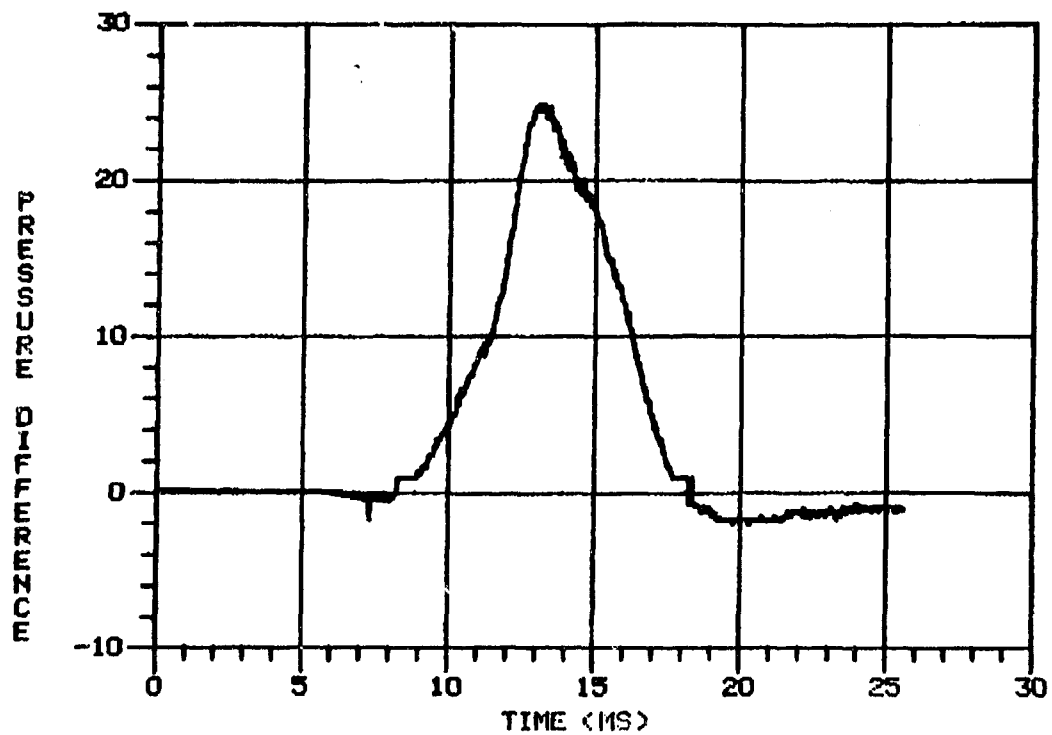
COMBUSTIBLE CASES

55

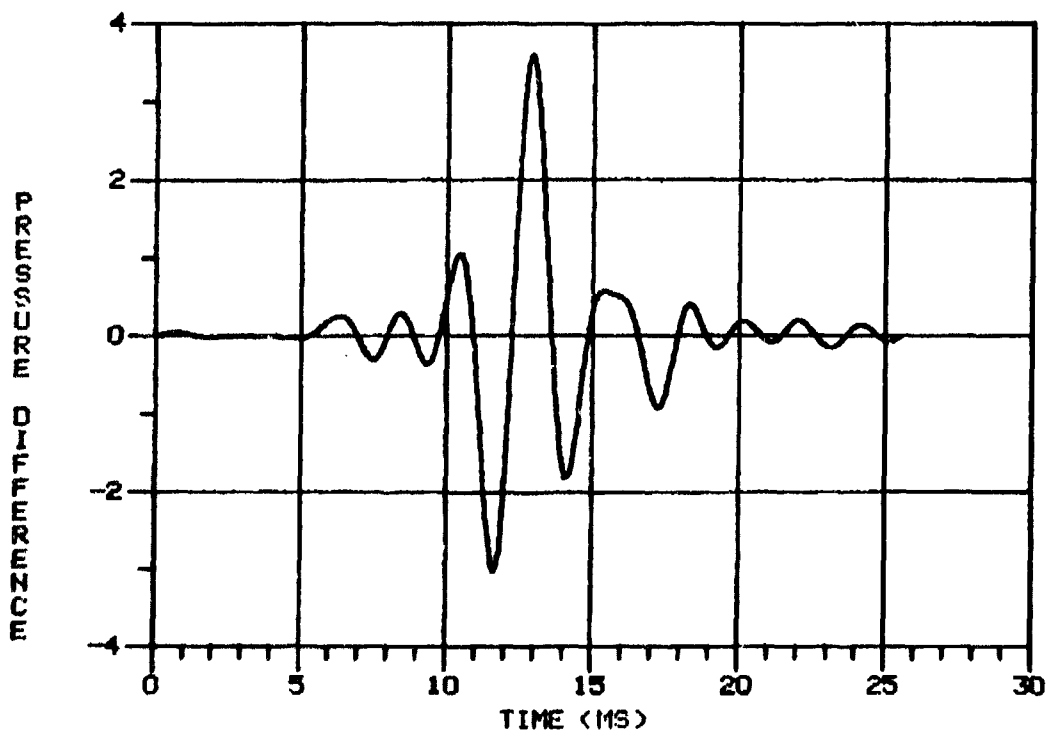


DOUBLE-BP-FILTERED DATA





DOUBLE-BP-FILTERED DATA



DISTRIBUTION LIST

<u>No. of Copies</u>	<u>Organization</u>	<u>No. of Copies</u>	<u>Organization</u>
12	Commander Defense Technical Info Center ATTN: DDC-DDA Cameron Station Alexandria, VA 22314	1	Director US Army ARRADCOM Benet Weapons Laboratory ATTN: DRDAR-LCB-TL Watervliet, NY 12189
1	Commander US Army Materiel Development and Readiness Command ATTN: DRCDMD-ST 5001 Eisenhower Avenue Alexandria, VA 22333	1	Commander US Army Aviation Research and Development Command ATTN: DRSAV-E P. O. Box 209 St. Louis, MO 63166
1	Commander US Army Materiel Development and Readiness Command ATTN: DRCDE-DW 5001 Eisenhower Avenue Alexandria, VA 22333	1	Director US Army Air Mobility Research and Development Laboratory Ames Research Center Moffett Field, CA 94035
10	Commander US Army Armament Research and Development Command ATTN: DRDAR-TSS (2 cys) DRDAR-LCA H. Fair S. Einstein S. Bernstein P. Kemmey D. Downs L. Schlosberg DRDAR-LCE, R. Walker DRDAR-SCA, L. Stiefel Dover, NJ 07801	1	Commander US Army Communications Rsch and Development Command ATTN: DRDCO-PPA-SA Fort Monmouth, NJ 07703
1	Commander US Army Armament Materiel Readiness Command ATTN: DRDAR-LEP-L, Tech Lib Rock Island, IL 61299	1	Commander US Army Electronics Research and Development Command Technical Support Activity ATTN: DELSD-L Fort Monmouth, NJ 07703
1	Commander US Army Watervliet Arsenal ATTN: SARWV-RD, R. Thierry Watervliet, NY 12189	1	Commander US Army Missile Command ATTN: DRSMI-R Redstone Arsenal, AL 35809
		1	Commander US Army Missile Command ATTN: DRSMI-YDL Redstone Arsenal, AL 35809

DISTRIBUTION LIST

<u>No. of Copies</u>	<u>Organization</u>	<u>No. of Copies</u>	<u>Organization</u>
1	Commander US Army Natick Research and Development Command ATTN: DRXRE, D. Sieling Natick, MA 01762	5	Commander Naval Surface Weapons Center ATTN: Code G33, J. East D. McClure W. Burrell J. Johndrow Code DX-21, Tech Lib Dahlgren, VA 22448
1	Commander US Army Tank Automotive Research & Development Cmd ATTN: DRDTA-UL Warren, MI 48090	3	Commander Naval Surface Weapons Center ATTN: S. Jacobs/Code 240 Code 730 K. Kim/Code R-13 Silver Spring, MD 20910
2	Commander US Army Materials and Mechanics Research Center ATTN: DRXMR-ATL Tech Lib Watertown, MA 02172	1	Commander Naval Underwater Systems Ctr Energy Conversion Dept. ATTN: Code 5B331, R. Lazar Newport, RI 02840
1	Commander US Army Research Office ATTN: Tech Lib P. O. Box 12211 Research Triangle Park NC 27706	2	Commander Naval Weapons Center ATTN: Code 388, R. Derr C. Price China Lake, CA 93555
1	Director US Army TRADOC Systems Analysis Activity ATTN: ATAA-SL, Tech Lib White Sands Missile Range NM 88002	1	Superintendent Naval Postgraduate School Dept of Mechanical Engineering ATTN: A. Fuhs Monterey, CA 93940
1	Chief of Naval Research ATTN: Code 473, R. Miller 800 N. Quincy Street Arlington, VA 22217	2	Commander Naval Ordnance Station ATTN: P. Stang C. Smith Indian Head, MD 20640
1	Commander Naval Sea Systems Command ATTN: SEA-62R2, J. Murrin National Center, Bldg. 2 Room 6E08 Washington, DC 20360	1	AFOSR (L. Caveny) Bolling AFB, DC 20332

DISTRIBUTION LIST

<u>No. of Copies</u>	<u>Organization</u>	<u>No. of Copies</u>	<u>Organization</u>
2	AFRPL (DYSC) ATTN: D. George J. Levine Edwards AFB, CA 93523	1	General Electric Company Armament Systems Dept. ATTN: M. Bulman, Rm. 1311 Lakeside Avenue Burlington, VT 05402
1	AFATL/DL DL (O. Heiney) Eglin AFB, FL 32542	1	Hercules, Inc. Allegheny Ballistics Laboratory ATTN: R. Miller P. O. Box 210 Cumberland, MD 21502
1	Aerofjet Solid Propulsion Co. ATTN: P. Micheli Sacramento, CA 95813	1	Hercules, Inc. Bacchus Works ATTN: K. McCarty P. O. Box 98 Magna, UT 84044
1	ARO Incorporated ATTN: N. Dougherty Arnold AFS, TN 37389	1	Hercules, Inc. Eglin Operations AFATL/DL DL ATTN: R. Simmons Eglin AFB, FL 32542
1	Atlantic Research Corporation ATTN: M. King 5390 Cherokee Avenue Alexandria, VA 22314	1	IITRI ATTN: M. J. Klein 10 W. 35th Street Chicago, IL 60615
1	AVCO Corporation AVCO Everett Rsch Lab Div ATTN: D. Stickler 2385 Revere Beach Parkway Everett, MA 02149	1	Lawrence Livermore Laboratory ATTN: M.S. L-355, A. Buckingham P. O. Box 808 Livermore, CA 94550
1	Calspan Corporation ATTN: E. Fisher P. O. Box 400 Buffalo, NY 14221	1	Olin Corporation Badger Army Ammunition Plant ATTN: R. Thiede Baraboo, WI 53913
1	Foster Miller Associates, Inc. ATTN: A. Erickson 135 Second Avenue Waltham, MA 02154	1	Olin Corporation Smokeless Powder Operations ATTN: R. Cook P. O. Box 222 St. Marks, FL 32355
1	General Applied Science Labs ATTN: J. Erdos Merrick & Stewart Avenues Westbury Long Island, NY 11590		

DISTRIBUTION LIST

<u>No. of Copies</u>	<u>Organization</u>	<u>No. of Copies</u>	<u>Organization</u>
1	Paul Gough Associates, Inc. ATTN: P. Gough P. O. Box 1614 Portsmouth, NH 03801	2	Thiokol Corporation Wasatch Division ATTN: John Peterson Tech Lib P. O. Box 524 Brigham City, UT 84302
1	Physics International Company 2700 Merced Street Leandro, CA 94577	2	United Technologies ATTN: R. Brown Tech Lib P. O. Box 358 Sunnyvale, CA 94086
1	Princeton Combustion Rsch Labs ATTN: M. Summerfield 1041 US Highway One North Princeton, NJ 08540	1	Universal Propulsion Company ATTN: H. McSpadden 1800 W. Deer Valley Road Phoenix, AZ 85027
1	Pulsepower Systems, Inc. ATTN: L. Elmore 815 American Street San Carlos, CA 94070	1	Battelle Memorial Institute ATTN: Tech Lib 505 King Avenue Columbus, OH 43201
1	Rockwell International Corp. Rocketdyne Division ATTN: BA08, J. Flanagan 6633 Canoga Avenue Canoga Park, CA 91304	1	Brigham Young University Dept of Chemical Engineering ATTN: Dr. M. Beckstead Provo, UT 84601
1	Science Applications, Inc. ATTN: R. Edelman 23146 Cumorah Crest Woodland Hills, CA 91364	1	California Institute of Tech 204 Karman Lab Mail Stop 301-46 ATTN: F.E.C. Culick 1201 E. California Street Pasadena, CA 91125
1	Scientific Research Assoc. Inc. ATTN: H. McDonald P. O. Box 498 Glastonbury, CT 06033	1	California Institute of Tech Jet Propulsion Laboratory ATTN: L. Strand 4800 Oak Grove Drive Pasadena, CA 91103
1	Shock Hydrodynamics, Inc. ATTN: W. Anderson 4710-16 Vineland Avenue North Hollywood, CA 91602		
3	Thiokol Corporation Huntsville Division ATTN: D. Flanigan R. Glick Tech Lib Huntsville, AL 35807		

DISTRIBUTION LIST

<u>No. of</u> <u>Copies</u>	<u>Organization</u>	<u>No. of</u> <u>Copies</u>	<u>Organization</u>
1	Case Western Reserve University Division of Aerospace Sciences ATTN: J. Tien Cleveland, OH 44135	1	Purdue University School of Mechanical Engineering ATTN: J. Osborn TSPC Chaffee Hall West Lafayette, IN 47906
3	Georgia Institute of Tech School of Aerospace Eng. ATTN: B. Zinn E. Price W. Strahle Atlanta, GA 30332	1	Rutgers State University Dept. of Mechanical and Aerospace Engineering ATTN: S. Temkin University Heights Campus New Brunswick, NJ 08903
1	Institute of Gas Technology ATTN: D. Gidaspow 3424 S. State Street Chicago, IL 60616	1	Rensselaer Polytechnic Inst. Department of Mathematics ATTN: D. Drew Troy, NY 12181
1	Johns Hopkins University Applied Physics Laboratory Chemical Propulsion Infor- mation Agency ATTN: T. Christian Johns Hopkins Road Laurel, MD 20810	1	SRI International Propulsion Sciences Division ATTN: Tech Lib 333 Ravenswood Avenue Menlo Park, CA 94024
1	Massachusetts Institute of Technology Dept. of Mechanical Engineering ATTN: T. Toong Cambridge, MA 02139	1	Stevens Institute of Tech Davidson Laboratory ATTN: R. McAlevy, III Hoboken, NJ 07030
1	Pennsylvania State University Applied Research Lab ATTN: G. Faeth P. O. Box 30 State College, PA 16801	1	University of California Los Alamos Scientific Lab ATTN: T3, D. Butler Los Alamos, NM 87554
1	Pennsylvania State University Dept. of Mechanical Engineering ATTN: K. Kuo University Park, PA 16802	1	University of Southern California Mechanical Engineering Dept ATTN: OHE200, M. Gerstein Los Angeles, CA 90007
		1	University of California, San Diego AMES Department ATTN: F. Williams P. O. Box 109 La Jolla, CA 92037

DISTRIBUTION LIST

<u>No. of Copies</u>	<u>Organization</u>
1	University of Illinois AAE Department ATTN: H. Krier Transportation Bldg. Rm 105 Urbana, IL 61801
1	University of Massachusetts Dept. of Mechanical Engineering ATTN: K. Jakus Amherst, MA 01002
1	University of Minnesota Dept. of Mechanical Engineering ATTN: E. Fletcher Minneapolis, MN 55455
2	University of Utah Dept. of Chemical Engineering ATTN: A. Baer G. Flandro Salt Lake City, UT 84112
1	Washington State University Dept. of Mechanical Engineering ATTN: C. Crowe Pullman, WA 99163

Aberdeen Proving Ground

Dir, USAMSAA
ATTN: DRXS-D
DRXS-MP, H. Cohen
Cdr, USATECOM
ATTN: DRSTE-TO-F
Dir, USACSL, Bldg. E3516, EA
ATTN: DRDAR-CLB-PA

USER EVALUATION OF REPORT

Please take a few minutes to answer the questions below; tear out this sheet, fold as indicated, staple or tape closed, and place in the mail. Your comments will provide us with information for improving future reports.

1. BRL Report Number _____

2. Does this report satisfy a need? (Comment on purpose, related project, or other area of interest for which report will be used.)

3. How, specifically, is the report being used? (Information source, design data or procedure, management procedure, source of ideas, etc.) _____

4. Has the information in this report led to any quantitative savings as far as man-hours/contract dollars saved, operating costs avoided, efficiencies achieved, etc.? If so, please elaborate.

5. General Comments (Indicate what you think should be changed to make this report and future reports of this type more responsive to your needs, more usable, improve readability, etc.) _____

6. If you would like to be contacted by the personnel who prepared this report to raise specific questions or discuss the topic, please fill in the following information.

Name: _____

Telephone Number: _____

Organization Address: _____

FOLD HERE

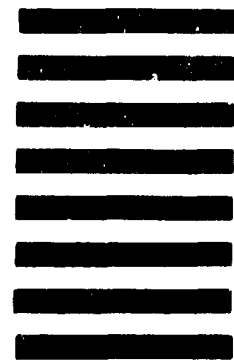
Director
US Army Ballistic Research Laboratory
Aberdeen Proving Ground, MD 21005



NO POSTAGE
NECESSARY
IF MAILED
IN THE
UNITED STATES

OFFICIAL BUSINESS
PENALTY FOR PRIVATE USE, \$300

BUSINESS REPLY MAIL
FIRST CLASS PERMIT NO 12062 WASHINGTON, DC
POSTAGE WILL BE PAID BY DEPARTMENT OF THE ARMY



Director
US Army Ballistic Research Laboratory
ATTN: DRDAR-TSB
Aberdeen Proving Ground, MD 21005

FOLD HERE